

Department of Biomaterials, Institute of Clinical Sciences,  
Sahlgrenska Academy at University of Gothenburg, Göteborg, Sweden

Mechanisms of Osseointegration: Experimental Studies on Early Cellular  
and Molecular Events in vivo

By

Omar Omar



UNIVERSITY OF GOTHENBURG

2010

© 2010 Omar Omar

Department of Biomaterials  
Institute of Clinical Sciences  
Sahlgrenska Academy  
University of Gothenburg

Correspondence:  
Omar Omar  
Department of Biomaterials  
Institute of Clinical Sciences  
Sahlgrenska Academy at University of Gothenburg  
Box 412  
SE 405 30 Göteborg  
Sweden

E-mail: [omar.omar@biomaterials.gu.se](mailto:omar.omar@biomaterials.gu.se)

ISBN: 978-91-628-8072-9

Printed in Sweden  
Geson Hylte Tryck

Printed in 200 copies



## Abstract

The early cellular and molecular activities determining the early tissue response and bone formation at bone/implant interface are not fully understood. The general aim of the current thesis was to develop a model for studying the early molecular and cellular activities in different bone types, and in response to different implant surface properties. The studies were performed by analyzing gene expression of implant-adherent cells using a sampling procedure and subsequent qPCR. The developed model was combined with histology and immunohistochemistry to study cellular relations and early tissue organization at the interface with the implant, governing the early structural basis of osseointegration. The ultimate aim was to determine the strength of the early formed bone/implant interface, by measuring the removal torque forces, and thereby to correlate the results with the degree of inflammation, bone formation and bone resorption, as measured by a gene expression panel. The evaluation time for the studies ranged between 3 hours up 28 days from implantation. The present studies provided a combination of gene expression, morphological, and biomechanical data.

The present results demonstrated biological differences between cortical and trabecular bone types, both in the normal steady-state condition and in response to biomaterial. During steady-state conditions, bone with trabecular architecture expressed higher level of bone turnover markers compared to cortical bone, while the latter had a higher inflammatory constitutive expression. The response to anodically oxidized titanium implants was different in trabecular and cortical bone sites after 3 days of implantation. Early differences in gene expression in cells associated with different implant materials can be detected as early as 3 hours after implantation. Higher level of osteogenic activity indicated by significantly higher expression of mesenchymal stem cell recruitment and adhesion markers and higher expression of markers for coupled bone formation and resorption, were found at oxidized surfaces. A higher expression of CXCR4 homing receptor for stem cells, and the integrins,  $\alpha v$ ,  $\beta 1$  and  $\beta 2$  were detected in cells at oxidized surfaces. On the other hand, higher proinflammatory activity was detected at the machined surfaces, as exemplified by the expression of TNF- $\alpha$  and IL-1 $\beta$ . Scanning electron microscopy and immunohistochemical analysis confirmed the presence of both inflammatory monocytes/macrophages and mesenchymal stem cells at the implant surfaces with predominance of the mesenchymal cells on the oxidized surfaces. Gene expression analyzed on the screw level provided additional information in comparison with that of surrounding bone. The rapid recruitment and adhesion of mesenchymal stem cells, the rapid triggering of gene expression crucial for bone remodeling and the transient nature of inflammation correlated with higher stability of the oxidized implants. In conclusion, the combination of the *in vivo* experimental model, qPCR and morphological and biomechanical techniques provided hitherto unexplored opportunities to analyze in detail the mechanisms of osseointegration. A major conclusion of the studies is that material surface properties elicit early, significant differences in gene expression in interfacial cells. This observation is important in order to understand the mechanisms behind osseointegration and the role of material surface properties. Furthermore, this knowledge is essential for the ability to design the material and biological conditions for optimal tissue regeneration in association with implanted medical devices.



## List of Papers

I. O. Omar, F. Suska, M. Lennerås, N. Zoric, S. Svensson, J. Hall, L. Emanuelsson, U. Nannmark, P. Thomsen, *The influence of bone type on the gene expression in normal bone and at the bone-implant interface: experiments in animal model*, Clin Implant Dent Relat Res 2009, [Epub ahead of print]

II. O. Omar, M. Lennerås, S. Svensson, F. Suska, L. Emanuelsson, J. Hall, U. Nannmark, P. Thomsen, *Integrin and chemokine receptor gene expression in implant-adherent cells during early osseointegration*, J Mater Sci: Mater Med. 2010 Mar; 21(3): 969-80

III. O. Omar, S. Svensson, N. Zoric, M. Lennerås, F. Suska, S. Wigren, J. Hall, U. Nannmark, P. Thomsen, *In vivo Gene expression in response to anodically oxidized versus machined titanium implants*, J Biomed Mater Res A. 2010 Mar 15;92(4):1552-66

IV. O. Omar, M. Lennerås, F. Suska, L. Emanuelsson, J. Hall, A. Palmquist, P. Thomsen, *Interfacial gene expression and stability of oxidized and machined titanium implants*, In manuscript



## Abbreviations

AES	Auger electron spectroscopy
ALP	Alkaline phosphatase
BMP-2	Bone morphogenetic protein-2
BSP	Bone sialoprotein
CATK	Cathepsin K
CCL2/MCP-1	Chemokine (C-C motif) ligand 2/Monocyte chemoattractant protein-1
CXCR2/IL-8R	Chemokine (C-X-C motif) receptor 2/Interleukin-8 receptor
CXCR4/SDF-1R	Chemokine (C-X-C motif) receptor 4/Stromal derived factor-1 receptor
CXCL8/IL-8	Interleukin-8
CXCL12/SDF-1	Stromal derived factor-1
Dlx	Distal-less homeobox
ECM	Extracellular matrix
EDS	Energy dispersive X-ray spectroscopy
FIB	Focused ion beam
IL-1 $\beta$	Interleukin-1beta
MAPK	Mitogen-activated protein kinase
M-CSF	Macrophage-colony stimulating factor
MSCs	Mesenchymal stem cells
OC	Osteocalcin
ON	Osteonectin
OPG	Osteoprotegerin
OPN	Osteopontin
PDGF	Platelet-derived growth factor
PMN	Polymorphonuclear leukocytes
PPAR- $\gamma$	Peroxisome proliferator-activated receptor-gamma
qPCR	Quantitative polymerase chain reaction
RANKL	Receptor activator of nuclear factor-kappaB ligand
RANK	Receptor activator of nuclear factor- $\kappa$ B
Runx2	Runt related transcription factor-2
SEM	Scanning electron microscopy
TCP	Tissue culture polystyrene
TEM	Transmission electron microscopy
TGF- $\beta$	Transforming growth factor-beta
TNF- $\alpha$	Tumor necrosis factor alpha
TNFR	Tumor necrosis factor receptor
TRAP	Tartrate-resistant acid phosphatase
Wnt signaling	Wingless signaling pathway



# Content

<b>ABSTRACT</b>	<b>3</b>
<b>LIST OF PAPERS</b>	<b>5</b>
<b>ABBREVIATIONS</b>	<b>7</b>
<b>CONTENT</b>	<b>9</b>
<b>INTRODUCTION</b>	<b>13</b>
<b>Osseointegration</b>	<b>13</b>
<b>Bone</b>	<b>14</b>
<b>Cellular components of bone</b>	<b>14</b>
Osteoprogenitors	14
Preosteoblasts and osteoblasts	15
Osteocytes	15
Bone lining cells	16
Osteoclasts	16
<b>Woven vs. lamellar bone</b>	<b>17</b>
<b>Cortical vs. trabecular bone types</b>	<b>17</b>
<b>Intramembranous vs. intracartilaginous bone formation</b>	<b>18</b>
<b>Biological aspects of bone healing</b>	<b>18</b>
Cellular components	19
Molecular components	19
Pro-inflammatory cytokines	20
<i>TNF-<math>\alpha</math></i>	20
Chemokines	21
<i>CCL2/MCP-1</i>	21
<i>CXCL8/IL-8</i>	21
<i>CXCL12/SDF-1</i>	22
Integrins	22
Growth factors	23
<i>TGF-<math>\beta</math>1</i>	23
<i>PDGF</i>	23
<i>BMP-2</i>	24
Transcriptional regulators	25
<i>Runx2</i>	25
<i>PPAR-<math>\gamma</math></i>	26
Osteogenic differentiation, bone formation and remodeling	26
<i>ALP and OC</i>	27
<i>TRAP and CATK</i>	27

---

<b>Effect of titanium surfaces on cellular and molecular activities</b>	<b>28</b>
<b>Biomechanical stability during development of osseointegration</b>	<b>34</b>
<b>In vivo cellular and molecular techniques in relation to bone-implant interface</b>	<b>35</b>
Immunohistochemistry and protein targeting procedures	35
RNA targeting procedures	35
<i>Northern analysis</i>	35
<i>In situ hybridization</i>	36
<i>Polymerase chain reaction</i>	36
<i>Reverse transcription-polymerase chain reaction (RT-PCR)</i>	37
Quantitative polymerase chain reaction (qPCR)	37
<i>Relative gene expression analysis</i>	38
<i>Normalization</i>	38
<b>AIMS</b>	<b>39</b>
<b>MATERIALS AND METHODS</b>	<b>41</b>
<b>Implants</b>	<b>41</b>
<b>Surface characterization (paper IV)</b>	<b>41</b>
Profilometry	41
Scanning electron microscopy	41
Auger electron spectroscopy	41
Transmission electron microscopy	41
Endotoxin test	42
<b>Animal model and surgical procedures (papers I-IV)</b>	<b>43</b>
<b>Gene expression analysis (papers I-IV)</b>	<b>45</b>
<b>Histology (papers I - IV) and immunohistochemistry (papers II and III)</b>	<b>46</b>
<b>Scanning electron microscopy (papers II - IV)</b>	<b>47</b>
<b>Removal torque analysis (paper IV)</b>	<b>47</b>
<b>Statistics</b>	<b>48</b>
<b>RESULTS</b>	<b>49</b>
<b>Surface characterization</b>	<b>49</b>
Surface morphology	49
Surface topography	49
Surface chemistry	49
Oxide thickness and ultrastructure	51
Endotoxin test	51
<b>Molecular activity of different bone types (paper I)</b>	<b>51</b>
Steady-state gene expression in cortical and trabecular bone types	51
Gene expression at oxidized implants in cortical and trabecular bone types	52

---



---

<b>Cellular and molecular activities at different implant surfaces (papers II - IV)</b>	<b>52</b>
Cellular and molecular activity during first day of implantation (paper II)	52
Gene expression in implant-adherent cells	53
Scanning electron microscopy of the implant-adherent cells	55
Immunohistochemistry of the interface	56
Cellular and molecular activity during first week of implantation (paper III)	56
Gene expression in the implant-adherent cells	57
Gene expression in the peri-implant bone	58
Scanning electron microscopy of the implant-adherent cells	58
Histology and immunohistochemistry of the interface	59
Cellular and molecular activity during first month of implantation (paper IV)	60
Gene expression in implant-adherent cells	60
Gene expression in the peri-implant bone	61
<b>Biomechanical evaluation (paper IV)</b>	<b>62</b>
Histology and backscattered scanning electron microscopy (paper IV)	63
Correlations between expression of individual genes and between individual genes and biomechanical torque (paper IV)	65
<b>DISCUSSION</b>	<b>67</b>
<b>In vivo interfacial gene expression model</b>	<b>67</b>
<b>Gene expression in trabecular and cortical bone types</b>	<b>68</b>
Steady-state gene expression	68
Gene expression at cortical and trabecular bone interfaces with oxidized implants	69
<b>Interfacial gene expression at machined and oxidized implants</b>	<b>70</b>
Gene expression at the interface: Initial inflammation, cell recruitment and adhesion	70
Inflammatory, osteogenic and osteoclastogenic gene expression at the interface	72
Transcriptional and growth factor regulators of interfacial gene expression	75
Molecular activities in the peri-implant bone	76
<b>Biomechanics and the correlation with the molecular activities at the interface</b>	<b>77</b>
<b>SUMMARY AND CONCLUSIONS</b>	<b>81</b>
<b>TOPICS FOR FUTURE RESEARCH</b>	<b>83</b>
<b>ACKNOWLEDGEMENTS</b>	<b>85</b>
<b>REFERENCES</b>	<b>87</b>



# Introduction

## ***Osseointegration***

Osseointegration is the privileged outcome of bone tissue healing around titanium implant. It is a biological process in which a direct anchorage is established by formation of bone tissue around the implant without the growth of fibrous tissue at the bone-implant interface [1, 2]. The regenerative process described by this definition and other definitions represent a part of multiple phases of healing which are governed by series of cellular and molecular events. The current knowledge on the process of healing at titanium implants is predominantly gained from histological data and correlation with normal fracture healing. In addition, few studies have addressed the early events during the healing process, and the cellular behavior at the interface has been largely neglected. Histologically, it has been shown that the process of bone formation at titanium implants is preceded by recruitment of cells of different types and at different levels of morphological differentiation [3, 4]. However, the functional activities of the different cells and the roles of cells other than osteogenic ones in the healing process have not been clearly defined. Such mechanisms underlying bone formation and maintenance at the implants surface *in vivo* are yet to be understood.

Histological and biomechanical evidence strongly suggest that bone would respond differently by alteration of the implant surface properties [5]. Subsequently, great attention has been given to study, *in vitro*, the cellular behavior on different substrates and to extrapolate the results to the actual interfacing between implant and living bone tissue. Taking into account the important information acquired from these studies, however, they remain to large extent unrepresentative for the actual paradigm of the *in vivo* implantation. The great advances in research technologies have made it possible to apply molecular techniques to analyze the interface between the living tissues and implant surface. Such tools can be used at high degree of precision to discover mechanisms that govern bone healing at the implant surface including events of early inflammation, mesenchymal cell recruitment and cell-cell communication. Nevertheless, the advent of these approaches requires establishing reliable procedures to collect cell samples from within the *in vivo* interface in the way that their spatial distribution can be determined.

Despite the high success/survival rate of osseointegrated implants, failure of developing and/or maintaining osseointegration is still happening and in many cases as early as before implant loading [6]. Irrespective of the etiological factors, the biological failure of an implant is underlined by unfavorable biological processes, including inflammation which adversely influences the regeneration process. As specific biological sequences characterize the healing at the bone-implant interface, possibly unique biological markers would also characterize pathological responses resulting in fibrosis and failure. An increased understanding of the cellular and molecular mechanisms of osseointegration will provide new tools for the screening, diagnosis and monitoring of implants in clinical care.

## ***Bone***

Bone is a viable, cellular, highly mineralized connective tissue and although one of the hardest tissues in the body, still maintaining some degree of elasticity due to its structure and composition. The mineral constituent of bone is mainly hydroxyapatite crystals laid down in organic matrix. Collagen fibers, mainly of type I, form approximately 95 % of the total protein in bone and the rest being extracellular substance containing proteoglycan and non-collagenous proteins. Bone exists in different shapes which include long bone, like tibia and femur, flat bone, like bones of skull and mandible, and irregular bone, like hip bone. The internal (endosteal) and external (periosteal) surfaces of bone are each lined with cellular layers called the endosteum and periosteum, respectively. The interior of bone is filled with loose vascular connective tissue, the bone marrow, which reside in direct contact with the endosteal surfaces. Bone marrow contains multipotent stem cells, localized in a defined microenvironment, i.e. niches, [7]. These primitive cells are capable for differentiation along multiple mesenchymal and hematopoietic lineages. The mesenchymal stem cells (MSCs) differentiate into various cell types which include cells from osteoblastic lineage in addition to chondroblasts, fibroblasts, adipocytes and myoblasts [8], whereas the hematopoietic stem cells give rise to erythrocytic, leukocytic and thrombocytic lineages. Osteoclasts, the major bone resorptive cells, are derived from the hematopoietic lineage.

In addition to its fundamental roles, bone serves as the major reservoir for calcium and inorganic ions, regulating the mineral homeostasis in the whole body. Bone marrow is the site where hematopoiesis and synthesis of blood cells take place. Bone matrix also has endocrinal contributions by serving as a storage site for different growth factors and proteins.

## ***Cellular components of bone***

Under control of specific growth and transcriptional factors, mesenchymal stem cells differentiate toward osteogenic lineage during a number of developmental stages, starting from commitment to osteoprogenitors, through preosteoblasts and osteoblasts and finally osteocytes or lining cells [9]. It is thought that during the early stages, commitment osteoprogenitors maintain certain degree of plasticity allowing de- and trans-differentiation to other mesenchymal lineages whereas osteoblasts and osteocytes represent a terminal differentiation stage as they become specialized functional cells [10]. However, it has also been suggested that even mature osteoblasts are being able to trans-differentiate to other phenotypes [8].

## **Osteoprogenitors**

Osteoprogenitor cells are committed to the bone cell lineage, i.e. restricted to osteoblast development and bone formation. These cells are from mesenchymal origin and have the properties of stem cells: the potential for proliferation and a capacity to differentiate. However, they lack the self-renewal capacity [9]. A wide range of cytokines and growth factors control the differentiation of osteoprogenitors to preosteoblasts and osteoblasts. These include, but not limited to, transforming growth factor-beta (TGF- $\beta$ ), bone morphogenetic protein-2 (BMP-2), insulin-like growth factor-I (IGF-I), fibroblast growth

factor (FGF), parathyroid hormone-related protein (PTHrP), vitamin D (1,25(OH)<sub>2</sub>D<sub>3</sub>), leptin and members of interleukin-6 (IL-6) family. The regulations are precisely controlled by specific transcription factors that ensure the osteogenic differentiation and, later on, bone matrix formation and mineralization. Runt related transcription factor 2 (cbfa1/Runx2) is considered as a master gene for osteogenic differentiation and has the major role in maintaining the osteo-phenotype [11]. Furthermore, other transcription factors like the activator protein (AP) family, osterix and Dlx5 (Distal-less homeobox), and intracellular signaling pathways such as the mitogen-activated protein kinase (MAPK) system, Wnt and Smad signaling pathways are majorly involved [12].

### **Preosteoblasts and osteoblasts**

Preosteoblasts are less cuboidal in shape and less matrix producing than osteoblasts. These cells are localized adjacent to the osteoblasts and represent a transitional stage between the highly proliferative osteoprogenitor cells and the mature osteoblast [9]. Despite their low production of matrix proteins, preosteoblasts still have the ability to divide. Studies have also shown that preosteoblasts can produce collagen I precursors [13] and express a panel of early bone formation markers such as alkaline phosphatase (ALP), growth factor receptors, several integrins and osteoblast specific factor-2 (periostin) [8, 13]. Preosteoblasts differentiate into osteoblasts which are typically cuboidal in shape and actively and ultimately secrete the organic bone matrix. Osteoblasts show the characteristics of protein producing cells with eccentric nuclei, prominent Golgi apparatus and rough endoplasmic reticulum. The early secretion of osteoblasts, the osteoid, contains collagen type I and other non-collagenous proteins including osteopontin (OPN), bone sialoprotein (BSP) and osteocalcin (OC). During the early stage of bone formation, osteoblasts express high activity of ALP enzyme. They also express growth factors and molecules involved in auto- and para-crine regulations and cell-cell interactions. As the osteoid formation proceeds, osteoblasts extend cellular protrusions or pseudopodia toward the osteoid seam, and adhere to the existing matrix and neighboring cells via integrins, predominately of  $\beta$ 1 type, and other adhesion molecules. As the bone matrix form, osteoblasts regulate the mineralization process by mechanisms that are not completely understood. Small membrane-bound matrix vesicles are budded from the processes of the osteoblast cell membrane and secreted to the matrix. These vesicles contain ALP and other phosphatases that neutralize the effect of pyrophosphate, which is a major inhibitor of calcium and phosphate deposition [14]. The deposition of hydroxyapatite, the predominant mineral crystal phase present in bone matrix, occurs both within and between the collagen fibrils which act as a template for the crystal initiation and propagation. A layer of unmineralized osteoid is always present on the bone surface under the osteoblasts. As bone matrix deposition and mineralization continue, some osteoblasts periodically become embedded in the osteoid and become osteocytes. Prior to mineralization, the buried cells establish numerous cytoplasmic connections with the surface osteoblasts and the adjacent osteocytes [15].

### **Osteocytes**

The osteocyte is a mature osteoblast, embedded in the bone matrix and plays an important role in its maintenance. At the early stage of osteoblast to osteocyte

differentiation these cells assume larger size and hence are called large osteocytes or osteoid-osteocytes [15]. On maturation of the osteoid, osteocytes becomes smaller in size with prominent reduction in the protein forming organelles. Hereby, many of the previously expressed bone markers, such as collagen I, ALP, periostin, OC and integrins are down regulated or switched off. Nevertheless, they still have the capacity to sanitize matrix and further they can resorb bone to a limited extent. Further, osteocytes are also implicated as the major mechanosensory cells in bone [16, 17].

### **Bone lining cells**

Lining cells are flat elongated and inactive cells that cover the surfaces of quiescent bone sites. The nature and function of these cells are not well-recognized and generally considered as mature late stage osteoblasts [8]. However, lining cells have also been speculated to be precursors for osteoblasts [14]. Increasing evidence suggest important roles of endosteal lining cells in maintaining and supporting hematopoietic stem cells [18-20]. They have also been shown to have important roles in coordination of bone resorption and formation [21].

### **Osteoclasts**

Osteoclasts are derived from hematopoietic origin and are primarily involved in bone resorption. The osteoclast is an end-differentiated multinucleated cell generated by differentiation and fusion of precursors from monocyte/macrophage lineage [22, 23]. Key cytokines are crucial for the process of osteoclastogenesis and osteoclast development. Several investigations have shown that osteoclastogenesis is critically dependent on Macrophage-colony stimulating factor (M-CSF) and receptor activator of nuclear factor-kappaB ligand (RANKL) [24-26]. M-CSF is considered to be critical for the proliferation of the osteoclast precursors as well as survival of mature osteoclasts, whereas RANKL appears to directly control the differentiation process upon binding to the receptor activator of nuclear factor- $\kappa$ B (RANK) expressed on the surface of osteoclast precursor [24]. Binding of M-CSF and RANKL to M-CSF receptor and RANK, respectively, initiates intracellular cascade and stimulates series of events inside the cell leading eventually to the development of mature osteoclast. In addition to M-CSF and RANKL, pro-inflammatory cytokines, tumor necrosis factor alpha (TNF- $\alpha$ ) and member of TNF receptor family, osteoprotegerin (OPG), have been shown to encompass crucial positive and negative roles on osteoclast differentiation, respectively [24]. TNF- $\alpha$  binds to TNFR1 and augments the RANK-RANKL pathway. Furthermore, in vitro studies have shown that TNF- $\alpha$  promotes osteoclast formation independently of RANKL, through other pathways [27, 28]. On the other hand, OPG has high affinity to RANKL and act as inhibitor to it and hence block its binding to RANK. Moreover, other cytokines and growth factors, including interleukin-beta1 (IL-1 $\beta$ ), IL-6 and TGF- $\beta$ 1, are known to exert direct positive effects on osteoclastogenesis. It is worthwhile that marrow stromal cells and their derivative osteoblasts, express most of these cytokines and growth factors which are absolutely required for osteoclastogenesis. Furthermore, some of these ligands, particularly RANKL, are membrane bound which indicate that differentiation of osteoclasts requires direct interaction of the non-hematopoietic, bone cells, with osteoclast precursors. Such interactions outline the mechanisms by which the processes

of bone resorption and formation are finely coupled between osteoclasts and osteoblasts during physiological and fracture remodeling.

During bone resorption, osteoclast precursors are recruited and subsequently differentiated at the site of prospected bone resorption. It is not clear how specific sites are chosen for resorption and how the earliest steps in resorption start. It is thought that cells from osteoblastic lineage, probably lining cells, prepare and condition the sites of resorption before and after the resorption takes place by osteoclasts [29]. During osteoclastogenesis, the precursor cells express a variety of integrins including those specific for monocyte lineage, integrin- $\beta$ 2. On maturation osteoclasts predominantly express  $\alpha$ v $\beta$ 3 integrins, which recognize exposed, specific, sequences of some bone proteins such as OPN and BSP [30]. Binding of integrins forms a tightly sealed zone under which bone resorption proceeds by creation of highly acidic microcompartment where the dissolution of mineral phase take place followed by enzymatic degradation of organic components by lysosomal proteases such as cathepsin K (CATK). Bone resorption is followed by bone formation as the osteoclasts are leaving the resorption pits. The signals that lead to recruitment and differentiation of osteogenic cells, for the subsequent bone formation, are unclear. It is possible that the release of growth factors, crucial for bone formation, such as TGF- $\beta$ 1, IGF-I and BMP-2, from the dissolved matrix, plays important role in providing directional information for osteoblastic bone formation. Furthermore, direct effects from osteoclasts on osteoblastic cells, by synthesizing growth factors such as TGF- $\beta$ 1 [31] and IGF-I [32], or by cell-cell contact, via ephrine and ephrine receptor signaling pathway [33], have been described. Interestingly, recent investigations indicate that osteoclasts may recruit osteoprogenitors to the site of bone remodeling through mechanisms which involve secretion of chemokines and BMP-6, and stimulate bone formation through increased activation of Wnt/BMP pathways [34].

### ***Woven vs. lamellar bone***

Woven bone is the name given to the early developed bone during embryogenesis. It is also the first bone to form during fracture healing and repair. This primitive bone is produced when osteoblasts produce osteoid rapidly. It is characterized by thick, irregular "woven" network of collagen fibers in the matrix and the lack of order of osteocytes. Woven bone is more flexible than lamellar bone and is mechanically weak. Once formed, woven bone is rapidly resorbed and replaced by mature lamellar bone. Lamellar bone is the mature bone where the tissue is well organized and regular. Lamellar bone formation takes place more slowly, and it is characterized by regular and parallel alignment of collagen into concentric sheets (lamellae) and regularly arranged osteocytes which have lower proportion and more flattened shape as compared to woven bone. Lamellar bone is mechanically stronger and it can be formed as a solid mass (cortical bone) or in an open sponge-like manner (trabecular bone).

### ***Cortical vs. trabecular bone types***

Morphologically, bone is divided into cortical (compact or dense) and trabecular (cancellous or spongy). Cortical bone forms the hard outer layer of bones and it is formed by overlapping cylindrical units termed osteons. Trabecular bone is found principally at

the ends of long bones, and in the vertebral bodies and the flat bones. It is composed of a meshwork of trabeculae within which are intercommunicating spaces allowing room for blood vessels and bone marrow. It is considered that the differences in structure are related mainly to their functions [14]. Cortical bone provides mechanical and protective functions while trabecular bone provides metabolic functions. Nevertheless, studies showed that there are also differences in their protein contents [35] and the basal gene expression of the members of bone morphogenetic proteins [36].

### ***Intramembranous vs. intracartilaginous bone formation***

Bone formation occurs by either direct (intramembranous) or indirect (intracartilaginous) processes. Intramembranous ossification occurs during embryonic development (cranial vaults, major part of mandible, maxilla and some facial bones and clavicle) [14]. It also forms an essential process during the natural healing of bone fractures. During intramembranous ossification, a group of mesenchymal cells within a highly vascularized area of the embryonic connective tissue, and the hematoma of fracture site, proliferates forming early mesenchymal condensations within which cells differentiate directly into osteoblasts. Bone Morphogenetic Proteins, as well as other growth factors appear to be essential in the process of mesenchymal cell condensation. Runx2 transcription factor is critical and decisive element for intramembranous bone formation [37]. The newly differentiated osteoblasts will synthesize a woven bone matrix, while at the periphery mesenchymal cells continue to differentiate into osteoblasts. Blood vessels are incorporated between the woven bone trabeculae and will form the bone marrow. Later, the woven bone will be remodeled through the classical remodeling process, resorbing the woven bone and progressively replacing it with mature lamellar bone.

Intracartilaginous ossification takes place majorly during embryonic development of long bones and postnatal growth of long bones and mandible. It also forms a part of the natural healing process of bone fracture. It begins with the formation of a cartilage analogue (model) from a mesenchymal condensation. Members of Sox transcription factor family, namely Sox9, L-Sox5, and Sox6, are the master regulators of the early chondrogenesis [38]. Runx2 and related isoforms are also indispensable [37]. Mesenchymal cells undergo division and differentiate into chondroblasts rather than directly into osteoblasts. These cells secrete the cartilaginous matrix, where the predominant collagen type is collagen II. Like osteoblasts, the chondroblasts become progressively embedded within their own matrix, where they lie within lacunae, and they are then called chondrocytes. Chondrocytes undergo well-ordered and controlled phases of cell proliferation, maturation, and apoptosis. Hypertrophic chondrocytes express predominantly type X collagen and mineralize the surrounding matrix. The hypertrophic chondrocytes (before apoptosis) secrete vascular endothelial growth factor and bone morphogenetic proteins that induces the invasion of blood vessels, hematopoietic cells and osteoprogenitor cells leading finally to replacement of the cartilaginous matrix by trabecular bone.

### ***Biological aspects of bone healing***

Bone regeneration around titanium implants has classically been regarded as similar to that observed after injury or fracture. This healing is based traditionally on the succeeding phases of inflammation, regeneration and remodeling with possible overlapping at certain



occasions. However, the presence of biocompatible, not inert, material in close vicinity to the healing tissue would largely influence the critical steps during the regeneration process. Therefore, it is likely that events that occur during normal healing are modulated in the presence of a biomaterial. Nevertheless, for proper interpretation of the cascades of cellular and molecular signaling, encompassing the recruitment of inflammatory and progenitor cells and the expression of different cytokines, matrix protein and growth factors at the implant interface, it requires proper understanding of such events during early healing processes after bone injury.

Healing of bone injury has been widely investigated in different models including: transverse long bone fracture [39], distraction osteogenesis [40], large segmental bone defect [41], injured growth plate model [42], marrow ablation model [43] and drill-hole injury [44]. Despite the fact that in most cases bone will heal in a very orchestrated manner of events with formation of new bone tissue without any scar formation, there are differences in the way how the bone will be formed, i.e. intramembranous, intracartilaginous or a combination of both. The cellular and molecular signals that underlay these types of healing would also be different. During healing of a drill-hole, which is the case when preparing an implant site, and marrow ablation injury, the intramembranous route is the principle mechanism of bone formation. Whether intramembranous or cartilaginous, several factors influence which type of ossification will occur. These factors include the defect size, stability of fracture site, blood supply and oxygen tension together with the spectrum of cytokines and growth factors at the site of fracture. The time factor is important depending on which events are taking place.

Based on histological observations, healing involving cartilaginous ossification may take several weeks for complete replacement of cartilaginous tissue with bone. On the other hand, intramembranous healing occurs within few days after injury. In femur diaphysis transverse fracture [39], woven bone produced by osteoblasts appeared within 3 d after fracture and was associated with upregulation of ALP and collagen I on d 3, and maximum early peak of these genes on d 5. In the same fracture site, cartilage was evident on d 9 in conjunction with increased expression of ALP and collagen. The expression of these two genes showed early peak after 15 d in the soft callus cartilaginous site.

### **Cellular components**

Healing of bone fracture is not exclusively limited to osteogenic cells *per se*, but a complex interplay of sequential, yet overlapping phases of establishing hemostasis, inflammation, tissue regeneration and remodeling. These events are orchestrated by both hematopoietic progenies: platelets, neutrophils, monocytes/macrophages, lymphocytes, endothelial cells and osteoclasts together with mesenchymal progenies of osteogenic and/or chondrogenic phenotypes.

### **Molecular components**

Multiple factors control the coordinated complex interactions of hematopoietic and immune cells and the mesenchymal skeletal cells during fracture healing. Plethora of cytokines, chemokines, integrins, growth, and differentiation factors are temporally and

spatially affecting the different stages of healing during processes such as inflammation, migration and chemotaxis, adhesion, proliferation, differentiation and extracellular matrix synthesis.

### **Pro-inflammatory cytokines**

TNF- $\alpha$  and IL- $\beta$  are major proinflammatory cytokines secreted primarily by hematopoietic immune cells, such as monocytes/macrophages and neutrophils, and also by cells from mesenchymal osteogenic lineage [45]. They have wide range of effects and can either trigger cell death or promote cell survival depending on the specific cell surface receptor they bind, the cell type, and the intracellular signaling cascade that is subsequently activated [46]. The central effect of IL-1 $\beta$  has been shown to contribute to the inflammation associated pain and fever [47]. In relation to bone injury, studies suggested that osteoblasts were removed from the injury site via a coordinately regulated apoptosis during bone healing [48] and evidence were found suggesting that IL-1 $\beta$  mediated the appearance and disappearance of osteoblasts, possibly by affecting the rates of differentiation and apoptosis [49]. Besides, positive effects of proinflammatory cytokines on osteoclastic differentiation have been documented. The critical roles of TNF member (RANKL) and the member of TNF receptor family (OPG) and the direct effect of TNF- $\alpha$  and IL-1 $\beta$  on osteoclastogenic differentiation have been largely investigated [24]. Generally, proinflammatory cytokines have been considered to be crucial regulatory component during bone healing. The expression of these cytokines significantly increases during the initial inflammatory phase after bone injury and show peak expression within the first 24 h following fracture [50]. Their levels are seen to reduce during the regenerative phase and increase again during the remodeling phase.

#### *TNF- $\alpha$*

Despite the numerous investigations on the role of TNF- $\alpha$  and their receptors, TNFR1 and TNFR2, on the osteogenic cells, their exact effects and mechanisms are still unclear. Studies with marrow ablation model in TNFR1 and TNFR2 knockout mice have indicated that TNF- $\alpha$  signaling is necessary for intramembranous ossification [51]. Furthermore, TNF- $\alpha$  is strongly implicated in the induction of ectopic calcification, for instance in arteries during atherosclerosis or aortic valve disease [52, 53]. These in vivo observations are in agreement with in vitro data showing that human MSCs increase their proliferation and invasion in response to TNF- $\alpha$  via inhibitor of NF- $\kappa$ B kinase (IKK-2) [54]. Recent in vitro work showed that TNF- $\alpha$  increased the matrix mineralization, BMP-2 and ALP expression by activating the NK- $\kappa$ B signaling pathway in hMSCs during osteogenic differentiation [55]. Furthermore, the activated NK- $\kappa$ B has led to inhibition of the differentiation of hMSCs toward myogenic [56] and chondrogenic [57] direction by down-regulating the critical transcription factors MyoD and Sox9, respectively. In addition, other in vitro data showed that TNF- $\alpha$  may stimulate the recruitment of MSCs by a process related to the expression of intercellular adhesion molecule 1 (ICAM-1) with possible involvement of p38 signaling pathway [58].

Nevertheless, it is generally recognized that TNF- $\alpha$  contributes to a decrease of bone mineral density by inhibiting osteoblast differentiation and bone formation. For instance, in growth plate injury model, TNF- $\alpha$  has been reported to activate p38 pathway and, yet, results in recruitment and proliferation of mesenchymal cells; however, by suppressing

expression of *cbfa1/Runx2*,  $\text{TNF-}\alpha$  signaling inhibited bone cell differentiation and bone formation [59]. In addition, several *in vitro* data showed that  $\text{TNF-}\alpha$  may decrease or inhibit *Runx2* expression [60-62] and promote its degradation [63].

## **Chemokines**

Healing of bone injury requires continuous influx of various cell types for each ongoing process, whether inflammation, regeneration and/or remodeling. Whereas the mechanisms by which inflammatory cells are recruited to the injury site are well characterized, the trafficking of mesenchymal stem cells to the healing site is still largely unknown. The local release of inflammatory mediators, such as the chemicals released from injured tissue (e.g. prostaglandins), products of coagulation and complement (e.g. C5a) and products of fibrinolysis, initiates the cascade that controls early inflammatory events. These events involve the production and release of primary acute phase cytokines (such as  $\text{TNF-}\alpha$ ,  $\text{IL1}\beta$  and  $\text{IL-6}$ ). By activation of their target cells, these cytokines generate a second wave of cytokines, including members of the chemokine family. The latter are small inducible secondary cytokines with a characteristic cysteine residue motif. Chemokines are divided into four families depending on the spacing of their first two cysteine residues, namely CC, CXC, C and  $\text{CX}_3\text{C}$  [64]. Binding of chemokines to their specific receptors start a complex biological process, the chemotaxis, which involves the rolling, adhesion to and penetration of blood vessel and migration toward the site of highest chemokine concentration.

### *CCL2/MCP-1*

CC-chemokines act primarily on monocytes/macrophages and they are further subdivided into 8 ligands. *CCL2*, also named *MCP-1* (Monocyte Chemoattractant Protein-1), is majorly responsible for monocyte trafficking in the body. In mice that lack *MCP-1* receptor (*CCR2*) gene, the recruitment of monocytes/macrophages to sites of injury is impaired [65, 66]. The receptor of *MCP-1* is also involved in osteoclast differentiation were *CCR2*-mutant mice developed osteopetrosis (increased bone mass and density), and this was not caused by osteoblasts but mainly due to altered number and function of osteoclasts [67]. In tibial fracture site in normal mice, the expression of *MCP-1/CCL2* and its receptor was closely related to the recruitment and function of macrophages. Furthermore, similar fracture in *CCR2* mutant mice revealed significantly fewer macrophages, altered vascular response, impaired osteoclast function and delayed fracture healing [68]. It is worthwhile that *MCP-1* is expressed by osteoblasts *in vitro* [69] and during healing of bone lesion *in vivo* [70].

### *CXCL8/IL-8*

Interleukin-8 (*CXCL8/IL-8*) is a major chemokine involved in neutrophil chemotaxis by binding to its receptors *CXCR1* and *CXCR2* [71]. Large induction of *CXCL8/IL-8* expression was revealed in injured growth plate on d 1 coinciding with neutrophil influx and was associated with increased expression of  $\text{TNF-}\alpha$  and  $\text{IL-1}\beta$  [42]. Using neutrophil-neutralizing antiserum in that model decreased neutrophil infiltration by 60 % which although did not affect mesenchymal cell infiltration on d 4, it significantly reduced the proportion of mesenchymal repair tissue on d 10 and tended to increase osteogenic differentiation by increased expression *cbfa1/Runx2* and OC [42].

### *CXCL12/SDF-1*

Stromal derived factor-1 (SDF-1) is a growth-stimulating factor belonging to the CXC subfamily of chemokines, which was initially identified as a bone marrow stromal cell-derived factor. SDF-1 plays many important roles through activation of its exclusive, a G protein-coupled receptor, CXCR4. Developmentally, SDF-1 and its receptor direct the migration of hematopoietic cells from liver to bone marrow. Mice which were knocked-out for CXCL12 or its receptor CXCR4 were lethal before birth or within 1 h of life [72]. CXCR4 is broadly expressed by hematopoietic leukocytes, especially neutrophils, and regulates their homing, retention and mobilization [73, 74].

Accumulating data have supported an emerging hypothesis that SDF-1/CXCR4 also plays a critical role in the biologic and physiologic functions of MSCs [75-79]. In segmental femoral defect in mice, the expression level of SDF-1 mRNA was significantly increased on d 2 when compared with its level at d 0, and the new bone formation was inhibited by the administration of anti-SDF-1 antibody [78]. Similar defect in mutant mice partially lacking SDF-1 and CXCR4 (SDF-1<sup>+/-</sup> and CXCR4<sup>+/-</sup> mice) showed reduced bone formation after 14 d as indicated histologically (the area of new bone formation was significantly reduced in both SDF-1<sup>+/-</sup> and CXCR4<sup>+/-</sup> mice, by 55 % and 65 %, respectively) [78].

### **Integrins**

Integrins are heterodimeric receptors that mediate cell-cell and cell-ECM attachment. They also play important roles in cell signaling and thus control cellular shape, mobility and regulate the cell cycle. They consist of two non-covalently linked molecules, alpha and beta subunits. Integrins are thought to be expressed by virtually every cell type. Cells of the osteoblastic lineage predominantly express  $\beta 1$ ,  $\alpha 4$ ,  $\alpha 5$  and  $\alpha v$  integrins in various combinations while the osteoclast exhibits higher levels of  $\alpha v \beta 3$  complexes in addition to  $\alpha 1$  and  $\alpha 2$  heterodimers [80]. On the other hand, at least 13 integrins are expressed by leukocytes, among which the  $\beta 2$  is a unique leukocyte-specific integrin [81], with putative roles in leukocyte chemotaxis, phagocytosis, and other adhesion-dependent processes [82]. The  $\beta 2$  integrin has also been shown to be expressed by monocytes committed towards the osteoclast lineage [83]. With respect to MSCs, it was shown that MSCs are capable of rolling and adhering to blood vessel walls in a P-selectin and integrin- $\beta 1$ /VCAM-1 dependent manner [84]. Transgenic mice with impaired integrin- $\beta 1$  function showed reduced bone mass, with increased cortical porosity in long bones and thinner flat bones in the skull [85]. On the other hand, healing of tibial fracture in integrin- $\beta 3$  null mice revealed significantly increased amount of new bone within the fracture callus after 7 d, compared to wild type mice [86]. Furthermore, twenty-three genes, that were primarily related to osteogenesis, were up-regulated at least twofold in  $\beta 3$ -null mice compared to wild type mice [86]. However, the null mice had fewer red blood cells, less hemoglobin, fewer neutrophils and prolonged bleeding time compared to the wild type mice.

## **Growth factors**

Fracture repair is controlled by several growth factors, hormones and hormone-related proteins. Several of these factors are already stored within the mineralized bone matrix and released during the active remodeling occurring as a part of tissue repair. In addition, most of the cells, whether inflammatory, osteogenic, angiogenic or osteoclastic, are known to synthesize and release many of these factors. TGF- $\beta$ , BMP-2, PDGF-bb, IGF-I, FGF, VEGF and PTHrP have been largely studied during bone development, healing [87, 88] and physiological remodeling. Most of these factors are pro-osteogenic. However, degrees of diversity in their effects are also known. As with cytokines and related proteins, growth factors act mainly by binding to specific or non-specific cell surface receptors thereby stimulating the proliferation and/or differentiation of the target cells. Furthermore, some of these factors elicit strong chemotactic effects for osteogenic as well as inflammatory cells.

### *TGF- $\beta$ 1*

Transforming growth factor-beta1 is a member of large family of secreted proteins including at least 3 members TGF- $\beta$ 1, 2 and 3 and also bone morphogenetic proteins, activins, inhibins, and growth and differentiation factors [89]. During early fracture healing it is widely thought that the degranulated platelets are the primary source for TGF- $\beta$ 1. However, it known that TGF- $\beta$ 1 is produced by several cell types, including osteoblasts [90] and fibroblasts [91]. Most leukocytes express TGFs and their expression serve in both autocrine and paracrine modes to control the differentiation, proliferation, and state of activation of these immune cells [92, 93]. TGF- $\beta$ 1 influences a wide range of cellular events by activating specific receptors on target cells, which generally consist of type I and II serine/threonine kinase subunits [94]. Binding of TGF- $\beta$ 1 leads to activation of Smad signaling pathway with major effects on osteogenic differentiation. In addition to the classical Smad pathway, TGF- $\beta$ 1 also activates other signaling cascades through its ability to phosphorylate TGF-activated kinase-1 (TAK1), which in turn activates the MAPK system [95, 96]. This wide range of activity explains in part the diversity of effects of TGF- $\beta$ 1 on cellular activations. TGF- $\beta$ 1 has been also implicated in committing monocytes to the osteoclast lineage in the presence of RANKL or TNF- $\alpha$ . However, it was also suggested that TGF- $\beta$ 1 may inhibit osteoclastic activation and promote osteoclast apoptosis [97]. Large scale gene expression analysis during intramembranous ossification in rat femoral ablation model showed suppression of TGF- $\beta$ 1 expression at d 1 and stimulation at d 5 – 14, with a distinct peak at d 7 [43]. In rat tibial drill-hole defect, TGF- $\beta$ 1 together with TNF- $\alpha$  peaked on d 1 [98]. Comparable results were observed in transverse, diaphyseal fractures of mice tibia where TGF- $\beta$ 1, which was expressed at very high levels in unfractured bones, showed a sharp rise 1 d after fracture, but then returned to the baseline level seen in unfractured bone [99].

### *PDGF*

Platelet derived growth factor is one of the numerous growth factors that regulate cell growth and division with significant role in formation of blood vessels (angiogenesis) [100]. It exist as a homo- or heterodimeric polypeptide consisting of A and B chains and exerts its effects by binding to, and activating, specific high-affinity cell surface receptors that have tyrosine kinase activity [101]. It is synthesized by platelets, monocytes,

macrophages, endothelial cells and osteoblasts. PDGF-BB is a potent mitogen for mesenchymal cells and also strongly induces their proliferation and migration [102, 103]. It is assumed to recruit MSCs to lesion sites to accelerate the repair process [104], although its effects on MSCs are largely contradictory. Interestingly, mutant mice depleted for PDGF receptor, PDGFR $\beta$ , significantly increased the ratio of woven bone to callus after 7 d in tibial fracture [103]. The results were supported by the accompanying in vitro data where the depletion of PDGFR $\beta$  in MSCs enhanced osteogenic differentiation as indicated by increased expression levels of ALP, OC, BMP-2, Runx2, and osterix. However, depletion of these receptors decreased the mitogenic and migratory responses of the MSCs. Gene expression of PDGF-B was upregulated on d 3 after drill-hole injury in proximal tibia [98].

### *BMP-2*

Bone morphogenetic proteins are growth factors that belong to the TGF- $\beta$  superfamily of proteins. There are more than 25 bone morphogenetic proteins (BMPs) divided into at least four separate subgroups depending on their primary amino acid sequence. Group one consists of BMP-2 and BMP-4, and group two includes BMP-5, -6, and -7. The main difference from other TGF- $\beta$  members is the ability of BMPs to induce bone formation in non-skeletal tissue sites (e.g. muscular or subcutaneous) [105]. As for TGF- $\beta$ , BMP ligand signal is mediated by type 1 and 2 serine/threonine receptor kinases which activate receptor substrates, the Smad proteins that move into the nucleus. Once activated, receptor kinases phosphorylate R-Smads (regulatory Smads), and the phosphorylated R-Smads then complex with C-Smads (common-mediator Smads). The complexes, which act as transcriptional regulators, then translocate into the nucleus [24]. BMP-2, -6, -7 and -9 may be the most potent to induce osteoblast lineage-specific differentiation of MSCs [106]. BMP-2 and BMP-7 induce the critical transcription factors Runx2 and Osterix in mesenchymal stem cells and promote osteoblast differentiation [107, 108]. The extracellular matrix comprises a main source of BMPs and further they are produced by osteoprogenitors, mesenchymal cells, osteoblasts, and chondrocytes. BMPs induce ordered cascades of events for osteogenesis, including chemotaxis, mesenchymal and osteoprogenitor cell proliferation and differentiation, angiogenesis, and controlled synthesis of extracellular matrix [50]. Recent investigations revealed that hematopoietic cells secrete and express BMP-2 and BMP-6 [109] and BMP receptor (BMPRII) [20], mediating important interactions between hematopoietic and mesenchymal osteoblastic lining cells. During healing of bone injury, BMP-2 expression increased along the days 1 – 21 of bone healing where it was one of the earliest genes to be induced with second elevation during osteogenesis [99, 110]. In intramembranous healing of rat femoral ablation, BMP-2 showed sharp increase from d 1 to d 3 and continuously increased with peak at d 7 and a second peak, slightly lower, at d 10 [43]. In rat ulnar stress fracture, the peak of BMP-2 was attained already after 1 d and maintained until d 4 [111]. Different model with transverse diaphyseal tibia fracture in mice revealed that the maximum peak of BMP-2 was on d 1, suggesting its role as an early response gene in the cascade of healing events [99]. In contrast, BMP-3, BMP-4 and BMP-7 showed a restricted period of expression from d 14 through d 21 corresponding to the period of cartilage replacement with bone [99].

## Transcriptional regulators

During the different phases of fracture healing, binding of cytokines, chemokines and growth factors to their respective receptors leads to the induction of intracellular transduction systems. The signal transduction via phosphorylation-dephosphorylation mechanisms results in activation of target transcription factors which enter the nucleus and binds to specific region of DNA resulting in up- or down-regulation of gene expression determining the activity of the target cell. Throughout the different phases of healing, several transcriptional factors are activated depending on the cells present, the receptor expressed and the availability of specific ligands. Inflammatory events are regulated by several transcription factors with major contribution of NF- $\kappa$ B as well as other transcription factors including AP-1 and STATs (signal-transducer and activator of transcription proteins). Similarly, osteogenic commitment, differentiation and functions are governed by several transcription factors. Major transcription factor in osteogenic differentiation is the Runx2 [37]. However, given the multiple stages of osteogenic differentiation, other transcriptional factors are also involved, including members of AP and Dlx families, Smads, CCAAT/enhancer binding protein beta (C/EBP $\beta$ ) and delta (C/EBP $\delta$ ), members of Wnt signaling pathways, activating transcription factor 4, and peroxisome proliferator-activated receptor-gamma (PPAR- $\gamma$ ). Transcriptional regulations during healing events are highly-controlled, complex processes owing to the multiplicity of many cells types with different levels of differentiation and the several cross-talks between the different factors. In rat femoral fracture, microarray analysis revealed that at least 18 molecular pathways were potentially involved and 11 of these were active at more than one cellular event [112].

### *Runx2*

Runx2 is a transcription factor that belongs to the Runx family. Runx2 is an osteoblast-specific transcription factor necessary for the differentiation of pluripotent mesenchymal cells to osteoblasts. The transcriptional control of Runx2 is required for commitment of progenitor cells to the osteoblast lineage and to exclude options for divergence towards other lineages [113]. It has been clearly demonstrated that Runx2 is essential for in vivo bone formation. Runx2 null mice exhibited complete absence of intramembranous and intracartilaginous bone formation despite the normal cartilaginous skeletal patterning [114]. The binding elements of Runx2 are present in the promoter region of collagen I, OPN, BSP and OC genes. Activation of Runx2, for example by MAPK via stimulation of integrin  $\alpha$ 2 $\beta$ 1 [115], results in translocation of Runx2 into the nucleus where it triggers the expression of the responsive genes during the early stage of osteoblast differentiation. The subnuclear activity of Runx2 is regulated by several factors resulting in either enhancing or inhibiting effects. Major co-activator is the core binding factor-beta (Cbfb) since the activity of Runx2 is largely dependent on dimerization with this factor [116]. Several other transcriptional factors interact with Runx2 with major enhancing effects. On the other hand, factors like Dlx3, PPAR- $\gamma$ , Stat1 and inhibitory Smads (Smad 3 and 4) have mainly inhibitory effects of Runx2 activity. The inhibition of Runx2 in mature osteoblasts does not reduce the expression of collagen I and OC in mice [117]. Thus, Runx2 is suggested to direct pluripotent mesenchymal cells to the osteoblast lineage, triggers the expression of major bone matrix protein genes during early osteoblast differentiation but does not play a major role in the maintenance of the expression of

collagen I or OC in mature osteoblasts [117]. Runx2 has also been shown to negatively control osteoblast proliferation by acting on pathways associated with cell cycle [118]. Furthermore, Runx2 may indirectly affect osteoclast differentiation by modulation of RANKL gene expression by the osteoblasts [119]. The expression pattern of Runx2 showed large variation between different fracture models. For example, in rat femoral ablation, with mainly intramembranous ossification, the expression of Runx2 increased steadily from d 1 to peak at d 7, with first peak at d 3 and relatively high levels at d 1 [43]. In ulnar stress induced fracture in rat, the expression of Runx2 showed a peak after 4 d [111]. Drill-hole defect in rat femoral diaphysis showed sharp decline of Runx2 expression from d 0 (non-injured) to d 3 followed by maximum peak at d 5 and decline thereafter [120].

### *PPAR- $\gamma$*

Peroxisome proliferator-activated receptor-gamma is a member of the nuclear receptor super family and was originally shown to be the master transcription factor for adipogenic differentiation of mesenchymal stem cells [121]. However, it has also been shown to play roles in the control of proliferation, differentiation and survival of various cell types [121]. PPAR- $\gamma$  is ligand-dependent transcription factor, which associate with retinoic acid receptor, binds to specific response element termed peroxisome proliferator-response element (PPRE), and regulates the expression of target genes [122]. During mesenchymal stem cell differentiation, activation of PPAR- $\gamma$  inhibited Runx2 expression in mouse osteoblastic MC3T3-E1 and rat osteogenic sarcoma cell lines, and hence hindered the expression of OC [123]. On the other hand, in vitro data using human marrow mesenchymal progenitors showed the coexistence of osteogenic transcription factor, Runx2, and PPAR- $\gamma$  at higher levels in ALP-positive cells compared the ALP-negative population, and upon osteogenic stimulation, the increased expression of OC was accompanied by increased expression of PPAR- $\gamma$  [124]. It was also shown that activation of PPAR- $\gamma$  pathway inhibits osteoclast differentiation [125]. Furthermore, using transgenic mice, that lack PPAR- $\gamma$  in osteoclasts, it was suggested that PPAR- $\gamma$  functions as a direct regulator of c-fos expression, an essential mediator of osteoclastogenesis, and thereby promote osteoclastogenesis [126]. In addition, evidence is available describing roles of PPAR- $\gamma$  on regulation of monocyte/macrophage gene expression and activities [122, 127].

### **Osteogenic differentiation, bone formation and remodeling**

During their differentiation along the osteogenic lineage, osteogenic cells start to express and release components specific with the developmental stage of the osteoblastic cells and the ongoing activity during healing cascades. Likewise, and owing to the availability of cytokines and factors required for their differentiation, osteoclasts develop and switch on specific mediators responsible for the resorptive activity. The gene expression of these markers has been shown to be largely correlated with the prospective phase whether bone formation or resorption. Nevertheless, many of these genes are active at more than one cellular event, indicating the complex and interdependent nature of the bone repair processes.



### *ALP and OC*

ALP is a hydrolase enzyme responsible for removing phosphate groups from many types of molecules. Several possible roles for ALP in bone formation have been proposed. It may increase local concentrations of inorganic phosphate, destroy local inhibitors of mineral crystal growth, transport phosphate, or act as calcium-binder.

OC was first discovered as a calcium binding protein in bone. It is characterized by three residues of K-dependent  $\gamma$ -carboxyglutamic acid (Gla), and has a very narrow expression pattern being expressed only by the osteoblasts and osteocytes in bone. Whereas ALP represents an early marker during osteogenic differentiations for MSCs in vitro, and bone formation in vivo, OC is considered as a late differentiation marker of osteogenesis and bone formation. In the locations of intramembranous ossification during healing of femur diaphysis fracture, the expression of ALP peaked at d 5 and then declined, while OC levels were very low during the first 7 d [39]. Comparable results were observed during healing of marrow ablation injury where the peak of ALP was attained at d 5, however, OC expression showed a high peak of expression at d 7 in this model [43].

### *TRAP and CATK*

Tartrate-resistant acid phosphatases (TRAPs) are a class of metalloenzymes that catalyze the hydrolysis of various phosphate esters under acidic conditions. TRAP is a characteristic constituent of osteoclasts and some mononuclear preosteoclasts and, therefore, used as a biochemical and immunohistochemical marker for osteoclasts and bone resorption [128]. In bone, TRAP is found not only in osteoclasts but also in mononuclear cells presumed to represent osteoclast precursor cells [129]. Nevertheless, histological, immunohistochemical and biochemical studies have shown that osteoblasts and osteocytes also express TRAP, albeit the expression level is much lower than that in osteoclasts [130].

Several cathepsins including CATK have been localized in vacuoles at the ruffled border membrane of osteoclasts [131]. CATK is a member of the cysteine protease family that, unlike other cathepsins, has the unique ability to cleave both helical and telopeptide regions of collagen I, the major type of collagen in bone [132]. CATK has the ability to catabolize collagen, allowing it to break down bone and cartilage, and it is required for osteoclastic resorption. Cathepsin K null mouse manifested osteopetrosis and osteoclasts isolated from CATK null mice showed severely impaired function in vitro [133]. In situ hybridization studies in mandibular distraction osteogenesis and transverse tibial fracture showed that the expression signals for CATK and for TRAP and CATK, respectively, were restricted to osteoclasts [134, 135]. The expression of TRAP and CATK in the transverse fracture showed first significant increase after 7 d, peak of expression after 14 d and decreased at d 28 [134]. Comparable results were observed in femoral ablation model for CATK where first peak of expression was attained at d 7 and continued at high levels at d 10 and 14 [43].

***Effect of titanium surfaces on cellular and molecular activities***

Unlike fracture healing, cellular and molecular activities regulating the in vivo bone formation for osseointegration are largely unknown. Even though bone healing around titanium implants is regarded to simulate fracture healing with the hallmark cascade of hemostasis, inflammation, regeneration and remodelling, the presence of foreign, yet biocompatible but not inert, titanium implant may influence these phases [5]. A simple and obvious support of this statement is that while fracture healing will finalize in reproduction of the original bone shape and its associated tissues, healing around titanium implant will end, preferentially, in a distinctive continuous layer of mature bone in intimate contact with the implant surface. Besides, it is generally observed that the process of bone formation at the interface is not preceded or accompanied by obvious chondrogenic activity [136], which represents a prominent phase during fracture healing. In the same context, histological and biomechanical data indicate that bone respond differently when interfacing to different titanium implant surfaces [137, 138]. Different surface alteration techniques such anodization, blasting, etching, surface coating, and combinations of some of these techniques are increasingly used, and claimed to induce prompt tissue healing and stronger bone formation than the original machined implant surface. While these asserts have largely been addressed morphologically and biomechanically, the potentially different in vivo cellular and molecular responses to such surfaces have not been established.

Inflammation during early osseointegration is obscure and has not received similar attention as that given during soft tissue integration [139]. Histological studies in bone revealed that macrophages and multinucleated cells from monocytic lineage are present at the interface with machined titanium [3, 4] and hydroxyapatite coated [140, 141] implants during early phases after implantation. The exact role of these cells during implant integration in bone is not known. Further, the relationship between their gradual disappearance in parallel with the bone apposition at the implant surface is largely unexplored [3-5]. These cells are known to express a wide range of proinflammatory and anti-inflammatory cytokines, growth and differentiation factors and chemotactic mediators which would be expected to influence the ultimate bone response. For instance, titanium discs with various degrees of roughness, from smoothly polished to coarsely rough, were placed in contact with the periosteum of rat parietal bone. On the first week, rough, but not the polished, surfaces formed an interface dominated by ED1-positive recruited macrophages [142]. These implants were associated with higher mineralization and bone nodule formation over the following weeks [142]. In agreement, J774A.1 murine macrophage cell plated on polished, machined, and blasted surfaces in vitro showed faster and higher expression of BMP-2 on the machined and blasted surfaces [143]. In soft tissue healing around titanium discs, higher release of TNF- $\alpha$  was observed in response to porous titanium with and without plasma protein layer compared to machined titanium after 3 h [144], as well as for machined titanium compared to copper after 12 h [145]. The soft tissue data presents strong evidence on the modulation of inflammatory cell responses by titanium surface roughness and composition, respectively. From these examples, it is suggested that material surface properties influence the activity of inflammatory cells which in turn may modify the elaboration of

extracellular matrix. Nevertheless, in order to verify such possible effects in bone, quantitative data on the recruitment and adhesion of inflammatory cells, solely or in parallel with matrix forming cells, to the implant surface and surrounding matrix are essentially required.

The mechanisms of cellular recruitment and adhesion to titanium implants *in vivo* are hitherto unknown. Available *in vitro* data has focused on the adhesion of cells to titanium surfaces rather than how different cells would be recruited to the surfaces, and whether or not the implant surface will influence the magnitude of the chemotactic signals. So far, most of the available literature on the chemotactic signals at biomaterials is based on the cellular response to particulates and debris. In one *in vitro* study, murine macrophage-like RAW 264.7 cell line, were cultured on titanium-coated epoxy resin replicas of polished, coarsely blasted, acid etched and blasted/acid etched titanium surfaces. The results showed roughness-, time- and stimulation- dependant expression of MCP-1 with highest expression at blasted/acid etched after LPS stimulation [146].

The extensive *in vitro* data on cell-on-substrate response have demonstrated that cellular adhesion, morphology, differentiation and/or the abilities to synthesize or release organic or inorganic components are largely dependant on the physico-chemical properties of the titanium surfaces [147]. For instance, early studies on osteoblastic cell adhesion to polystyrene and titanium and cobalt chromium alloys, with or without protein coatings, showed specific pattern of integrin expression for each material and this was largely dependent on the type of protein coating whether fibronectin, laminin or collagen [148]. Using pure titanium modified with machining, grit blasting or with calcium phosphate coating, Ter Brugge *et al.* showed temporal difference in the expression of different integrins expressed by rat bone marrow cells cultured on these surfaces in osteogenic media [149, 150]. In another study [151], cellular attachment was decreased on calcium phosphate coated titanium after a pre-treatment with either anti-integrin- $\beta$ 1 or anti-integrin- $\beta$ 3 antibodies, whereas on the pure titanium, cell adhesion was only slightly affected after a pre-treatment with anti-integrin- $\beta$ 3 antibodies. While many of these *in vitro* studies show prominent effect of surface physico-chemical properties on cellular adhesion, with the ability of different osteoblastic cell-lines to attach directly to the implant surface, it is unknown if similar scenario will take place in the *in vivo* surrounding and whether or not the cell-to-surface migration and contact will be influenced by the implant surface.

Likewise the inflammation and inflammatory cells, the importance of osteoclasts and the bone remodeling at implants have either been neglected or, considered as processes in the late stage of bone healing at titanium implants. In conjunction with the bone-forming osteoblasts, the long term significance of osteoclasts on the renewal and repair of interfacial bone, by replacing the old and damaged foci while maintaining the structural integrity of the interface, is obvious [152].

On the other hand, the exact role and participation of these sophisticated cells during the early process of osseointegration is yet to be detailed. Such demands for understanding are gained from the *in vivo* morphological studies showing bone remodeling as an

integral early component after implantation irrespective of the implant surface properties [153]. In addition, there are other circumstances which have prompted the current work, examining e.g. the contribution of these cells during the early events after the titanium implantation in bone. The first line is the established mutual cross-talk between osteoblasts and osteoclasts at different stages of differentiation with possibility of such cross-talk at the titanium implant interface. Secondly, osteoclasts have been shown in vitro, to resorb hydroxyapatite, [154, 155] and calcium phosphate [156, 157] substrates. In most cases the resorption was influenced by the roughness of the substrate [155] or the precoating with collagen [154] or extracellular matrix [156]. While there is no evidence that osteoclasts can resorb metallic titanium surface in vivo, however, it does not seem unlikely the possibility that osteoclasts can condition the biologically coated titanium implant or, may be, expose the implant surface parameters to allow other cells for direct contact with the surface.

Table I: A number of in vitro experiments investigating cellular and molecular activities on substrates with different surface properties.

Implant/surface	Cells and time	Factors	Main findings	Ref.
Titanium <ul style="list-style-type: none"> <li>Polished</li> <li>Grit blasted</li> </ul>	Mouse macrophage cell line J774A.1  24, 48 and 72h	IL-1 $\beta$ , IL-6  Gene expression analysis	<b>Unstim.</b> <b>IL-1<math>\beta</math></b> : increased on rough>smooth at 24 and 48h. <b>IL-6</b> : Significantly increased from 24 to 48h for both surfaces, smooth>rough at 72h. <b>LPS stim.</b> <b>IL-1<math>\beta</math></b> : Significantly increased for both surfaces at 24h. Significantly lower at 48 and 72h for both surfaces. Inhibition of NF-kB resulted in significant decrease of IL-1 $\beta$ on rough and smooth surfaces.	[158]
Titanium-coated epoxy-resin replicas of the following surfaces <ul style="list-style-type: none"> <li>Polished (PO)</li> <li>Blasted (CB)</li> <li>Acid etched (AE)</li> <li>Blasted/acid etched (HCl/H<sub>2</sub>SO<sub>4</sub>) (B/AE)</li> </ul> Tissue culture polystyrene (TCP)	Murine macrophage-like cells RAW 264.7  6, 24, and 48h	TNF- $\alpha$ , IL-1 $\beta$ , IL-6, MCP-1  Cytokine secretion (ELISA)	<b>Unstim.</b> <b>TNF-<math>\alpha</math></b> : increased on AE>other surfaces at 6 and 48 h. Increased on AE and B/AE>other surfaces at 24h. <b>IL-1<math>\beta</math></b> and <b>IL-6</b> : Undetectable. <b>MCP-1</b> : lower on B/AE < other surfaces at 6, 24 and 48h. <b>LPS stim.</b> <b>TNF-<math>\alpha</math></b> : increased on B/AE >all surfaces>TCP. <b>IL-1<math>\beta</math></b> : TCP>all surfaces; PO>B/AE at 6h. B/AE >PO and AE at 24h. <b>IL-6</b> : B/AE>TCP at 6h. B/AE >TCP, PO and AE at 24h. B/AE and AE>all surfaces at 48h. <b>MCP-1</b> : Increased significantly at all time points on B/AE surface compared with unstim B/AE. B/AE>PO, AE and TCP at 24h. B/AE and AE >all surfaces at 48h. Surface topography influenced the release of cytokines from unstim. and stim. macrophages. Roughness and LPS show synergistic effect on cytokines and chemokines secretion, particularly in B/AE.	[146]
Titanium <ul style="list-style-type: none"> <li>Blasted</li> <li>Grooved</li> </ul> Tissue culture polystyrene (TCP)	Human embryonic palatal mesenchymal cells  3 weeks	Runx2, OC  Gene expression analysis	<b>With <math>\beta</math>-glycerophosphate and ascorbate treatment:</b> Runx2 increased significantly (2-fold) on both grooved and rough surfaces compared to TCP. OC increased significantly (5-fold) on grooved and (2.5-fold) rough surface as compared to TCP. <b>Without treatment:</b> No differences.	[159]

<p>Titanium</p> <ul style="list-style-type: none"> <li>• Blasted, (RBM)</li> <li>• P-incorporated (P)</li> <li>• P/Sr incorporated (SrP)</li> </ul>	<p>MC3T3-E1</p> <p>7 and 14d</p>	<p>Runx2 ALP OPN BSP OC</p> <p>Gene expression analysis</p>	<p><b>Runx2:</b> Slightly increased on SrP at 7d. At 14d, Runx2 decreased on RBM compared with 7d, but increased on P and SrP compared with 7d. Higher on P and SrP than on RBM (3.8-fold) at 14d.</p> <p><b>ALP:</b> increased with incubation time on all groups. ALP was higher on RBM than P (2.9-fold) and SrP (2.2-fold) at 7d. This pattern was reversed at 14d where ALP on P and SrP was higher than on RBM (2.4- to 3.4-fold).</p> <p><b>OPN:</b> higher on P and SrP than on RBM (8- to 11.2-fold) at 7d. At 14d: OPN on P and SrP decreased or maintained a level similar to 7d, but increased on RBM.</p> <p><b>BSP:</b> in all groups, levels at 14d were greater than at 7d. BSP levels were similar between groups at 7d. At 14d, higher on P and SrP than on RBM (3.1- to 4.1-fold).</p> <p><b>OC:</b> no differences between groups at 7d. OC on P and SrP was higher than on RBM (1.4-fold) at 14d.</p>	<p>[160]</p>
<p>Titanium</p> <ul style="list-style-type: none"> <li>• Smooth (S)</li> <li>• Blasted (GB)</li> <li>• Blasted/acid-etched H<sub>2</sub>SO<sub>4</sub>/H<sub>2</sub>O<sub>2</sub> (Nano)</li> </ul>	<p>hMSCs</p> <p>3, 7, 14, and 28d</p>	<p>Runx2 Osterix (OSX) ALP OPN BSP OC</p> <p>Gene expression analysis</p>	<p><b>Runx2:</b> was 3.5-fold higher on Nano at 14 and 28d. For GB, varied to 2.5-fold over same period. On S increased to 2-fold at 14d.</p> <p><b>OSX:</b> was 2.5-, 3.5-, and 4- fold higher at 7, 14 and 28d on Nano. For the S, OSX was 2.5-fold on 7d and then decreased to baseline. OSX on GB reached 4-fold at 7d, but subsequently dropped to baseline levels.</p> <p><b>ALP:</b> was 12-fold and 38-fold higher on Nano compared to S (6-fold) and (13-fold) and GB (5-fold) and (19-fold) at 14d and 28d, respectively.</p> <p><b>OPN:</b> constant for (S) throughout the 28d. At 28d, OPN on GB and Nano &gt; 50-fold.</p> <p><b>OC:</b> modestly increased (3-fold) on S and Nano at 14d and kept the same rate at 28d for Nano. OC on S dropped close to the baseline level at 28d. For GB, OC reached 2-fold at 7d and kept constant thereafter.</p>	<p>[161]</p>
<p>Titanium</p> <ul style="list-style-type: none"> <li>• Acid etched (HCl/H<sub>2</sub>SO<sub>4</sub>) (AE)</li> <li>• Blasted/etched (B/AE)</li> <li>• Plasma-sprayed (TPS)</li> <li>• Pretreated Hydrofluoric/nitric acid (PT)</li> </ul> <p>TCP</p>	<p>MG63 osteoblast-like cells</p> <p>7d</p>	<p>ALP</p> <p>(Enzyme specific activity)</p>	<p><b>ALP</b> activity was significantly higher on B/AE and TPS compared to TCP. Further enhanced with 1<math>\alpha</math>,25(OH)2D3.</p> <p>Inhibition of MAP kinase inhibited ALP activity on TCP, PT, and B/AE surfaces. On TPS, there was only a partial inhibitory effect of MAP kinase inhibitor (PD98059). The effects of surface roughness and 1<math>\alpha</math>,25(OH)2D3 on ALP activity were mediated through (MAPK) pathway.</p>	<p>[162]</p>

<p>Titanium</p> <ul style="list-style-type: none"> <li>• Pretreated (PT)</li> <li>• Blasted/acid etched (B/AE) (HCl/H<sub>2</sub>SO<sub>4</sub>)</li> <li>• Blasted/acid etched and protected (mod.B/AE)</li> </ul> <p>Tissue culture polystyrene (TCP)</p>	<p>MSCs</p> <p>7d</p>	<p>Runx2 OC DKK1 DKK2 Intg-<math>\alpha</math>2 Intg-<math>\beta</math>1</p> <p>OC secretion (ELISA)</p>	<p><b>RUNX2:</b> increased on titanium and higher on mod.B/AE compared to TCP.  <b>OC:</b> significantly upregulated on mod.B/AE surfaces.  <b>Intg-<math>\alpha</math>2:</b> slightly increased on mod.B/AE, but the expression on mod.B/AE was significantly increased when compared to TCP and PT.  <b>Intg-<math>\beta</math>1:</b> expression increased 30% on mod.B/AE compared to other surfaces.  <b>DKK1:</b> was slightly lower on mod.B/AE surfaces and significantly down regulated on B/AE than on TCP and PT.  <b>DKK2:</b> was 200% higher on B/AE and mod.B/AE than on TCP or PT.  When MSCs cocultured with MG63, OC secretion was significantly higher in cells adherent to B/AE and mod.B/AE.  Knockdown of integrin-<math>\alpha</math>2 and silencing Dickkopf-2 resulted in reduced osteogenic differentiation of the MSCs.</p>	<p>[163]</p>
<p>Titanium</p> <ul style="list-style-type: none"> <li>• Machined (Ti-m)</li> <li>• Oxidized (Ti-ox)</li> </ul> <p>Zirconia with different surface roughnesses and crystallinity</p> <p>Tissue culture polystyrene (TCP)</p>	<p>Human fetal-osteoblast cell line, hFOB 1.19</p> <p>From 3 up to 28d</p>	<p>Including: Runx2 and 3, ALP, Collagen1A1, Collagen2A1, OPN, BSP, OC, TGF-<math>\beta</math>1, Intg-<math>\beta</math>1, Intg-<math>\beta</math>3, PCNA (gene marker for proliferation)</p>	<p>Compared to TCP, rough surfaces showed roughness-specific modulation. Independent of the material (titanium, zirconia), higher Runx2, Runx3 and BMP-7 were observed for Ti-ox, rough polycrystal zirconia at 3d. PCNA did not seem to be affected. After the cells started to differentiate at d7, roughness led to a specific and significant up-regulation of Intg-<math>\beta</math>3 at 21d. During the differentiation at the onset of ECM mineralization, specific reaction to titanium started: On titanium, higher BSP and Intg-<math>\beta</math>1 at 21d, independent of roughness. OC was affected similarly, increased, however, only on Ti-ox.  <b>Differences in gene regulation assigned to three different phases</b>  <b>Proliferation:</b> Regulatory genes RUNX2, RUNX3 and BMP-7 showed up-regulation on all rough surfaces at 3d.  <b>ECM maturation:</b> higher BSP and Intg-<math>\beta</math>1 at 21d on Ti independent of roughness. TGF-<math>\beta</math>1, collagen1A1, collagen2A1, ALP, and OPN were not affected.  <b>ECM mineralization:</b> biglycan and decorin are switched on at 28d.</p>	<p>[164]</p>
<p>Titanium plates finished by:</p> <ul style="list-style-type: none"> <li>• 2000 grit</li> <li>• 1200 grit</li> <li>• 600 grit</li> <li>• 180 grit</li> </ul> <p>Tissue culture polystyrene (TCP)</p>	<p>RAW264 mouse/macrophage cell line</p> <p>In presence or absence of RANKL</p> <p>Up to 5d</p>	<p>TRAP CATK RANK TRAF6</p> <p>Enzyme activity of TRAP</p>	<p>In presence of RANKL, expression of TRAP and CATK was observed after 3d on titanium as well as on TCP. TRAP and RANK was higher on TCP compared to titanium. Higher TRAP expression in association with the increased roughness. Highest CATK was on the medium roughness samples. In presence or RANKL, multinucleated giant cells appeared at 5d. RANK and TRAF6 were expressed even in absence of RANKL.</p>	<p>[165]</p>

***Biomechanical stability during development of osseointegration***

A titanium implant is functionally and structurally defined to be osseointegrated when there is no progressive relative movement between the implant and the surrounding bone with which it has a direct contact [166]. The biomechanical stability of the machined screw-shaped titanium implant has been studied in detail during the healing period in different species [167]. The results of these studies in rats revealed unchanged torque values during the first four weeks but with significant increases after 8 and 16 weeks.

Biomechanical studies on implants with modified surfaces have largely focused on comparisons with controls or other surfaces, at specific time periods, rather than evaluating the development of torque strength for the same implant over different healing periods. Furthermore, large variations in torque results between the different surfaces have been observed with possible major influences by the different animal models, torque instruments and implant designs used.

Frequently, increased torque values have been revealed for many surface modifications [168-173]. For instance, comparisons were performed in distal femur of rabbit between three screw-shaped titanium implants with machined (MA), dual acid etched (H<sub>2</sub>SO<sub>4</sub>/HCl) (DAE) and titanium plasma sprayed (TPS) implants [170]. In that study, while the torque was relatively constant after 1, 2 and 3 months periods at the machined implants, it increased from 1 month to 2 months and kept similar levels after 3 months for the dual etched implants, and progressively increased during the three evaluation periods for the plasma sprayed implants. The increased torque values were: TPS>DAE>MA at every evaluation period.

Machined implants in previous studies [174] revealed positive correlation with healing time and bone formation parameters over the whole evaluation period. Furthermore, not only the implant surface properties appeared to influence the rate of biomechanical stability but also the bone type in which the implant is inserted [175]. In the latter study, Sennerby et al. evaluated the removal torque of machined implants in cortical tibial bone and trabecular intraarticular bone over periods of 6 weeks, 3 months and 6 months. The results showed that whereas higher and constant torques values were registered for the machined implants in the cortical sites, torque was lower at 6 weeks in the trabecular bone and increased over time to reach similar values as the machined implant in cortical bone after 6 month period.

From the available scientific data, whereas a relationship between biomechanical strength and the bone formation parameters and bone types has been demonstrated, the relationship between the biomechanical strength and the molecular activities during early stages of inflammation, regeneration and remodeling has yet to be determined.



### ***In vivo cellular and molecular techniques in relation to bone-implant interface***

Different approaches have been used to investigate the host response to titanium surfaces. The *in vitro* model has been applied extensively to determine the biological responses of single cell type, cultured on titanium surface. However, this model remains to a large extent limited prediction of the *in vivo* events. Such limitation has been largely addressed when biomaterials were investigated in soft tissue of animal models where the latter provided excellent information by taking the advantage that all potentially affected cells, blood and tissue components and biological molecules are present in contact with the surface. The kinetics of inflammatory cell responses, recruitment of different cell types and their molecular activities has been widely analyzed in soft tissue. However, the access to the bone/implant interface is a major challenge in order to apply the molecular tools.

### **Immunohistochemistry and protein targeting procedures**

Immunohistochemical analysis relies on the combination of histological, antibody-labeling and microscopic imaging procedures to identify different cell types and proteins. Different sets of mono- and poly-clonal antibodies can be used to reorganize and bind to specific epitopes in the plasma membrane and secreted proteins. At the implant interface, it can be used to study the distribution and localization of specific cell phenotypes, biomarkers and differentially expressed proteins. Visualization of the epitope-antibody binding can be performed using an antibody conjugated to an enzyme that can catalyze a colour-producing reaction. Difficulties of obtaining intact metallic titanium-bone interface sections, the semi-quantitative nature, destruction of the cell epitopes by fixation and decalcification steps and the limitation for using multiple antibodies on one section make the main drawbacks of immunohistochemistry in studying the temporal molecular processes at the implant-bone interface. Yet, immunohistochemical studies have been widely used with non-metallic implants in bone and with studies on titanium implant-bone interface, after implant removal using different approaches [176, 177].

### **RNA targeting procedures**

Translation or synthesis of any protein or glycoprotein, including all cytokines, chemokines, adhesion molecules, growth factors, enzymes and matrix components, is dependent on the presence of corresponding messenger RNA (mRNA) molecules in the cell. The expressions of different mRNA represent the dynamic activity of the cell as in most cases detection of specific mRNA molecules correspond to the proteins which is being actively synthesized.

### ***Northern analysis***

Northern blotting is the technique in which mRNA fragments harvested from cells are separated by electrophoresis and immobilized in agarose gel. Membrane-bound DNA, labeled with radioactive nucleotides is used as probe for the target gene of interest. When the probe find complimentary mRNA it anneal strongly to that area and upon exposure to x-ray it allow for detection and localization of the target mRNA. In relation to cellular

response to titanium this technique has mainly used in cell culture experiments in vitro. The low resolution of the gel and the limited sensitivity to low amount of mRNA constitute the main disadvantages for applying it to study the in vivo bone response to titanium implants. Northern blotting has e.g. been used to study the relative expression of osteoblastic genes in bone callus during fracture healing [39].

### *In situ hybridization*

In this technique, the expressed mRNA molecules are localized by applying labeled complementary DNA or RNA probes in place (i.e. in the tissue where they are expressed). The technique involves fixation of the target transcripts followed by hybridization to the target sequences at elevated temperature. The excess probes are then washed away and the antigen- or fluorescent-labeled probes are visualized and quantified in the section using enzyme-conjugated antibodies (immunohistochemistry) or fluorescence microscopy, respectively. This technique can be used to detect two or more transcripts on the same section. The main advantage of this technique, giving the ability to get intact bone-implant interface, is the possibility to determine the spatial distribution of the expressed gene marker in relation to the implant surface. Furthermore, it can be combined with immunohistochemical studies on separate sections to determine the cell specificity for the expressed genes. In situ hybridization has e.g. been used to study osteoblastic gene expression at non-metallic biomaterials in bone [178, 179]. It has also been used to study the sequential expression of osteoblastic genes in bone tissue collected from assembled titanium chambers retrieved from sheep tibia at different time periods [180].

### *Polymerase chain reaction*

The technology of PCR relies on the amplification of single or few double stranded DNA molecule/s to several thousand copies identical to the original starting template. The technique takes the advantage of the heat-stable enzyme, DNA polymerase, which assembles a new DNA strand using the single-stranded DNA as a template in the presence of DNA primers (the probe) and the building blocks, dNTPs (deoxynucleoside triphosphates). The reaction is performed by temperature cycling in special reaction tubes. The DNA double strand, which contains the sequence of interest, is first heated to a high temperature (around 95 °C) in order to separate the strands of the double helical DNA (denaturation temperature). The temperature is then lowered to about 65 °C (annealing temperature) which allow for the primers to anneal to the target sequences on the separated DNA strands. After that, the temperature is set around 72 °C (extension temperature) which is optimum for the polymerase that extends the primers by incorporating the dNTPs. By repeating these temperature cycles, the original single or few templates will be amplified in an exponential manner resulting in thousands of copies amenable for identification and quantification.

PCR is a common and often essential technique used in medical and biological research laboratories for a variety of applications. These include, but not limited to, DNA cloning for sequencing, DNA-based functional analysis of genes, and the diagnosis of infectious and hereditary diseases and cancers. In biomedical research field there is more interest to target the mRNA expression denoting for the biological events during tissue healing at

the implanted biomaterials. Therefore, modifications of the original PCR technique are quite often used in this field of research.

### *Reverse transcription-polymerase chain reaction (RT-PCR)*

In this technique, the mRNA molecules, isolated from individual cells or living tissue, are first transcribed into complimentary DNA (cDNA) using the enzyme, reverse transcriptase. The resultant cDNA template is amplified using the heat-stable DNA polymerase in a typical PCR procedure as described above. The resultant PCR product can be subsequently analyzed by size separation on agarose gel and visualization by ethidium bromide staining. The product identity, based on the starting mRNA transcripts in the sample, can be then confirmed using a Southern blotting technique, which is the DNA equivalent of the Northern analysis. This end-point RT-PCR can be used to measure changes in expression levels in different ways such as the relative and comparative methods. The relative quantification compares transcript abundance across multiple samples, using a co-amplified internal control for sample normalization. Results are expressed as ratios of the gene-specific signal to the internal control signal. Albeit the advantage of quantifying mRNA levels from much smaller samples, this method of analysis is at best semi-quantitative and it needs to ensure that the PCR is terminated when the genes of interest and the internal control are in the exponential phase of amplification. Furthermore, the low sensitivity and resolution of the agarose gel make it less valuable when compared with the new detection technologies used with the quantitative real-time PCR.

### **Quantitative polymerase chain reaction (qPCR)**

The major difference of the quantitative real time PCR from the conventional reverse transcription PCR is that the former incorporate fluorescent reporter that binds to the product formed and reports its presence by fluorescence. Reporter binding takes place during the cDNA amplification and upon accumulation the signal develops which increase exponentially until reaching a saturation level. A number of dyes and probes are available covering a range of non-specific fluorescent dyes, which react with all double-stranded DNA, and sequence-specific DNA probes. SYBR Green I fluorescent dye is one of the most commonly used reporters in gene expression analysis. These dyes do not fluorescence when they are free and become brightly fluorescent when they bind to cDNA, and the fluorescence increases with the amount of double stranded product formed. The amount of cDNA products during the exponential phase are determined by plotting fluorescence against cycle number. By setting a common threshold for the different cDNA products (representing the starting mRNAs to be quantified), the cycle at which the fluorescence from a gene crosses the threshold is called the cycle threshold, Ct value for that gene. The differences in the Ct values between the different cDNAs during the analysis reflect the differences in their initial amounts of template molecules. Ct value relates to the number of initial template molecules as:

$$N_{Ct} N_0 = (1 + E)^{Ct}$$

Where  $N_{Ct}$  is the number of double-stranded DNA molecules after  $Ct$  amplification cycles,  $N_0$  is the initial number of double-stranded target molecules, and  $E$  is the PCR

efficiency.  $E$  is assumed to be independent of  $N_0$  over the studied concentration range, and can be estimated from dilution series of mRNA, cDNA or genomic DNA, or from the real-time PCR amplification response curve.

### *Relative gene expression analysis*

Quantification by real-time PCR may be performed as either absolute measurements using an external standard, or as relative measurements, comparing the expression of a reporter gene with that of a presumed constantly expressed reference gene. Quantitative gene expression analysis is most commonly performed as a relative measurement between two genes. The expression ratio is given by an equation which is commonly referred to the delta delta Ct-method and it is a convenient way to analyze the relative changes in gene expression from real-time quantitative PCR experiments.

### *Normalization*

Real-time PCR is the method of choice for expression analysis of a limited number of genes. The measured gene expression variation between subjects is the sum of the true biological variation and several confounding factors resulting in non-specific variation. Comparing samples requires normalization to compensate for differences in the amount of biologic material analyzed. The purpose of normalization is to remove the non-biological (sample to sample and run to run) variations as much as possible. Several normalization strategies have been proposed, but the use of one or more reference genes is currently the preferred way of normalization. For each target gene sample, the relative abundance value obtained is divided by the value derived from the control sequence in the corresponding target gene. The normalized values for different samples can then directly be compared.

A standard gene expression analysis consists of sample collection, RNA isolation, removal of any possible DNA contamination, reverse transcription, real-time PCR and data analysis, respectively. Special attention should be given when designing the primers for the target genes ensuring the specificity, short amplicons production, minimum artifact formation and annealing at the specified PCR temperature. Furthermore, strict adherence to RNase-free procedure is required which include appropriate sample preservation, the use of RNase decontamination agents.

The quantitative PCR represent powerful, efficient, and highly reproducible and reliable methods for molecular analysis. In the present thesis, quantitative PCR together with histological, ultrastructural and biomechanical tools were used to explore the bone-implant interface during the early process of osseointegration.

## **Aims**

The main aim of the current thesis was to further understand the biological mechanisms of osseointegration. Therefore, the following specific aims were formulated:

To develop an in vivo model for molecular analysis of osseointegration by analyzing gene expression both at the immediate interface at implant surface and in the surrounding bone.

To compare gene expression denoting inflammation and bone remodeling between cortical and trabecular bone types both during steady-state condition and at the interface with titanium implants.

To investigate the cellular and molecular activities denoting cell adhesion, chemotaxis and inflammation at different titanium implants during the first day of implantation.

To investigate the cellular and molecular activities denoting inflammation, osteogenic activity and bone remodeling at different titanium implants during osseointegration (1d-28d)

To correlate the interfacial molecular activities with the bone response and biomechanical capacity at different titanium implants.



## Materials and Methods

### ***Implants***

Screw-shaped titanium implants, 2 mm in diameter and 2.3 mm in length were used. In paper I, anodically oxidized implants were used. In papers II, III and IV the implant surfaces were either machined or anodically oxidized (TiUnite) surfaces. All the implants were produced, sterilized and delivered in glass containers by the manufacturer (Nobel Biocare, Göteborg, Sweden).

### ***Surface characterization (paper IV)***

#### **Profilometry**

Topographical analysis of the two implant surfaces was performed using non contact 3D interference microscopy (WYKO NT-9100). The measurements were made over a  $125 \times 95 \mu\text{m}$  area on flanks, tops, and valleys of two nonadjacent threads of each implant type. Before calculating the topography parameters, raw data were processed with a tilt and cylindrical correction. A built-in median filter ( $5 \times 5$  pixel smoothing) was then applied for further reduction of noise. From the corrected and smoothed data the surface parameters  $S_a$  (arithmetic mean of the absolute values of deviations from a mean plane),  $S_t$  (peak-to-valley distance) and  $S_{dr}$  (developed interfacial area ratio) were derived.

#### **Scanning electron microscopy**

To evaluate the morphological features of the two surfaces, the implants were mounted on stubs by means of carbon-coated adhesive tape and sputter-coated with palladium. The samples were examined in a Zeiss DSM 982 Gemini scanning electron microscope.

#### **Auger electron spectroscopy**

The top atomic layers were analyzed using PHI 660 scanning Auger microscope to evaluate the chemical compositions of the implant surfaces. The analysis was made on the thread top and valley of the implant over  $30 \times 30 \mu\text{m}$  analysis area. The implants were analyzed either as-received or after short cleaning with argon ion resulting in approximately 3 nm reduction of the outer surface. The primary beam energy was 3.0 keV and beam current 300 nA. Five scans were performed per each analysis area and the analysis time was 50 ms/eV.

To determine the oxide thickness of the oxidized implants, AES analysis combined with argon ion etching was performed on one oxidized sample. The depth profiling was conducted on the top of the third thread using 3.5 keV Ar<sup>+</sup> ion gun with sputter rate at 32nm/min. The oxide thickness was calculated.

#### **Transmission electron microscopy**

Ultrathin sections for TEM analysis were prepared from machined and oxidized implants using focused ion beam microscope (Figure 1). Prior to ultrathin sectioning, the implants were embedded in LR White plastic resin and cut longitudinally into two halves using a band saw and grinding equipment (EXAKT<sup>®</sup> Apparatebau GmbH & Co, Norderstedt,

Germany). Sputter coat with a thin film of palladium was applied on the exposed side of the implant. The sample was mounted on stub by means of carbon-coated adhesive tape and placed into the focused ion beam (FIB) microscope (FEI Strata DB235, FEI Company, Eindhoven, Netherlands). Cross-section samples were prepared using an in-situ lift-out method, where the area of interest was protected by platinum deposition [181, 182]. A thick lamella ( $\approx 5 \mu\text{m}$ ) was cut and transferred to a TEM-grid. Final thinning using decreasing ion beam current was performed until a thickness of 100 nm was obtained. Bright field and dark field imaging, selected area electron diffraction analysis (SAED) and energy dispersive X-ray spectroscopy (EDS) were performed.

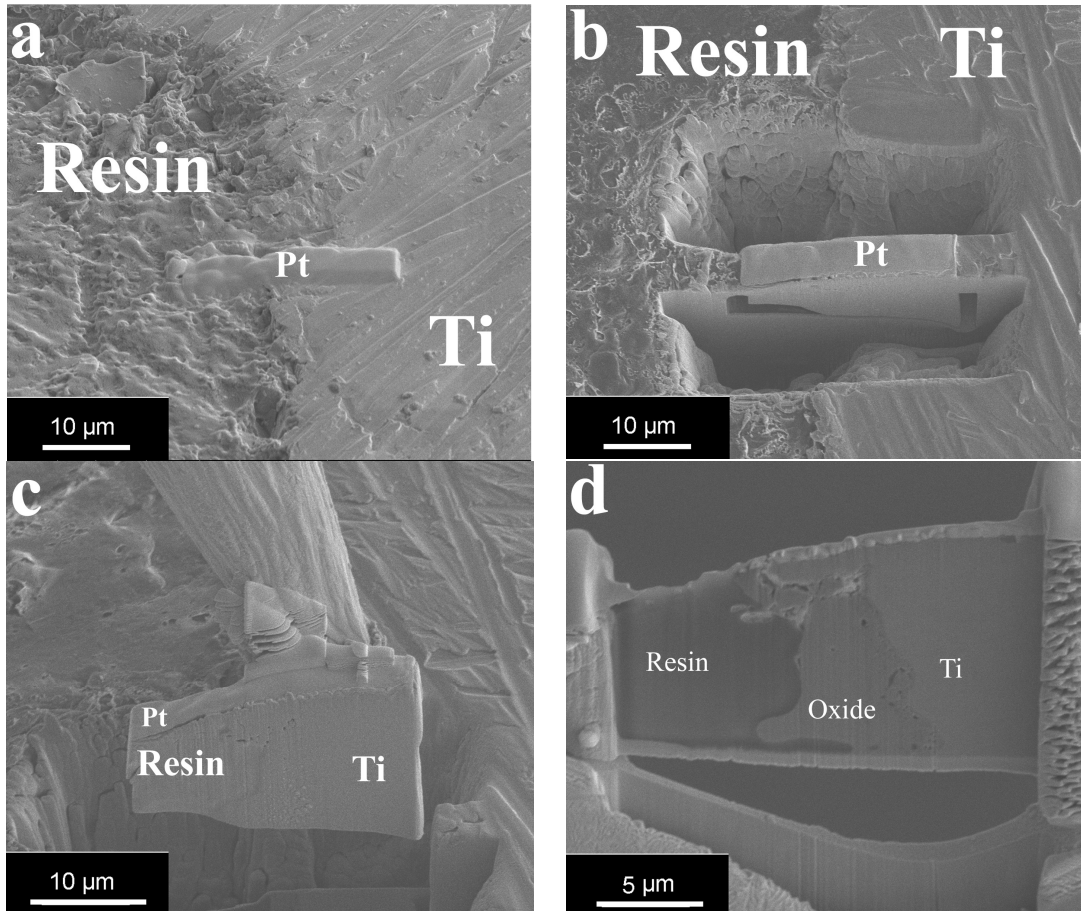


*Figure 1: Serial images of sample preparation steps using FIB technique. (a) Area of interest was selected at the interface of titanium implant (Ti) with the plastic resin and protected by platinum deposition (Pt). (b) Rough cutting of trenches on either side of the platinum (c) The lamella was transferred to a V shaped TEM grid (d) Final thinning of the lamella was performed using beam current down to 50 pA.*

### Endotoxin test

All the implants were sterilized and kept in glass containers until analysis. However, to exclude endotoxin contamination of the implants, limulus test was performed on machined and oxidized implants immediately after removal from glass storage containers.



### ***Animal model and surgical procedures (papers I-IV)***

The animal experiments were approved by the local ethical committee for laboratory animals, University of Gothenburg, Sweden (Dnr 306-2006 and 301-2009). Sprague–Dawley rats (200 – 250 g), fed on a standard pellet diet and water were used in the four studies. Implantation procedures were carried out under isoflurane inhalation anesthesia (Isoba Vet, Schering-Plough Uxbridge, England) using Univentor 400 anesthesia unit (Univentor, Zejtun, Malta). Each rat received analgesic (Temgesic 0.03 mg/kg, Reckitt & Coleman, Hull, Great Britain) subcutaneously prior to the implantation, and daily postoperatively. Prior to implantation, rats were shaved and cleaned (5 mg/mL chlorhexidine in 70 % ethanol). In papers II, III and IV machined and oxidized implants were installed in the left and right tibiae, two implants per tibia (Figure 2). The implantations were performed according to a predetermined schedule ensuring rotations between locations. The medial aspect of the proximal tibial metaphysis was exposed through an anteromedial skin incision, followed by skin and periosteum reflection with blunt instrument. Proximal and distal implant sites were prepared using Ø 1.4 and 1.8 mm round burs under profuse irrigation with NaCl 0.9 %. The implants were inserted with a hexagonal screw driver and the surgical wounds were sutured. The subcutaneous layer of the wound was closed with resorbable polyglactin sutures (5-0, Vicryl, Ethicon, Johnson & Johnson, Brussels, Belgium) and the skin was closed with transcutaneously placed nonresorbable nylon sutures (5-0, Ethilon, Ethicon, Johnson & Johnson, Brussels, Belgium). In paper I, oxidized implants were inserted in the proximal femoral epiphysis and distal tibial metaphysis. After surgery, the animals were allowed free postoperative movements with food and water *ad libitum*.

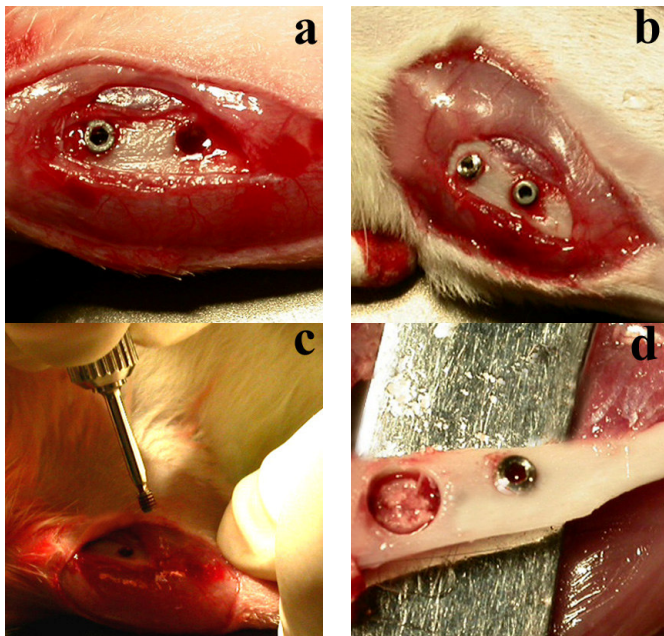


*Figure 2: Images from surgical procedure (paper II). (a and b) Two implants have been inserted in each tibia. (c and d) Implants were unscrewed by hexagonal screw driver and the peri-implant bone was retrieved by trephine.*

Table II: Summary of the number of rats and implants used for each analytical technique per each time period.

Paper	No. of rats	Analysis	Type of sample	Samples (n)
I	8	qPCR	Bone biopsies from femur, proximal and distal tibia (1 biopsy per site, right and left).	15
	18	qPCR	Oxidized implants in femur and tibia (1 implant per rat, left).	9
	4	H	Bone blocks with or without oxidized implants (1 block per site, left).	4
II	5	qPCR	Machined and oxidized implants (2 implants per tibia, right and left).	10
	2	SEM	Machined and oxidized implants (1 implant per tibia, right and left).	2
	2	H and IHC	Machined and oxidized implants (1 implant per tibia, right and left).	2
III	10	qPCR and SEM	qPCR: Machined and oxidized implants (2 implants per tibia, right and left).	15
			qPCR: Peri-implant bone of the machined and oxidized implants (right and left).	10
			SEM: Machined and oxidized implants (2 implants per tibia, right and left).	3
	3	H	Machined and oxidized implants (1 implant per tibia, right and left).	3
	3	IHC	Machined and oxidized implants (1 implant per tibia, right and left).	3
IV	7	qPCR and biomechanic test	qPCR and biomechanics: Machined and oxidized implants (2 implants per tibia, right and left).	BM (14) qPCR (10)
			qPCR: Peri-implant bone of the machined and oxidized implants (right and left).	10
	3	H and FIB-TEM (fractured interface)	Machined and oxidized implants (2 implants per tibia, right and left).	2
			H and FIB-TEM (intact interface)	Machined and oxidized implants (2 implants per tibia, right and left).

*qPCR* = quantitative polymerase chain reaction, *SEM* = scanning electron microscopy, *H* = histology, *IHC* = immunohistochemistry, *FIB-TEM* = focused ion beam-transmission electron microscopy, *BM* = biomechanical test.

Animal sacrifice was performed using intraperitoneal overdose of sodium pentobarbital (60 mg/mL; ATL Apoteket Production & Laboratories, Kungens Kurva, Sweden) under anaesthetisation with a 0.5-mL mixture of pentobarbital (60 mg/mL), sodium chloride, and diazepam (1:1:2). Sample retrieval was performed after 3 d (paper I), 3 h - 1 d (paper II), 1 d - 6 d (paper III) and 6 d - 28 d (paper IV). Different retrieval procedures were performed depending on the intended analyses. For qPCR analysis and SEM, implants

were unscrewed with adherent biological material by a hexagonal screw driver (papers I - IV). Trephines, with internal Ø 2.3 mm, were used to retrieve the peri-implant bone (papers III and IV). Similar trephines, with internal Ø 2.1 and 2.3 mm, were used to retrieve bone biopsies from femoral epiphysis, proximal, and distal tibial metaphysis (paper I). For histology and immunohistochemistry, the rats were first anaesthetized and fixated by perfusion of modified Karnovsky media (2 % paraformaldehyde, 2.5 % glutaraldehyde in 0.05 M sodium cacodylate) (pH 7.4) via the left heart ventricle. Implants with the surrounding bone were dissected *en bloc* using dental disc. In paper IV, the implants were tested for torsion torque before complete removal.

**Gene expression analysis (papers I-IV)**

Procedure	Bone	Implant
Sample preservation	Immediately after retrieval, implants, peri-implant bone or bone biopsies were preserved in separate tubes containing RNAlater <sup>®</sup> solution <sup>a</sup> . The samples were stored at 4°C overnight, and then at – 80°C until analysis.	
Sample homogenization	In phenol/guanidine-based Qiazol lysis reagent using 5 mm stainless steel bead and TissueLyser <sup>a</sup> .	In RLT Buffer and TissueLyser <sup>a</sup> .
RNA extraction	After adding chloroform and centrifugation, aqueous phase was used for RNA extraction. Total RNA was extracted using RNeasy <sup>®</sup> Mini kit <sup>a</sup> .	After centrifugation, aqueous phase was used for RNA extraction. Total RNA was extracted using RNeasy <sup>®</sup> Micro kit <sup>a</sup> .
RNA purification	DNase treatment was performed in order to eliminate any contamination from genomic DNA.	
Reverse transcription and cDNA synthesis	Reverse transcription was carried out using iScript cDNA Synthesis Kit <sup>b</sup> in a 10 µl reaction.	
Primer design	Design of primers was performed using the Primer3 web-based software [183]. Design parameters were: <ul style="list-style-type: none"> <li>• Minimum formation of artifact products.</li> <li>• Annealing temperature in the PCR at about 60 °C.</li> <li>• Short amplicons (preferably shorter than 200 bp)</li> <li>• Function well with SYBR Green I fluorescent dye.</li> </ul> The following primers were designed throughout the project: OC, ALP, TRAP, CATK, TNF- $\alpha$ , IL-1 $\beta$ , TGF- $\beta$ 1, BMP-2, PDGF-B, Runx2, PPAR- $\gamma$ IL-8R, MCP-1, CXCR4, vinculin, integrins $\alpha$ v, $\beta$ 1, $\beta$ 2, $\beta$ 3 and 18S	

Procedure	Bone	Implant
Real time polymerase chain reaction	<ul style="list-style-type: none"> <li>• Performed in duplicates using the Mastercycler ep realplex<sup>c</sup> in 20 µl reactions.</li> <li>• Cycling conditions were 95 °C for 3 min followed by 45 cycles of 95 °C for 20 s, 60 °C for 20 s and 72 °C for 20 s.</li> <li>• Fluorescence was read at the end of the 72 °C step.</li> <li>• Melting curves were recorded after the run by stepwise temperature increase (1 °C/5s) from 65 – 95 °C.</li> </ul>	
Quantification	Quantities of target genes were determined as either a total content or normalized using the expression of 18S ribosomal RNA. Normalized relative quantities were calculated using the delta Ct method and 90 % PCR efficiency ( $k*1.9^{\Delta Ct}$ ) [184].	

Table III: A description of different steps during gene expression analysis.

<sup>a</sup>QIAGEN GmbH, Hilden, Germany. <sup>b</sup>Bio-Rad, Hercules, USA. <sup>c</sup>Eppendorf, Hamburg, Germany

### **Histology (papers I - IV) and immunohistochemistry (papers II and III)**

For decalcified paraffin embedded section (papers I - III), bone and implant-bone specimens were post-fixed in modified Karnovsky media for 2 h, decalcified in 10 % EDTA for 10 d and embedded in paraffin. Implants were unscrewed from the blocks during paraffin embedding stage and the procedure was continued. Ten µm sections were produced, mounted on glass slides and stained with hematoxylin and eosin for light microscopy (Nikon Eclipse E600). For immunostaining, 4 µm sections were produced, mounted on poly-L-lysine slides (Menzel GmbH and Co KG, Braunschweig, Germany), deparaffinized, hydrated and incubated with primary antibodies CD163 (sc-58965, Santa Cruz Biotechnology), and periostin (ab14041, Abcam, Cambridge, UK). The immunoreactivity of CD163 labeled sections was detected and visualized using LSAB®2 System-HRP kit (K0609; DAKO, Sweden), diaminobenzidine (Victor's kit, Immunokemi, Sweden) and counterstained with Mayer's hematoxylin. Periostin staining was detected with PK6101 kit, diaminobenzidine (Victor's kit, Immunokemi, Sweden) and counterstained with Mayer's hematoxylin. The primary antibodies were diluted in 1% bovine serum albumin (BSA, Sigma A7638 from Sigma Aldrich, Sweden) in phosphate buffered saline (PBS). Negative control slides were prepared by omission of the primary antibody and incubation with 1% BSA in PBS.

For ground section preparations (paper IV), bone-implant specimens were fixated and dehydrated prior to plastic embedding (Technovit 7200, Heraeus Kulzer GmbH & co.KG). The implants were divided along the long axis (EXAKT® cutting and grinding equipment, EXAKT® Apparatebau GmbH & Co, Norderstedt, Germany). Ground sections were prepared by the method described elsewhere [185]. The ground sections were stained with 1 % toluidine blue before the histological examination in an optical microscope (Nikon Eclipse E600).

### ***Scanning electron microscopy (papers II - IV)***

In papers II and III, retrieved implants were fixed in modified Karnovsky solution (2 % paraformaldehyde, 2.5 % glutaraldehyde in 0.05 M sodium cacodylate) (pH 7.4) for 4 h. Implants were then rinsed with sodium cacodylate buffer and subsequently impregnated with a conductive, metallic layer of osmium using a modified osmium-thiocarbohydrazide-osmium technique (OTOTO). Specimens were then dehydrated in graded series of ethanol and dried with hexamethyldizilane for  $2 \times 5$  min. Specimens were mounted on stubs with carbon coated adhesive tape. In case of reduced conductivity, specimens were subjected to an additional sputter coating with palladium. All specimens were examined in a Zeiss DSM 982 Gemini scanning electron microscope.

For backscattered SEM analysis (paper IV), the other half of the embedded and divided bone-implant specimens was used. The blocs were glued on SEM stubs and coated with thin layer of palladium prior to mounting in the microscope.

### ***Removal torque analysis (paper IV)***

At different time points after surgery, the rats were sacrificed and implants retrieved using torque test equipment. The implants were exposed with careful dissection of the overlying soft tissues. Special hexagonal screw driver, connected to the torque test machine, was fitted into the implant internal hexagon (Figure. 3). The torque measuring equipment is an upgraded version of previously described set-up [174, 186]. The torque test equipment was calibrated prior to angular torque measurement. Torque was registered versus the rotation angle and followed in real time. After the break point was reached, the procedure was continued under the constant rotation to determine the pattern of deformation before the complete failure.

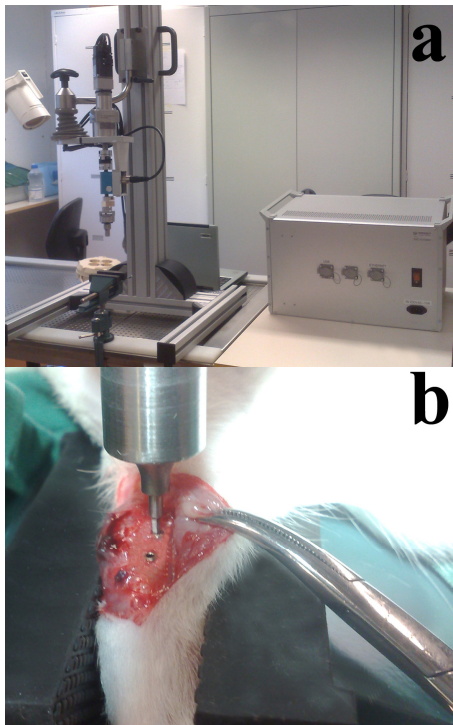


*Figure 3: Procedure during removal torque analysis. (a) Biomechanic equipment. (b) The screw driver was aligned with the implant while the tibia was firmly held using a vise.*

### ***Statistics***

Non parametric tests were used to compare gene expression between machined and oxidized samples (except for paper III where t-test was used). Multiple comparisons were performed using analysis of variance (ANOVA). Pearson correlation analyses were performed between removal torque values and the expression levels of different analyzed genes.

# Results

## Surface characterization

Oxidized and machined implants were characterized morphologically, topographically, chemically and ultrastructurally using SEM, profilometry, Auger electron microscopy and transmission electron microscopy, respectively. The main results of surface characterizations are presented in Table IV.

## Surface morphology

Different surface morphology was observed between machined and oxidized implants. Machined surface showed a smooth appearance, characterized by ordered grooves and ridges, due to the manufacturing process (Table IV). The oxidized surface was characterized by a porous surface texture with open pores, in micrometer range, protruding from the surface (Table IV). Small depressions, in submicron-micrometer range, were also observed on the oxidized surface.

## Surface topography

All averaged roughness parameters ( $S_a$ ,  $S_t$  and  $S_{dr}$ ) were significantly higher for the oxidized implants than those registered for the machined implants (Table IV). Site-specific comparisons showed oxidized implants to have greater height of deviation, surface enlargement as well as larger peak-to-valley distance at every location (flank, top or valley) compared to the equivalent locations on machined implants.

## Surface chemistry

AES analysis revealed the presence of Ti, O and C at machined and oxidized surfaces, both as received and after 3 nm sputter cleaning. Machined implants showed higher oxygen peak and less carbon at the outermost surface. Phosphorus was detected (about 3.6 %) in the oxidized surface and increased to 6.4 % after sputtering. EDS analysis confirmed the presence of substantial amount of phosphorus (Figure 4).

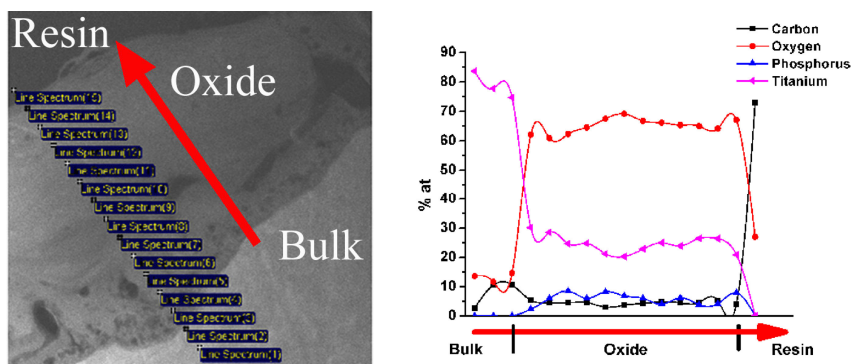
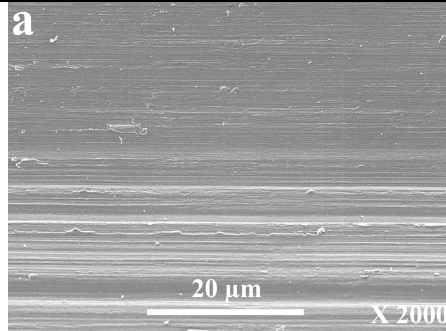
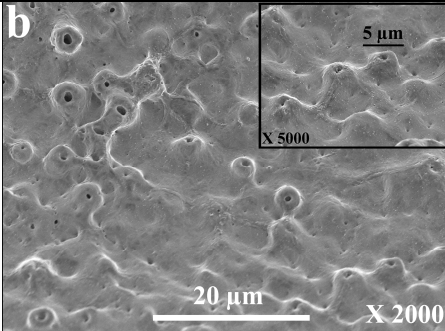
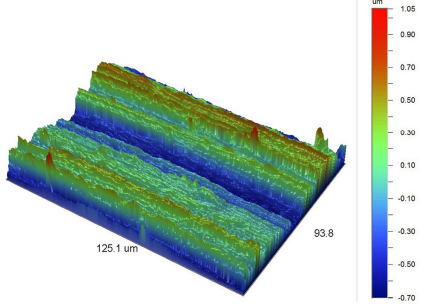
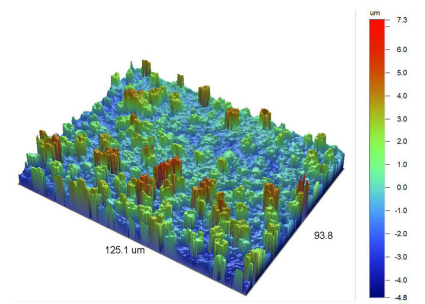
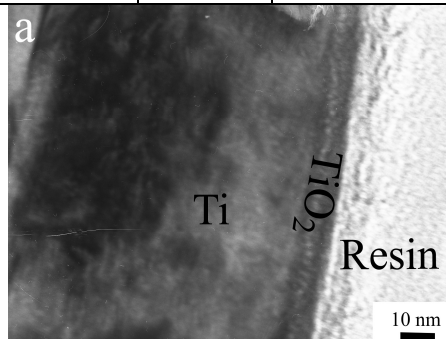
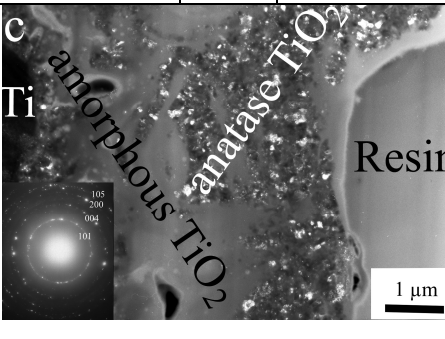


Figure 4: EDS scanning acquired in direction from the bulk to the surface of oxidized implant through the oxide layer. The graph shows the integrated intensities from Ti, O, C and P spectra along the line.



Table IV: Summary of the surface characterization of machined and oxidized implants (presented in paper IV)

	Machined	Oxidized				
Morphology						
	Smooth appearance Ordered grooves and ridges	Porous texture Open pores in $\mu\text{m}$ range Smooth edges (Insert shows lower right area in higher magnification)				
Topography	<b>Machined thread flank</b> 	<b>Oxidized thread flank</b> 				
	$S_a$	$S_t$	$S_{dr}$	$S_a$	$S_t$	$S_{dr}$
	0.28	2.31	5.03	1.2	8.4	75.51
Oxide thickness and Crystallinity						
	Thin native $\text{TiO}_2$ , about 10 nm. Crystallinity was not determined	Thick $\text{TiO}_2$ , up to 10 $\mu\text{m}$ . Crystalline clusters (anatase) embedded in amorphous $\text{TiO}_2$				
Chemistry	Mainly O, Ti, C Traces of B and Si detected	Mainly O, Ti, C Contains phosphorus				

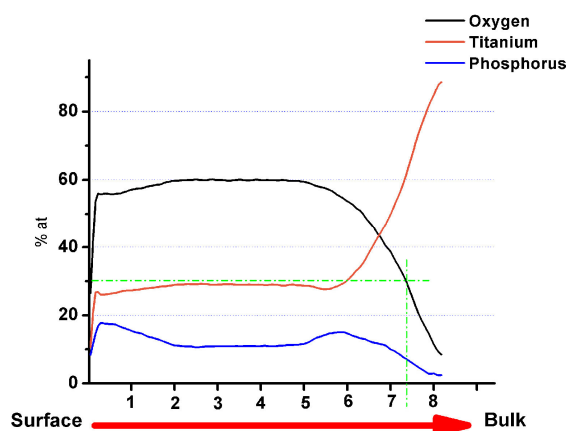


## Oxide thickness and ultrastructure

Depth profiling using a combination of argon ion sputtering and AES revealed that the oxide thickness of the oxidized implants was  $\approx 7.5 \mu\text{m}$  (Figure 5).

Low resolution examination of FIB produced sections of the oxidized implant showed a surface oxide layer with 2-10  $\mu\text{m}$  thickness range. High resolution imaging of the oxide layer showed both amorphous and crystalline phases (Table IV). SAED analysis revealed that the crystalline phase was anatase  $\text{TiO}_2$ . A surface layer of about 10 nm thickness was visible between bulk titanium of the machined implant section and the plastic resin, which is most likely the native titanium oxide. However, further analysis was difficult due to the limited thickness of the oxide.

*Figure 5: AES depth profile of oxidized implant. The oxide thickness, defined at which the oxygen signal has dropped to half its maximum value, was measured to be  $7.5 \mu\text{m}$ .*



## Endotoxin test

The results from Limulus test did not show any contamination for neither machined nor oxidized implants. The endotoxin contents were  $< 0.005$  and  $0.009 \text{ EU/ml}$  for oxidized and machined implants, respectively.

## Molecular activity of different bone types (paper I)

Gene expression of bone formation, bone resorption and pro-inflammatory markers was evaluated in bone samples from femoral epiphysis, proximal tibial metaphysis and distal tibial metaphysis representing trabecular, mixed cortico-trabecular and mainly cortical bone types, respectively. Then, the panel of genes was measured and compared in cells adherent to oxidized titanium implants after unscrewing them from either trabecular or cortical bone locations.

## Steady-state gene expression in cortical and trabecular bone types

The results are presented in Figure 6 a and b. Normalized ALP expression showed 3-fold higher expression in femoral epiphysis compared to proximal and distal tibia metaphysis. For OC, the normalized expression was significantly higher, by a factor of 2, in femur compared to the distal tibia. The normalized TRAP expression level was 5-fold higher in the femur compared to the proximal tibia. No significant differences in the normalized expression of CATK were observed among the different bone sites. Significantly higher expression levels of  $\text{TNF-}\alpha$  and  $\text{IL-1}\beta$  were detected in both proximal and distal tibia compared with femur.

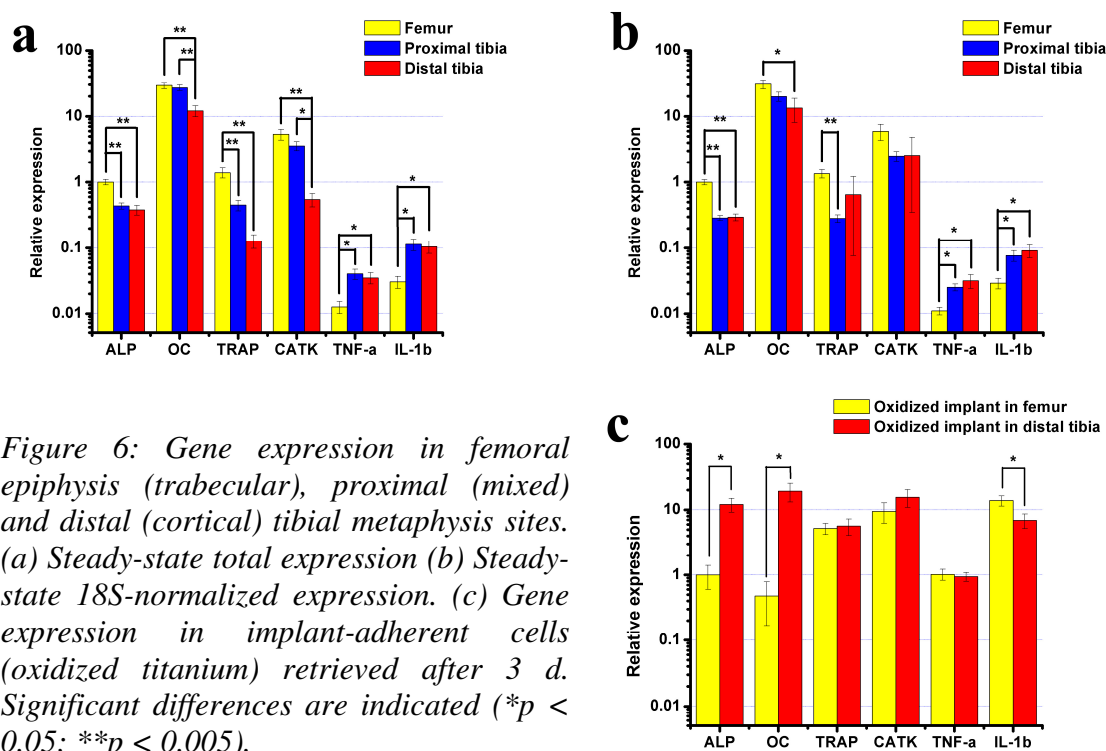


Figure 6: Gene expression in femoral epiphysis (trabecular), proximal (mixed) and distal (cortical) tibial metaphysis sites. (a) Steady-state total expression (b) Steady-state 18S-normalized expression. (c) Gene expression in implant-adherent cells (oxidized titanium) retrieved after 3 d. Significant differences are indicated (\* $p < 0.05$ ; \*\* $p < 0.005$ ).

## Gene expression at oxidized implants in cortical and trabecular bone types

The normalized expression of ALP and OC were 12- and 41-fold, respectively, higher at the implants retrieved from tibial cortical bone than those retrieved from the femoral trabecular bone (Figure 6c). No significant differences could be observed between the two locations when comparing the expression levels of the bone resorption markers at the implants retrieved from femur and tibia. Anodically oxidized implants retrieved from trabecular femoral bone showed 2-fold higher expression of IL-1 $\beta$  compared to similar implants retrieved from tibial cortical bone.

## Cellular and molecular activities at different implant surfaces (papers II - IV)

Studies on the interfacial gene expression were performed from 3 h until 28 d after implantation of machined and oxidized implants. In addition, electron microscopic and immunohistochemical observations were made during the early phase of osseointegration. Biomechanical and histological analyses were performed during the late phase.

## Cellular and molecular activity during first day of implantation (paper II)

Gene expression in cells adherent to machined and oxidized implants was evaluated 3, 12 and 24 h after implantation. Retrieved implants and bone were also examined with SEM and immunohistochemistry, respectively.

## Gene expression in implant-adherent cells

Gene expression of chemotaxis, cell adhesion and pro-inflammatory markers was analyzed. The total expression levels were normalized to 18S expression at the implant surfaces. The results are presented in Figure 7. Significantly higher expression of CXCR4 (at 12 h) and integrins,  $\alpha v$  (at 12 h),  $\beta 1$  (at 24 h) and  $\beta 2$  (at 12 and 24 h) was detected at the oxidized surfaces. On the other hand, higher TNF- $\alpha$  (at 3 h) and IL-1 $\beta$  (at 24 h) expression was demonstrated for the machined surface.

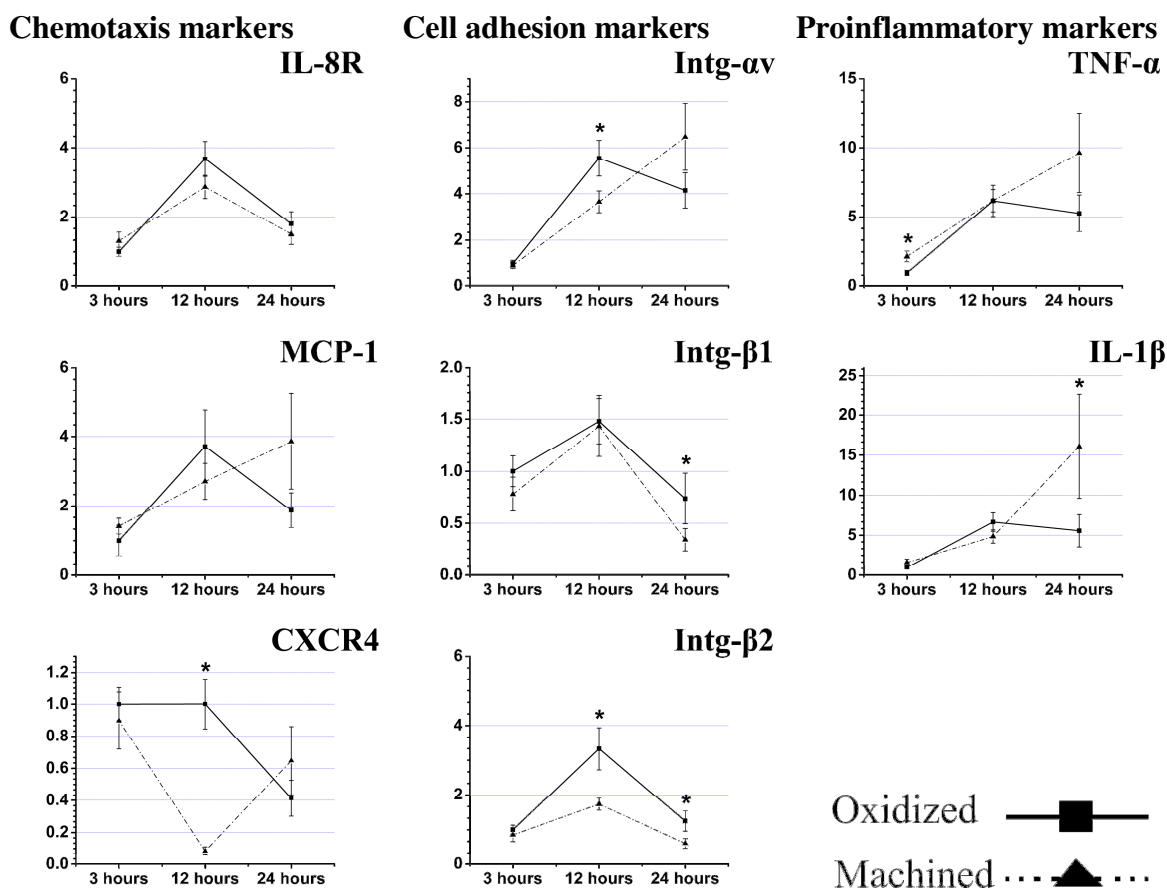


Figure 7: Gene expression at machined and oxidized implants retrieved 3, 12 and 24 h after implantation. Significant differences are indicated (\* $p < 0.05$ ).

Correlation analysis of gene expression at the oxidized surface during the 24 h period (Table V) revealed significant positive relationship between the expressions of chemokines and integrins. IL-8R was in correlation with integrins-  $\beta 2$  and  $\beta 3$  whereas MCP-1 showed correlation with all integrins except integrin- $\alpha v$ . CXCR4 exhibited association with integrin- $\beta 1$ . Strong correlation was also revealed at the oxidized implants between IL-8R, MCP-1 and integrin- $\beta 2$ .

At machined implants (Table VI), significant correlation was revealed between CXCR4, IL-8R and integrin- $\beta 2$ . Significant correlation was also revealed at the machined implants between MCP-1, TNF- $\alpha$  and IL-1 $\beta$ .

Table V: Correlation analysis of different genes expressed after 24 h in cells adherent to oxidized implants

		MCP-1	CXCR4	IL-1 $\beta$	TNF- $\alpha$	Intg- $\alpha$ v	Intg- $\beta$ 2	Intg- $\beta$ 1	Intg- $\beta$ 3
IL8R	Corr.	.892**	.592	.914**	-.136	.137	.935**	.552	.709*
	Sig.	.001	.093	.001	.727	.725	0.0002	.123	.049
MCP-1	Corr.		.770*	.910**	-.318	.201	.840**	.736*	.762*
	Sig.		.015	.001	.404	.605	.005	.024	.028
CXCR4	Corr.			.716*	-.038	.377	.394	.680*	.649
	Sig.			.030	.923	.317	.293	.044	.082
IL-1 $\beta$	Corr.				-.253	.145	.847**	.644	.732*
	Sig.				.511	.709	.004	.061	.039
TNF- $\alpha$	Corr.					.657	-.312	-.437	-.101
	Sig.					.055	.414	.240	.811
Intg- $\alpha$ v	Corr.						.027	.259	.555
	Sig.						.945	.502	.154
Intg- $\beta$ 2	Corr.							.565	.775*
	Sig.							.113	.024
Intg- $\beta$ 1	Corr.								.886**
	Sig.								.003

Table VI: Correlation analysis of different genes expressed after 24 h in cells adherent to machined implants

		MCP-1	CXCR4	IL-1 $\beta$	TNF- $\alpha$	Intg- $\alpha$ v	Intg- $\beta$ 2	Intg- $\beta$ 1	Intg- $\beta$ 3
IL8R	Corr.	-.320	.989**	-.163	-.175	.514	.857**	.087	.254
	Sig.	.402	.000005	.675	.653	.157	.003	.823	.543
MCP-1	Corr.		-.282	.896**	.891**	.561	-.231	-.349	.697
	Sig.		.462	.001	.001	.116	.550	.357	.055
CXCR4	Corr.			-.100	-.156	.517	.857**	.057	.283
	Sig.			.797	.688	.154	.003	.884	.497
IL-1 $\beta$	Corr.				.905**	.502	-.154	-.341	.728*
	Sig.				.001	.168	.693	.370	.041
TNF- $\alpha$	Corr.					.618	-.205	-.358	.631
	Sig.					.076	.597	.345	.093
Intg- $\alpha$ v	Corr.						.518	-.382	.745*
	Sig.						.153	.310	.034
Intg- $\beta$ 2	Corr.							.011	.283
	Sig.							.978	.498
Intg- $\beta$ 1	Corr.								-.546
	Sig.								.161

### Scanning electron microscopy of the implant-adherent cells

Retrieval of the implants after 24 h of implantation revealed high proportion of fibrinous material adherent to the machined implant surfaces. Numerous erythrocytes and leukocytes were captured within the fibrin-like mesh (Figure 8 a, c). Mesenchymal-like cells assumed more flat shape on the machined surfaces (Figure 8b). Oxidized implants showed more mesenchymal-like cells attached over the surfaces with predominance at the bottom valley of the threads (Figure 8d, f). Leukocytes and erythrocytes were also observed at the oxidized surface (Figure 8e). Firm anchorage of the mesenchymal-like cells on the oxidized implants was observed (Figure 8g).

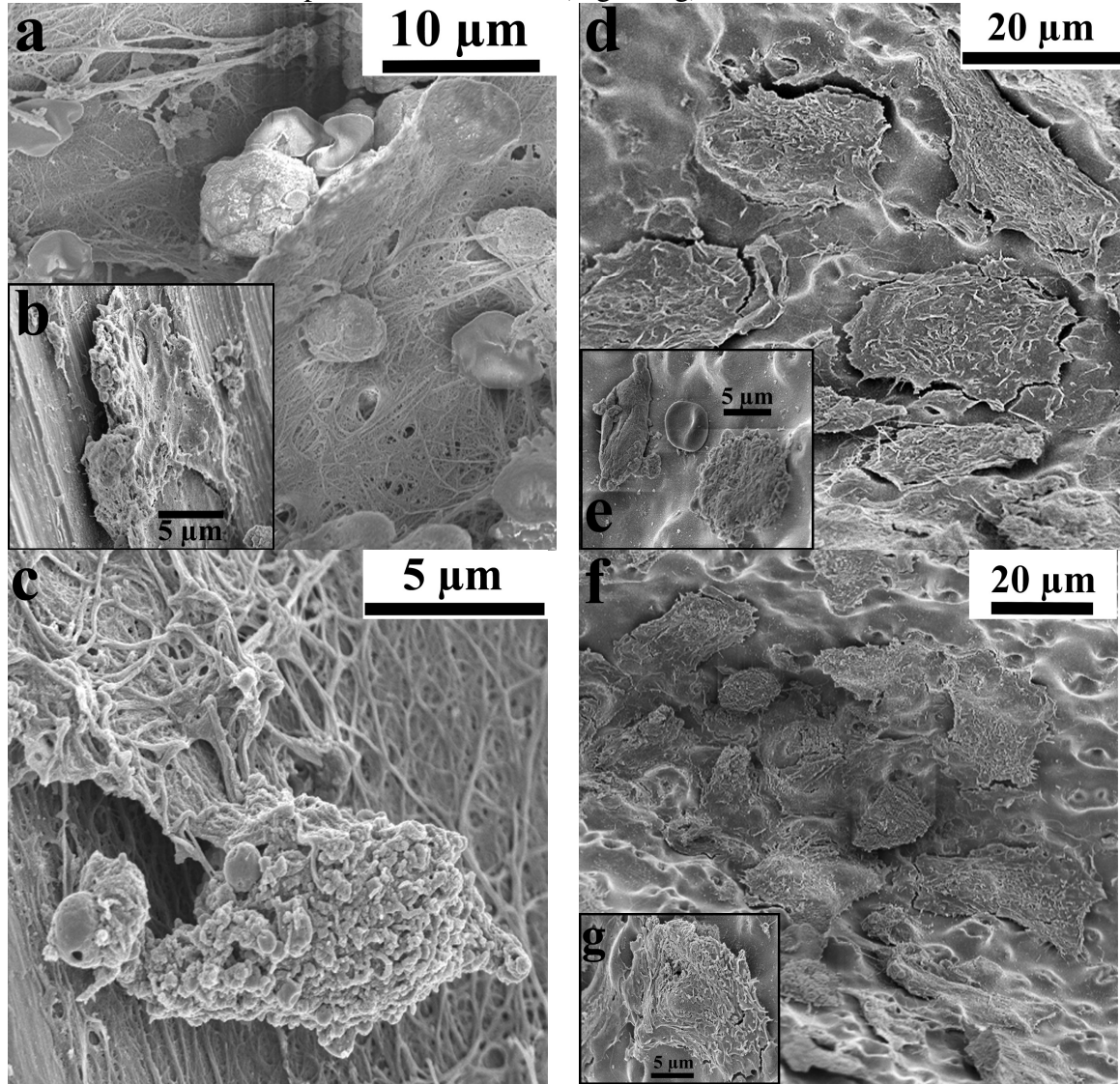


Figure 8: SEM images of machined and oxidized implant retrieved 24 h after implantation. Biological material adherent the machined implant was highly fibrinous with numerous erythrocytes and leukocytes (a, b and c). On the oxidized implants, mesenchymal-like cells are frequently seen (d, f and g). Leukocytes and erythrocytes are also evident (g).



### Immunohistochemistry of the interface

The immunohistochemically stained sections (Figure 9) revealed an early organization of blood hematoma within the threads of both implant types after 24 h of implantation. CD163 (a marker for monocytes and tissue macrophages) and periostin (a marker for mesenchymal and osteoprogenitor cells) positive cells were scattered into the newly formed hematoma within the threads and at some locations very close to implant surface. Fibrin-like strands running parallel to the implant surface were prominently seen at the machined surfaces but not the oxidized ones.

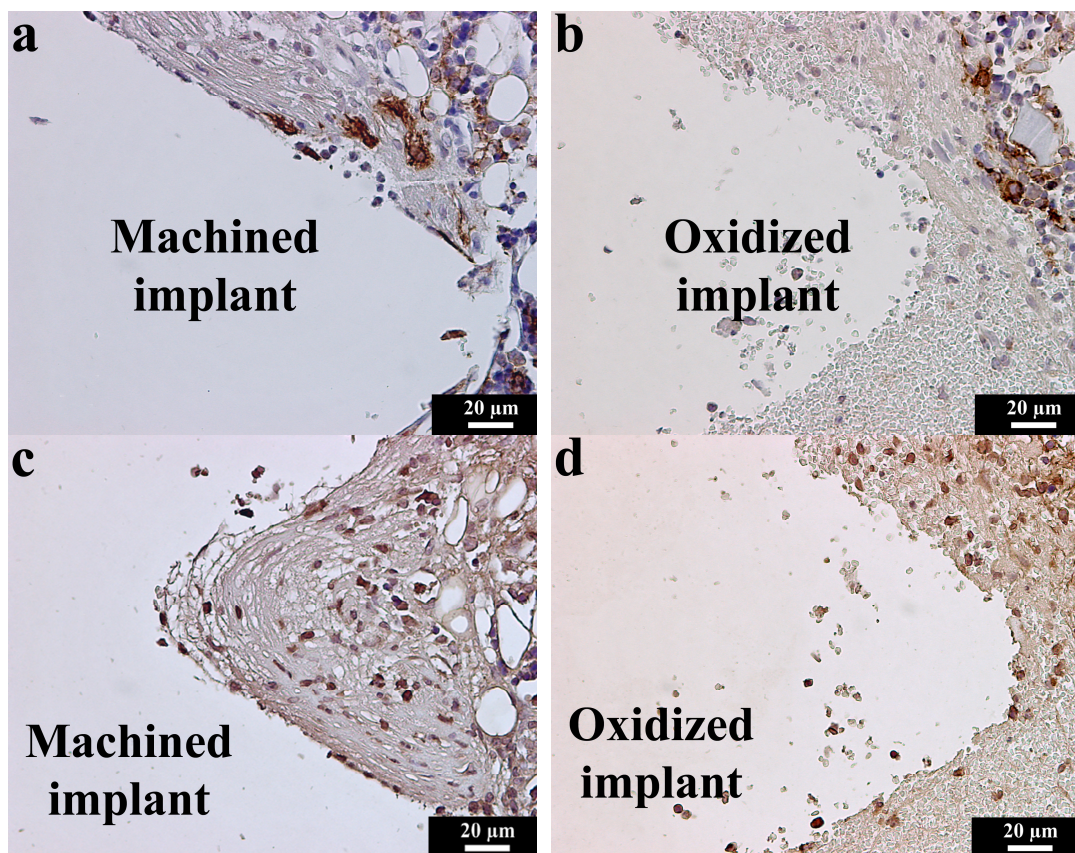


Figure 9: Immunohistochemical sections of the interface 24 h after implantation showing CD163 (a and b) and periostin (c and d) positive cells.

### Cellular and molecular activity during first week of implantation (paper III)

After 24 h, 3 d and 6 d, interfacial gene expression was evaluated in the implant adherent cells as well as in the peri-implant bone retrieved following implant unscrewing. Cellular and tissue organization on the retrieved implants were examined with SEM. Histological and immunohistochemical sections were prepared from bone-implant blocks after implant removal.

## Gene expression in the implant-adherent cells

The results are presented in Figure 10. Machined implants induced 2-fold and 5-fold higher level of TNF- $\alpha$  and IL-1 $\beta$ , respectively, after 1 d. 3-fold higher expression of IL-1 $\beta$  was also observed after 6 d at the machined implants. OC and ALP expression were 5-fold and 2-fold higher after 3 d and 6 d, respectively, at oxidized compared with machined surfaces. In addition, CATK was up-regulated 4-fold at the oxidized implants after 3 d.

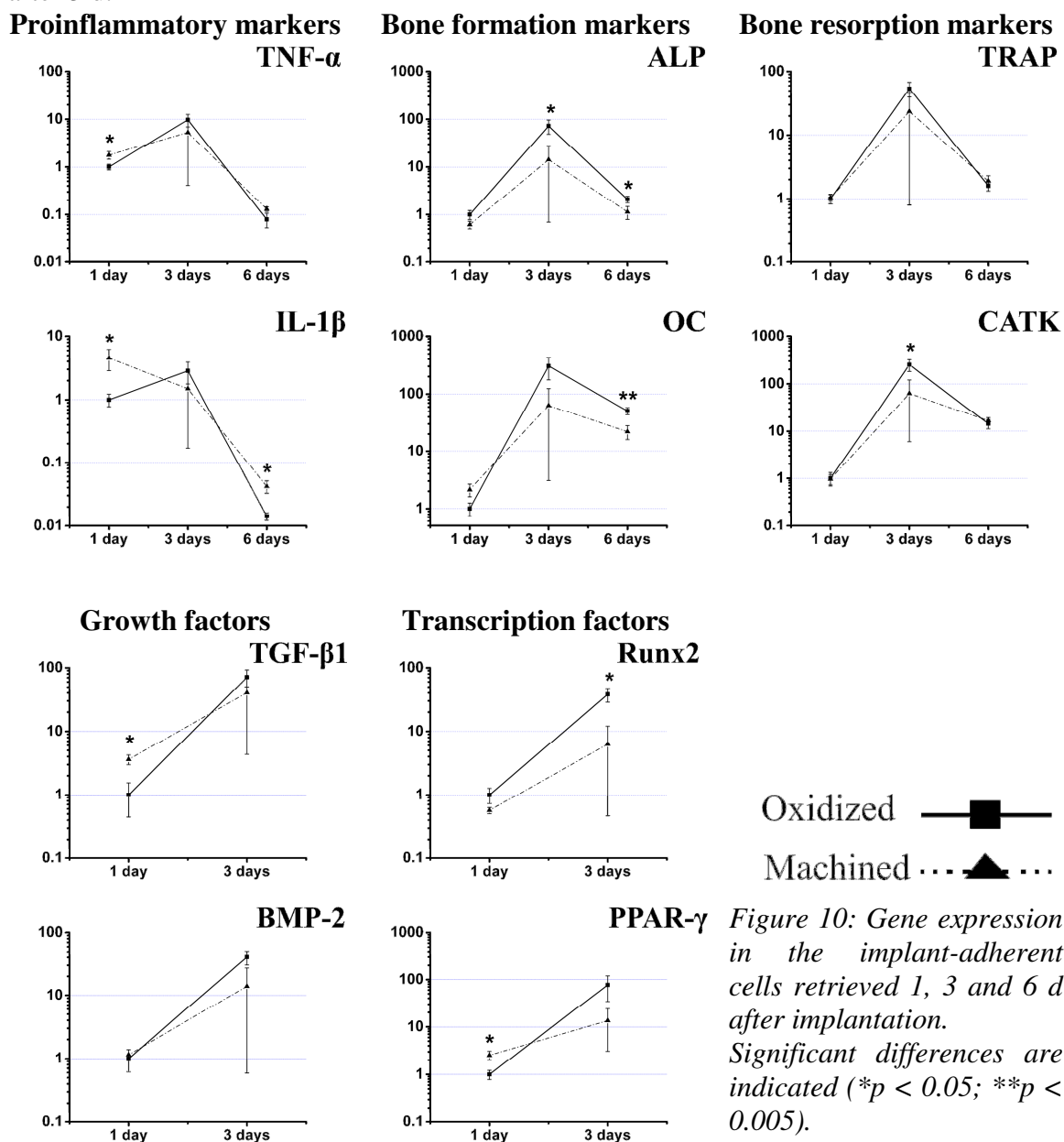


Figure 10: Gene expression in the implant-adherent cells retrieved 1, 3 and 6 d after implantation. Significant differences are indicated (\* $p < 0.05$ ; \*\* $p < 0.005$ ).

The expression of Runx2 was significantly higher (6-fold) at the oxidized compared to the machined surfaces 3 d after implantation (Figure 10). The expression of transcription factor PPAR- $\gamma$  was significantly higher by 3-fold at the machined surface compared to

oxidized surface 1 d after implantation. After 3 d, the expression of PPAR- $\gamma$  was 6-fold higher at the oxidized surface (Figure 10). TGF- $\beta$ 1 expression was significantly higher by 4-fold at the machined surfaces compared to the oxidized ones 1 d after implantation. Generally, the highest peaks of bone formation and remodeling markers were observed after 3 d of implantation. On the other hand, high peaks of inflammatory markers were detected 1 d after implantation and decreased to lower levels 6 d after implantation.

### Gene expression in the peri-implant bone

No significant differences in gene expression were observed between the peri-implant bone collars of machined and oxidized implants (Figure 11). The temporal pattern of the osteogenic markers was different in the peri-implant bone from that seen in the implant-adherent cells during the time course of implantation. 18S, OC, ALP, TRAP and CATK expression levels were increasing steadily with time with peak at 6 d after implantation. On the other hand, the pro-inflammatory marker expression in the peri-implant bone showed comparable pattern to that occurring in implant adherent cells with the lowest levels 6 d after implantation.

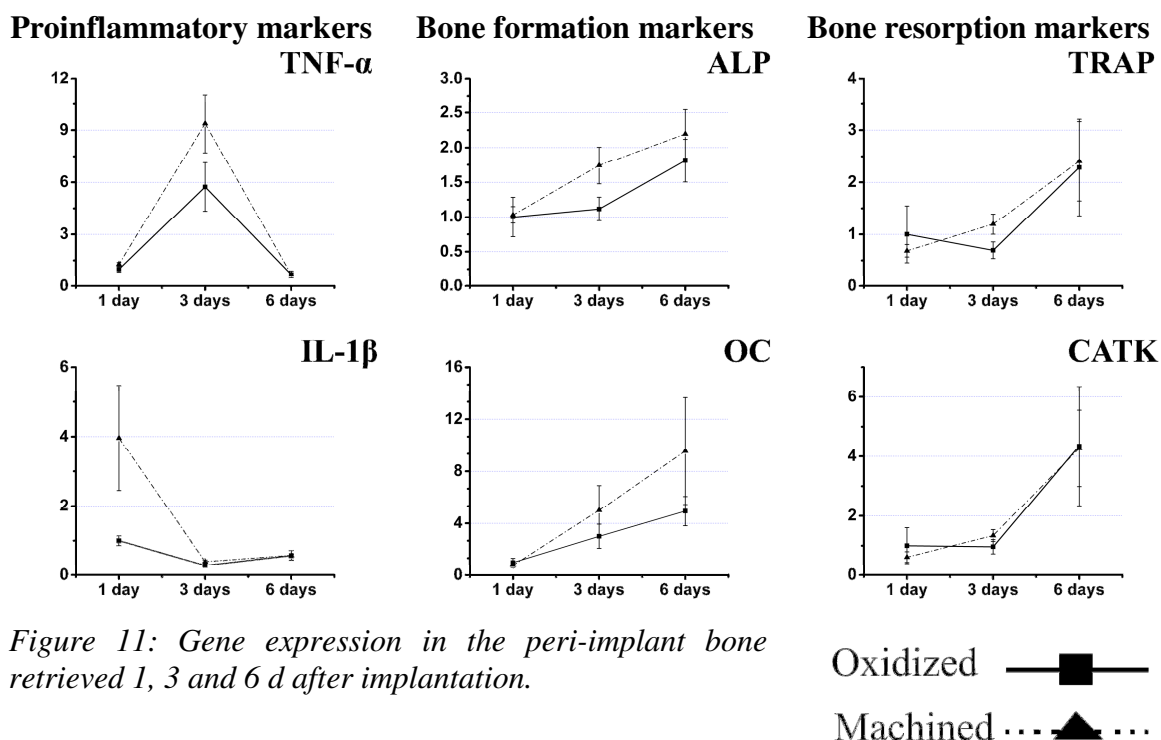


Figure 11: Gene expression in the peri-implant bone retrieved 1, 3 and 6 d after implantation.

### Scanning electron microscopy of the implant-adherent cells

At all the time points the oxidized surface showed better organization of tissue attached to the implants and more attached mesenchymal cells. At 6 d (Figure 12a, b), tissue adherent to the machined implant was loosely attached to the surface and less organized than that seen at oxidized surface. Numerous erythrocytes and white blood cells were captured within the fibrin-like tissue at different locations of the implant. On the other hand, SEM imaging of oxidized implants retrieved after 6 d (Figure 12c, d) showed fairly



organized tissue with bundles of collagen forming a mesh and mesenchymal-like cells on most parts of the implant surface.

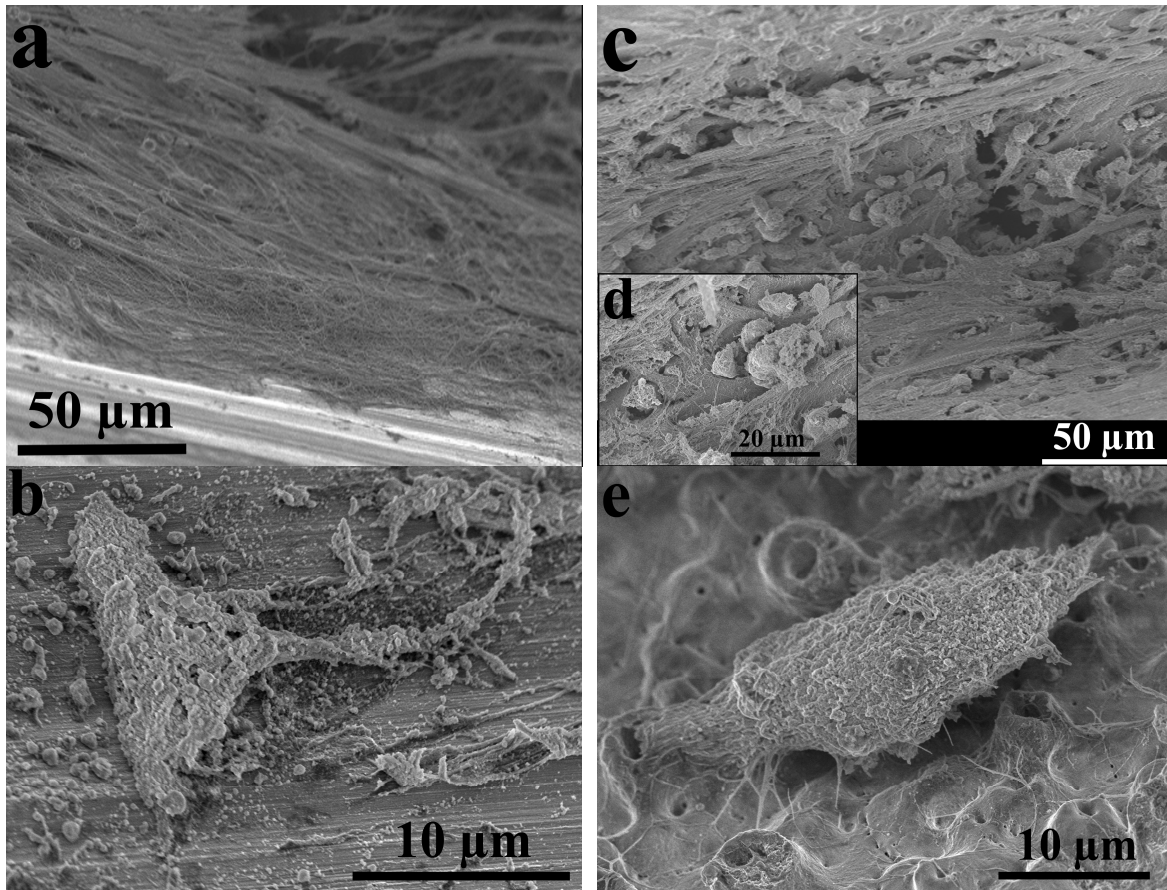


*Figure 12: SEM images of machined and oxidized implants retrieved 6 d after implantation. (a) Fibrinous mesh covered large part of the machined implant surface. (b) Infrequently, mesenchymal-like cells were observed at the machined surface. (c and d) Well-organized collagen network with numerous mesenchymal-like cells were observed on the oxidized implant. (e) Mesenchymal-like cell on the oxidized surface assuming more rounded shape with firm anchorage of cell extensions onto the pores of oxidized surface.*

### **Histology and immunohistochemistry of the interface**

For both types of implants the tissue located inside the threads was well organized and different cellular populations could be distinguished 3 d after implantation (Figure 13). The oxidized implants appeared to show a higher degree of vascularity and organization compared to machined implants. Substantial new bone formation was observed for both implant surfaces 6 d after implantation (Figure 14). Immunohistochemical studies showed high reactivity of the periostin (a marker for osteogenic cells and bone formation) throughout the regenerated tissue at both implant surfaces. Osteoblasts lining bone trabeculae stained strongly for periostin. Positively stained cells were also localized at interface. Macrophages, labeled positively with CD163 antibodies, were also scattered in the newly organized tissue within the threads.

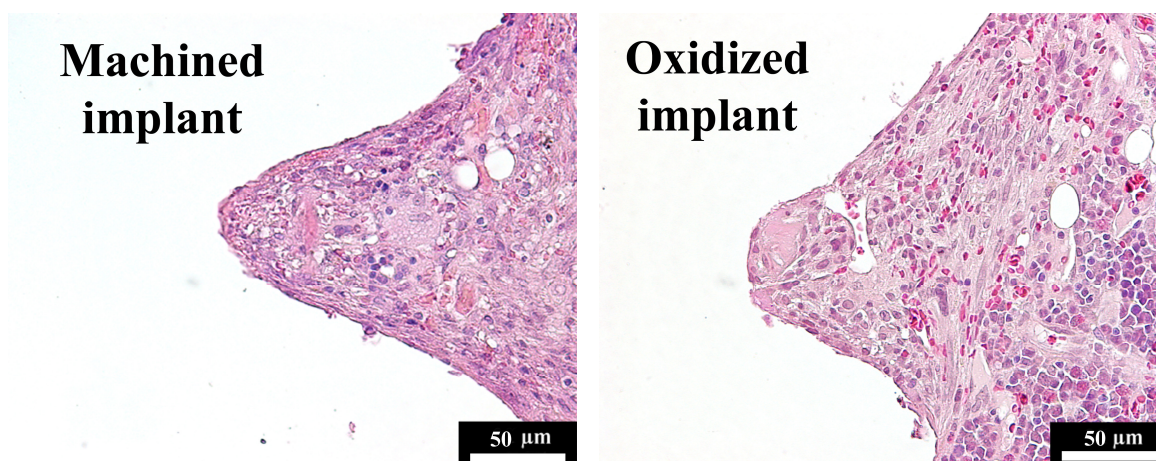


Figure 13: Decalcified paraffin-embedded and H&E stained sections of tissue-implant interface after 3 d of implantation (the implants are removed).

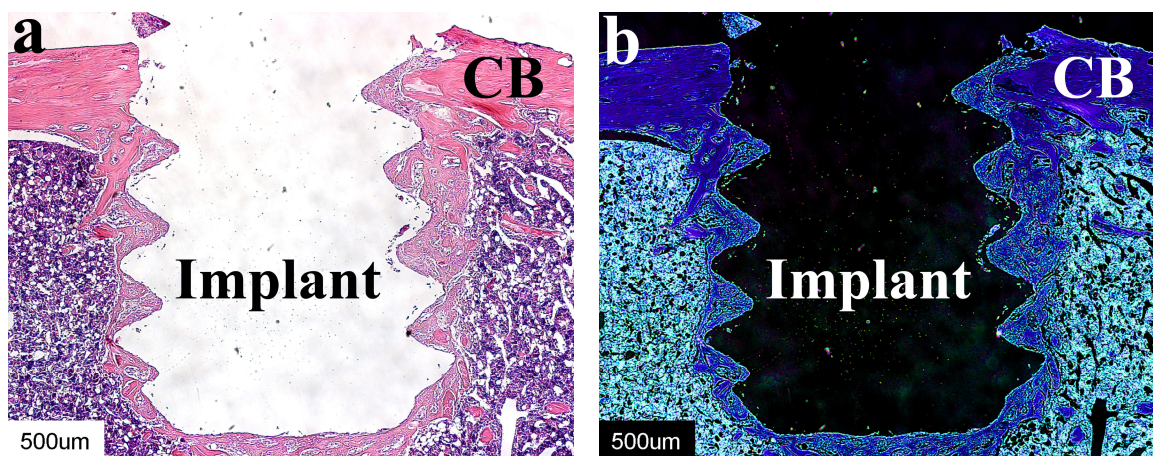


Figure 14: Decalcified paraffin-embedded and H&E stained section of tissue-implant interface 6 d after implantation (the implant is removed). (a) Bright-field. (b) Dark-field. The images show the newly formed bone almost all over the implant surface. The implant was unicortically inserted in the cortical bone (CB) of tibial metaphysis.

## Cellular and molecular activity during first month of implantation (paper IV)

### Gene expression in implant-adherent cells

The results are presented in Figure 15. IL-1 $\beta$  was significantly higher at the machined implants by factors of 3, 2.4 and 2.3 after 6, 14 and 28 d of implantation, respectively. The expression of TNF- $\alpha$  was higher by factors of 3 at the machined implants after 6 and 28 d of implantation. No significant difference in the cellular expression of ALP was detected between machined and oxidized implants at all evaluation periods. On the other hand, higher expression levels of OC were detected at the oxidized implants compared to the machined ones during all evaluation periods. This was indicated by 5.4-, 3- and 2.8-fold upregulated expression of OC at the oxidized implants after 6, 14 and 28 d, respectively. Statistically significant difference was also detected for the transcriptional

factor, Runx2, at the 28 d with higher expression by 1.7-fold at the oxidized implants. Oxidized implants were further associated with higher expression of bone resorption transcripts and this was demonstrated by about 2.5-fold upregulated expression for TRAP and CATK at the oxidized implants 6 and 14 d after implantation. At the 28 d, whereas CATK expression revealed comparable levels at both surfaces, the expression of TRAP kept twofold higher expression at the oxidized surface. Temporally, there were no statistically significant differences in the temporal courses for all genes at the machined implants. No major changes were detected in the temporal courses for the proinflammatory cytokines and OC at the oxidized implants. On the other hand, ALP demonstrated significant decrease from 6 to 14 d and kept constant level thereafter. Both CATK and TRAP showed constant temporal expression from 6 to 14 d and then significantly decreased at the 28 d.

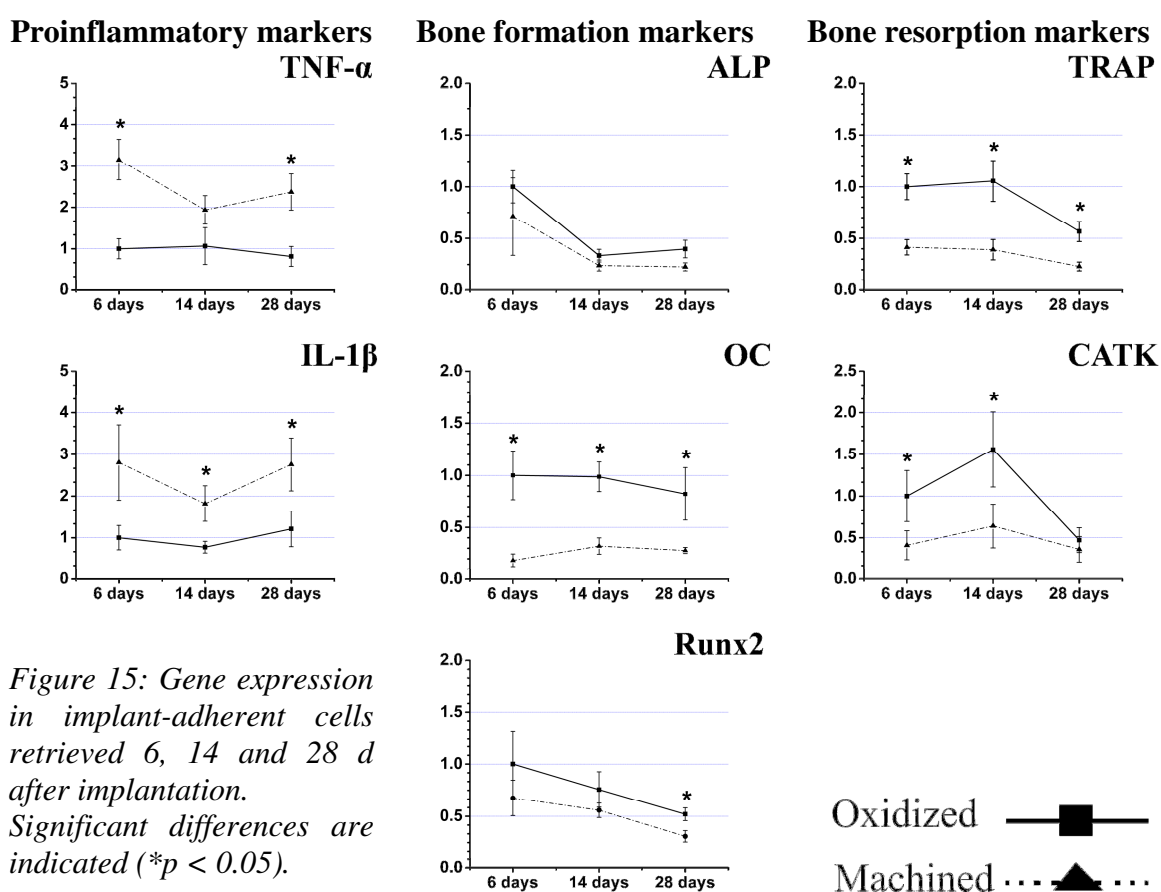


Figure 15: Gene expression in implant-adherent cells retrieved 6, 14 and 28 d after implantation. Significant differences are indicated (\* $p < 0.05$ ).

### Gene expression in the peri-implant bone

In contrast to gene expression during the early periods 1, 3 and 6 d (paper II), significant differences in gene expression levels were observed between peri-implant bone collars of machined and oxidized implants after 14 and 28 d (Figure 16). At 14 d period, IL-1 $\beta$  and CATK revealed higher expression in the peri-implant bone of machined compared to oxidized implants. At 28 d, TNF- $\alpha$  and IL-1 $\beta$  expression levels were about 3-fold higher in the peri-implant bone of the oxidized implants compared to the machined ones. At the same time, higher expression levels of Runx2 and ALP, by factor of 2 and OC, by factor



of 3 were detected in peri-implant bone of the oxidized implants. Similar expression levels of TRAP and CATK were observed in bone related to both implant types after 28 d. Temporally, peri-implant bone of the oxidized implants revealed upregulation of both inflammatory cytokine genes and osteoblastic genes from 14 to 28 d while osteoclastic genes revealed a trend for downregulation. Similar trend for downregulation was also observed for osteoclastic genes and OC in bone related to the machined implants, whereas all other genes revealed a relatively constant expression.

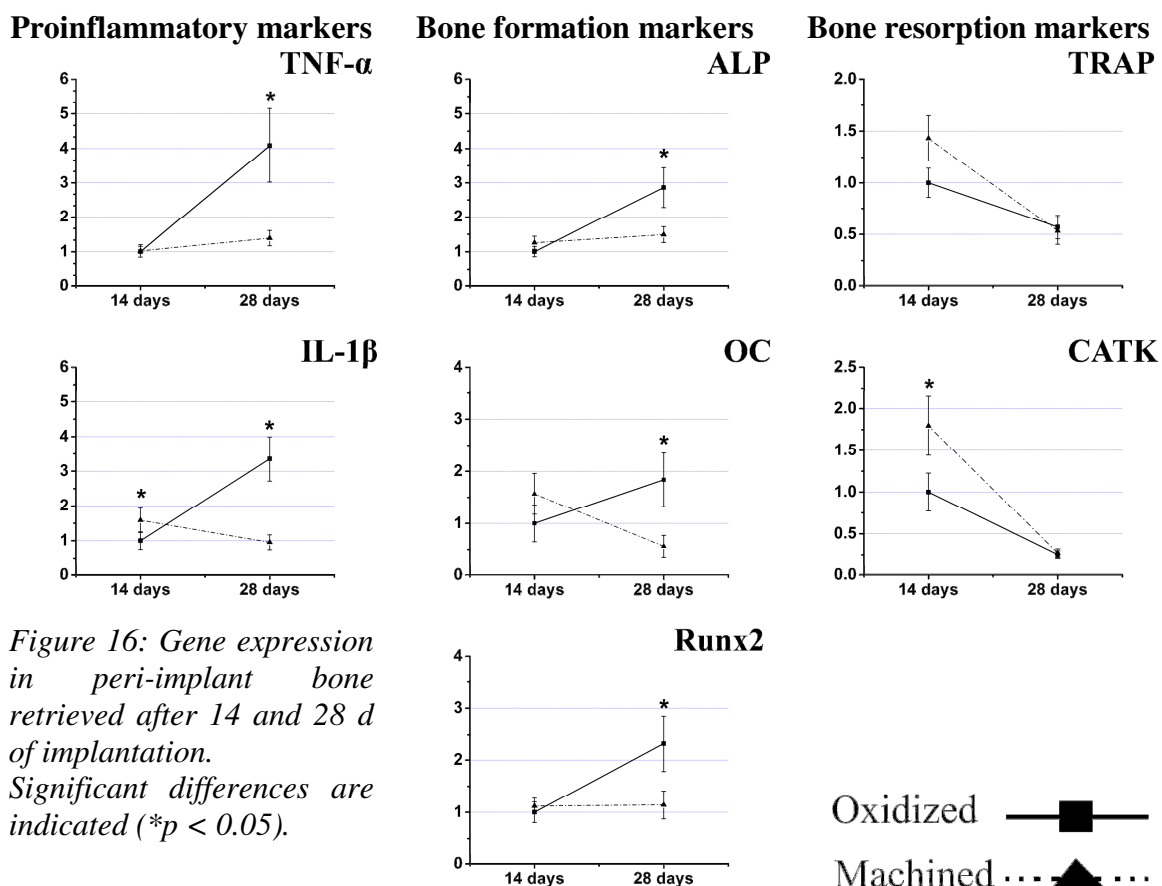


Figure 16: Gene expression in peri-implant bone retrieved after 14 and 28 d of implantation. Significant differences are indicated (\* $p < 0.05$ ).

### Biomechanical evaluation (paper IV)

In comparison to machined implants, significantly 170 % and 190 % larger removal torque values (breakpoints) were recorded for the oxidized implants after 14, and 28 d, respectively (Figure 17). Oxidized implants showed mean values of 3.37, 6.84 and 9.68 Ncm, while machined implants showed means of 1.4, 2.5 and 3.33 Ncm after the evaluation periods 6, 14 and 28 d, respectively. Significant temporal increases for the oxidized implants were, 102 % from 6 to 14 d and 41 % from 14 to 28 d. The resultant overall increase from 6 to 28 d for the oxidized implants was 187 %. On the other hand, the slightly increased removal torque for the machined implants was not significant during the all periods of evaluation. The tested implants showed distinctly different patterns of deformation (Figure 18). At all time points, machined implants showed a relatively similar load-deformation plot with less well defined break point and long

plateau phase. The oxidized implant curve showed sharp torque increase at larger torsion angles and distinct breakpoint with shorter or no plateau period.

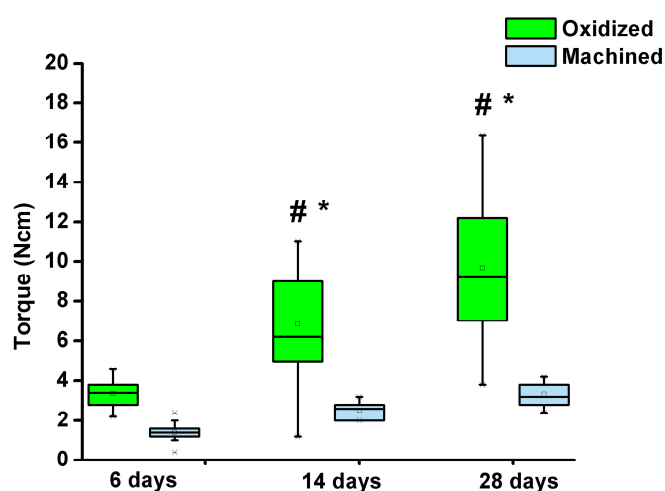


Figure 17: Removal torque analysis of the machined and oxidized implants. The box shows median, standard deviation and the range of values for each type of implant and time point. Mean values and standard error of the mean are given in the text.

\* $p < 0.05$  indicates significant differences between the mean values of the two implant types; # $p < 0.05$  indicates significant differences between different time points for each implant type.

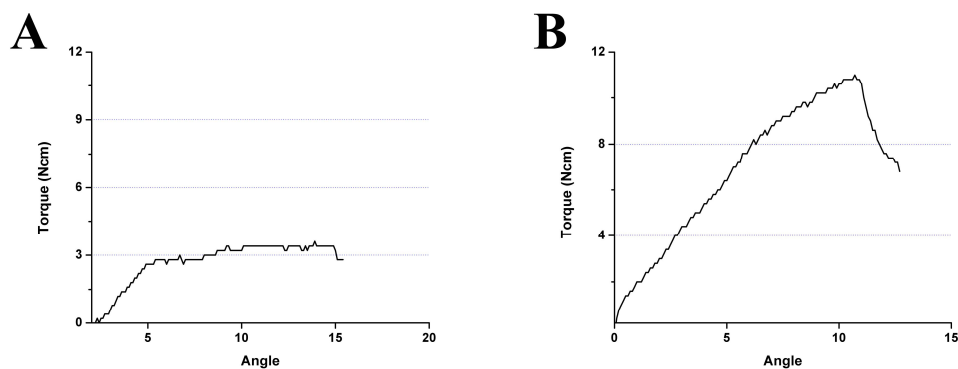


Figure 18: Typical load deformation curve for machined (A) and oxidized implants (B), 28 days after implantation.

## Histology and backscattered scanning electron microscopy (paper IV)

The histological evaluation in paper IV showed comparable appearance for the interface for machined and oxidized implants 28 d after implantation (Figure 19). Endosteal bone downgrowth was observed for all sections, irrespective of implant type. Remodeling within the original cortical bone as well as in the endosteal downgrowth was also evident.

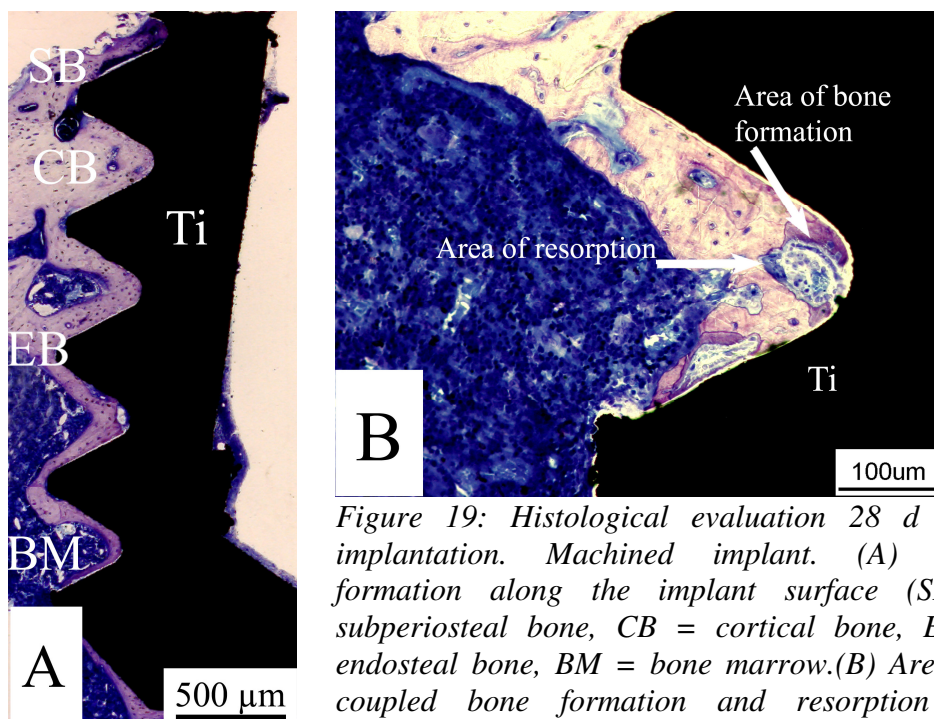


Figure 19: Histological evaluation 28 d after implantation. Machined implant. (A) Bone formation along the implant surface (SB = subperiosteal bone, CB = cortical bone, EB = endosteal bone, BM = bone marrow). (B) Areas of coupled bone formation and resorption are observed within the thread.

The implants in Figure 20 had been subjected to the removal torque. For the machined implants, the separation between the implant surface and the adjacent bone was not determined if it is due to the removal torque or an artifact due to sample preparation. However, no fracture lines were evident for the machined implants. For the oxidized implants, fracture lines appeared at many locations perpendicular to the implant surface.

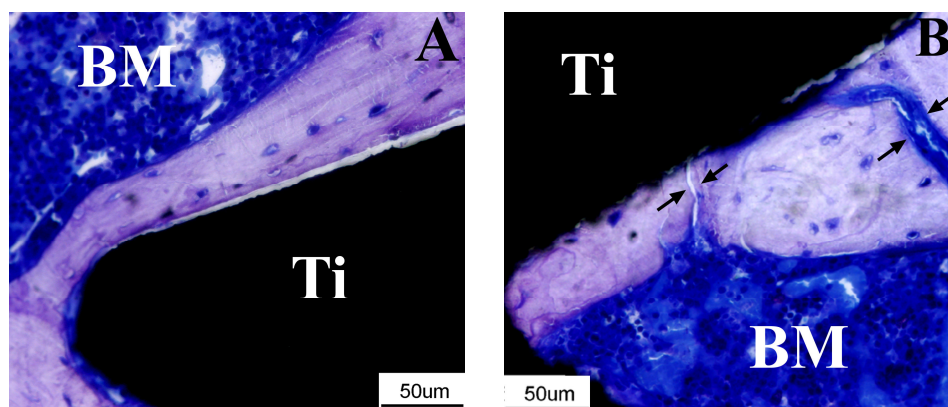


Figure 20: Light microscopy images for the titanium implants after torque removal test. (A) Machined implants. (B) Oxidized implants (fracture lines are indicated by arrows. Ti=titanium, BM=bone marrow).

Backscattered SEM evaluation of non-torqued implants (Figure 21) showed that the threads contained mineralized bone with typical osteocyte lacunae and blood vessel spaces. Often machined implant was separated from bone by a narrow gap (Figure 21A,

B). Direct contact of the bone with the oxidized implant was detected with generalized bone ingrowth into different sized micropores (Figure 21C, D).

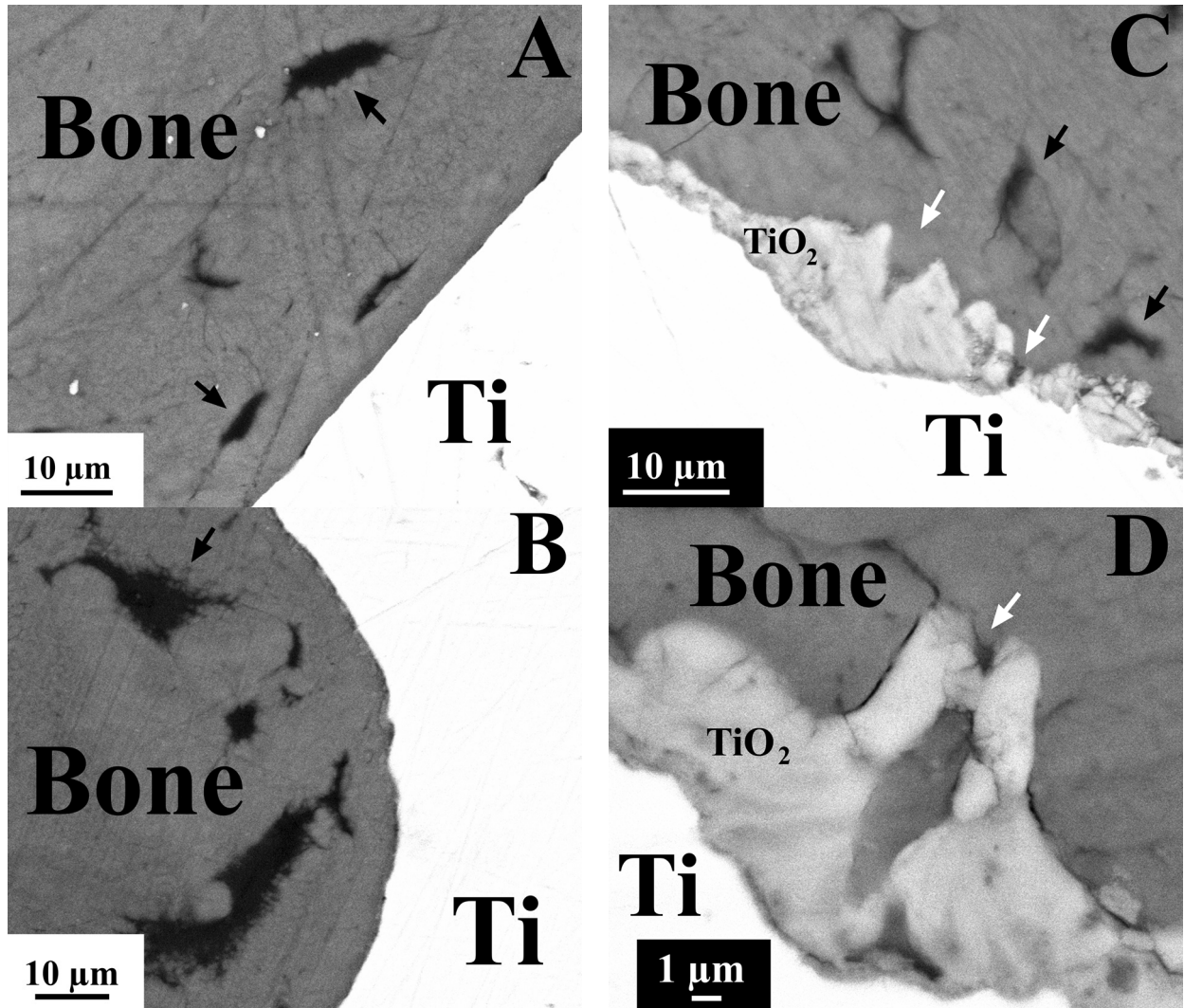


Figure 21: Backscattered SEM images (A and B) Machined implants. (C and D) Oxidized implants. The black arrows indicate some osteocyte lacunae. The white arrows indicate bone ingrowth.

### Correlations between expression of individual genes and between individual genes and biomechanical torque (paper IV)

After 28 d, gene expression in cells adherent to oxidized implants (Table VII) showed statistically significant correlation between Runx2 and all other genes except for IL-1 $\beta$ . Significant correlation was also detected between bone formation and bone resorption gene expression. No significant correlations were observed between the expression of individual genes at the machined implants except the significant positive correlation between TNF- $\alpha$  and Runx2 expression (data not shown).

No significant correlation was demonstrated between any of the analyzed individual gene expressions and the torque values after 28 d, irrespective of implant type.

*Table VII: Correlation analysis of genes expressed at the oxidized implants 28 d after implantation. Pearson correlation coefficients and p-values are presented.*

	<b>TNF-<math>\alpha</math></b>	<b>IL-1<math>\beta</math></b>	<b>ALP</b>	<b>OC</b>	<b>TRAP</b>	<b>CATK</b>	<b>Runx2</b>	
<b>TNF-<math>\alpha</math></b>		.351	.838	.876	.751	.641	.841	Pearson
		.319	.002	.001	.012	.046	.002	Sig.
<b>IL-1<math>\beta</math></b>			.368	.115	.519	.808	.357	Pearson
			.296	.752	.124	.005	.311	Sig.
<b>ALP</b>				.932	.966	.802	.975	Pearson
				.000085	.000005	.005	.000002	Sig.
<b>OC</b>					.828	.605	.917	Pearson
					.003	.064	.000192	Sig.
<b>TRAP</b>						.860	.952	Pearson
						.001	.000022	Sig.
<b>CATK</b>							.775	Pearson
							.008447	Sig.



## Discussion

### ***In vivo interfacial gene expression model***

In the present thesis, the combination of quantitative gene expression analysis, immunohistochemistry and biomechanical test was successfully used to analyze the process of osseointegration. In paper I, discrimination between cortical and trabecular bone gene expression was achieved, both constitutively and in response to titanium implants. The initial events of cell recruitment, adhesion and early phase inflammation were the focus of paper II, whereas the osteogenic, osteoclastic and later inflammatory phases were studied in papers III and IV. Furthermore, in paper IV, the molecular events were correlated with the temporal development of implant stability as judged by measurement of interfacial torsional strength.

An advantage with the experimental set-up in paper IV was the possibility to perform biomechanical torsion test on the same implant used for analysis of gene expression. The quality of RNA did not differ between implants that were torqued or not. Further, the torque analysis was performed using an upgraded version of a biomechanical instrument that has previously been applied on similar sized, machined, threaded titanium implants in same rat model [174]. The results for the machined implants in the present thesis were similar to the results after 14 d and 28 d in the latter study.

An advantage of the present method, utilized for the first time, was the possibility of isolating RNA from both the threaded implant surface and the peri-implant bone collar. Gene expression analyses were performed separately on the implant-adherent cells and on the peri-implant bone, allowing for spatial distinction of gene expression at the immediate vicinity to the implant surface from those occurring at some distance. The few available studies on the *in vivo* gene expression at interface have either examined the implant associated cells of disks [187, 188] or the overall expression in the bulk bone-implant unit [189-192]. With the present model, spatial differences were detected in material surface-triggered gene expression during the first week as well as at later time periods. For instance, different implant surface properties resulted in significant modulation of the gene expression in implant-adherent cells, whereas no major differences were detected in the peri-implant bone during the first week of implantation (paper III). After 14 d and 28 d, differences in gene expression between the two material surfaces, were also detected in the peri-implant bone, however, the gene expression fingerprint was not completely similar to that of implant-adherent cells (paper IV). These observations show that material surface properties are rapidly “sensed” by the biological system during the early phase of osseointegration (h - d), and that with time, material-specific differences are also expressed at a distance from the implant surface. In addition, the temporal change of ALP, OC, TRAP and CATK gene expression in the surrounding bone was different than that observed at the surface of the implants. In contrast, a similar time course was observed for the expression of pro-inflammatory TNF- $\alpha$  and IL-1 $\beta$  close to and distant to the implant. These observations suggest that, despite the differences in the magnitude, the inflammatory gene response, but neither the osteogenic nor the osteoclastic, follow similar time course at the immediate interface and some distance to the implant surface.

The distribution and localization of different cells adherent to the implant or in the nearby organizing tissue was qualitatively studied by SEM and immunohistochemistry, respectively. Due to the difficulty to section and perform immunoincubation of intact implant-undecalcified bone specimens, the true relationship between the cells and the implant surface was not possible to determine. Further, in order to determine the immune phenotype of implant surface-adherent cells, additional immunoincubation of the surface adherent cells, e.g. prepared for SEM, would probably have been providing additional data on the specific cell types in the interface.

### ***Gene expression in trabecular and cortical bone types***

Hitherto, major structural, mechanical, elemental and different responses to metabolic and hormonal disorders have been identified when comparing cortical and trabecular bone types. In paper I, the hypothesis was that the constitutive gene expression was different between the two different types. Further, it was of interest to determine if the molecular activities in the respective bone types would be differently triggered in response to titanium implants.

### **Steady-state gene expression**

The constitutive gene expression in trabecular, cortico-trabecular and cortical bone sites revealed significant differences with respect to “finger-print” markers of bone formation (ALP and OC), bone resorption (TRAP and CATK) and inflammation (TNF- $\alpha$  and IL-1 $\beta$ ). The differences were detected both in the total gene expression in the retrieved samples as well as in the 18S-normalized expression, indicating the relative expression per cell. In both cases, trabecular bone demonstrated higher levels of osteoblastic and osteoclastic activities and less inflammatory gene expression. In the total expression it was clearly evident that constitutive expression of bone formation and bone resorption decreased with the reduction of trabecular fraction. The normalized expression showed significant differences mainly between the trabecular femoral samples and the cortical tibial ones. The opposite was observed in the expression of TNF- $\alpha$  and IL-1 $\beta$  where both cytokines demonstrated higher expression levels in both tibial sites as compared to femoral trabecular site. Differences in the bone-related protein levels between spinal trabecular and tibial cortical biopsies have been previously reported [35] where trabecular bone showed higher and lower levels of osteonectin and OC, respectively, as compared to the cortical bone. Since the present results on OC are at variance with this finding, possible feedback mechanisms controlling the gene expression levels may be operative. Additionally, osteonectin has been reported to be critically effective modulator for the steady-state remodeling [193] which could explain the higher remodeling gene expression activity observed in the present data. In other reports, higher level of the BMP-2 gene expression was detected in epiphyseal trabecular bone than in cortical distal diaphysis of human femur [36].

### **Gene expression at cortical and trabecular bone interfaces with oxidized implants**

In response to the oxidized implants, trabecular bone expressed a higher level of IL-1 $\beta$ , whereas the implants in cortical bone were associated with higher expression of ALP and OC. The reason behind this reversal in the expression of some gene levels from their constitutive expression is not clear. It may be that different stimulation of osteogenic or inflammatory cells, in response to the surgical trauma and/or the presence of implant, in the two different bone environments would affect one type of cells which consequently regulate the other type. This would lead to a second question if there are important roles of cellular cross-talk between osteoblastic and inflammatory cells in such events? Emerging scientific data have shown important regulatory effects of osteoblasts on hematopoietic cells [19] and *visa versa* [109]. Bone type-specific mechanisms may involve signaling from osteogenic cells to existing inflammatory cells to change e.g. the cytokine environment. Transgenic mice targeted to express higher levels of M-CSF by osteoblasts, showed increased bone formation and thickness only in the cortical distal area of femur whereas the trabecular proximal area was not affected [194]. A second possible mechanism is that the upregulated expression of pro-inflammatory cytokines, such as TNF- $\alpha$ , in the trabecular bone environment may lead to inhibition of key osteogenic differentiation factors. For instance, *in vivo* [59] and *in vitro* [62, 195] studies have shown negative effects of TNF- $\alpha$  on the osteogenic response by the inhibition of Runx2. Nevertheless, and in order to approach such questions, it needed to further explore the two different bone types including additional time points and analyzing other cytokines and differentiation factors.

The demonstrated differences in the expression of genes important for inflammation and bone formation/remodeling could be important for explaining previous differences detected between cortical and trabecular bone with respect to implant performance (bone area, bone density and bone-implant contact). However, the available studies on such differences are largely contradictory. Whereas some authors have noticed a superior response of trabecular bone over the cortical type [196-198], others have proved stronger bone formation at implants in cortical bone locations [199-201]. Studies on oxidized implants with and without phosphorylcholine coating showed that the peri-implant bone density, within as well as immediately outside the implant threads, was considerably greater at the tibial cortical sites than at the femoral trabecular sites [200]. In another study [202], machined and anodically oxidized implants were inserted in cortical and trabecular bone sites of rabbit tibia and evaluated after 1 month of implantation. The results revealed significantly higher bone contact for the oxidized implants over the machined ones in both cortical and trabecular sites. On the other hand, the oxidized implants were associated with higher bone area only in cortical sites while no differences to machined implants were detected in the trabecular sites.

## ***Interfacial gene expression at machined and oxidized implants***

### **Gene expression at the interface: Initial inflammation, cell recruitment and adhesion**

In paper II (first 24 h after implantation), the material-specific and temporal pattern of gene expression of factors implicated in cell migration and adhesion was evaluated. This early phase coincided with a major influx of inflammatory cells after implantation. Results showed, for the first time, that the *in vivo* expression levels of members of chemokine system at the interface between materials and bone were largely influenced by the different implant surface properties. For both implant surfaces, significant temporal upregulation of IL-8R and MCP-1 gene expression was observed from 3 to 12 hours after implantation. IL-8R is a chemokine receptor involved in recruitment of PMN by binding to a specific chemokine IL-8 whereas MCP-1 is a major chemoattractant protein for monocytes/macrophages. Whereas the expression of IL-8R showed significant downregulation after 24 h for both surfaces, MCP-1 expression was continuously increasing at machined but not oxidized surfaces. These results are in agreement with previous *in vitro* studies on the participation of leukocyte subsets using titanium plates with different surface oxide thickness and roughness in contact with human blood [203]: a predominance of PMN during the first hours, subsequently decreasing to low numbers for all surfaces after 24 h of contact. In contrast, the number of monocytes increased to reach a peak after 24 h. At this time point, significant differences in the number of monocytes were detected between the different surfaces. The results obtained in the present *in vivo* model and the previous *in vitro* studies are consistent with the transient nature of PMN. Furthermore, the results demonstrate a strong influence of material surface properties on the accumulation of monocytes during the first 24 hours. The temporal expression profile for MCP-1 was similar to the expression of proinflammatory cytokines TNF- $\alpha$  and IL-1 $\beta$  suggesting that the recruitment of inflammatory cells was accompanied by cytokine activity at both material surfaces, but the prolonged signal of monocyte recruitment by the MCP-1 was coupled with prolonged expression of proinflammatory cytokines at the machined implants.

Immunohistochemical sections and SEM images of the retrieved implants showed CD163-labeled monocytes/macrophages together with periostin-positive osteoprogenitor cells. A general observation in all sections was that a large amount of fibrinous material covered the machined implants. Fibrin has been shown to enhance the proinflammatory response to biomaterials [204] which might explain the upregulated proinflammatory cytokine expression at this surface as early as 3 and 24 h (paper II) and at later time periods (paper III).

One of the major observations during the initial 24 h was the significant modulation of the chemokine receptor CXCR4 (paper II). As with other chemokines, the present study provided the first set of data on the expression of this chemokine receptor at titanium implants in bone. Already after 3 h there was significant expression of this receptor at both implant surfaces, however the expression thereafter was differently modulated depending on the implant surface. Whereas an upregulated level was demonstrated at oxidized implants after 12 h, a significant reduction was observed at the machined implants making 11-fold difference with the level at the oxidized implants at this time

point. From 12 to 24 h, CXCR4 expression was decreased at the oxidized surfaces while increased at the machined surfaces, being at comparable level at the two implant surfaces at 24 h. CXCR4 together with its exclusive ligand, chemokine SDF-1 $\alpha$ , form an important migration axis for both hematopoietic and mesenchymal stem cells and has recently gained significant attention as a major axis for local and systemic recruitment of MSCs to sites of tissue repair and regeneration [75, 205-207]. Blocking of CXCR4 significantly inhibited *in vivo* migration of circulating ALP positive osteoblast progenitor cells to subcutaneously implanted BMP-2 containing collagen pellets. Together with other evidences, the results strongly suggested that CXCR4 on the progenitor cells react with SDF-1 to induce their migration to the region of regenerating bone [208]. This study was further corroborated with bioluminescence imaging, demonstrating that MSC migration to a fractured tibia site was highly dependent on CXCR4 in a time- and dose-dependant manner [209].

Integrins contribute to the processes of chemotaxis, cellular adhesion and activation and cell-cell contact. The attachment to a surface is one of the first critical steps in the cell response to a biomaterial [147]. The results in paper II showed that, for both types of implants, all analyzed integrins showed peak expression at 12 h except for integrin- $\alpha$ v expression at the machined implants which peaked after 24 h. The early association between the upregulated expression of chemotactic signals and the expression of integrins has been documented [210]. It is therefore hypothesized that chemotactic signals and integrins have decisive roles in the recruitment of different cells toward the implant surface during the healing process, subsequent matrix deposition and bone formation. For instance,  $\beta$ 2 has been shown to be important integrin for rolling, adhesion and transvessel migration of leukocytes during chemotaxis [211]. Similarly, integrin- $\beta$ 1 has been suggested to be important for MSCs recruitment in the same manner as for hematopoietic cells [212]. In the present thesis, the correlation analysis of gene expression at the oxidized surface during the 24 h period revealed significant positive relationship between the expressions of chemokines and integrins. Particularly, IL-8R was in correlation with integrins- $\beta$ 2 and  $\beta$ 3 whereas MCP-1 showed correlation with all integrins except integrin- $\alpha$ v. On the other hand, CXCR4 exhibited association with integrin- $\beta$ 1 which with the increased expression of osteogenic markers demonstrated in study III and the higher number of mesenchymal cells, as shown in SEM observations, altogether suggests that the oxidized implant was associated with higher recruitment of MSCs through mechanisms which involve modulation of CXCR4 chemokine receptor and integrin- $\beta$ 1 expression. In contrast, strong correlation was revealed between CXCR4, IL-8R and integrin- $\beta$ 2 (specific for leukocytes) at the machined implants. Taken together with the prolonged and upregulated expression of proinflammatory cytokines (paper II and III), a potential role of CXCR4 and IL-8R expression for leukocyte activation is suggested.

Implant surface properties significantly influenced the level of expression of different integrins evaluated in paper II as demonstrated by the finding that oxidized implants were associated with about 2-fold higher expression levels of integrins  $\alpha$ v,  $\beta$ 2 (after 12 h) and  $\beta$ 1 (after 24 h). *In vitro* studies have demonstrated major influence of material surface properties on the patterns of cell attachment and integrin expression [148, 150, 160, 164, 213-215]. Hitherto, no *in vivo* data has been provided on the role of integrins for cell attachment to implant surfaces. At late time periods, T-shaped hollow titanium implants

treated with sulphuric and hydrochloric acids and implanted in rat femur showed higher expression levels of  $\beta 1$  and  $\beta 3$  integrins in the bone formed within the implants after 1 week in rat femur compared to bone related to the machined implants and in the non-implant defect [190]. In another study by the same research group [192], the T-shaped dual acid etched implants revealed 3- to 7-fold and 2- to 4-fold increased expressions of  $\beta 1$  and  $\beta 3$  integrins in the implant-associated bone compared to native bone and bone defects without implants after 2 and 4 w of implantation in rat femur. In the same study, ovariectomized rats were also operated and the expression of integrins  $\beta 1$  and  $\beta 3$  in the implant bone was lower in the ovariectomy group compared to the normal rats. Interestingly, the expression of the two integrins in the ovariectomy group was neither affected in the native bone nor in the defect site, as compared to the normal rats.

The present upregulated expression of specific integrins may reflect specific temporal and conformational changes in protein adsorption influenced by the physico-chemical properties of the surface. In vitro observations on the stromal cell response to different proteins precoated on tissue culture plastics showed protein-specific expressions of integrins  $\beta 1$ ,  $\alpha v$  and  $\beta 3$  [216]. It was also shown that osteoblast-like cells growing on orthopedic materials appear to be capable of attaching directly to implant materials through integrins, whereas the type of substrate determines which integrins and extracellular matrix proteins are expressed by these cells [217]. The latter in vitro data have also shown that, among many upregulated integrins, integrin- $\beta 1$  was the integrin subunit with the greatest increase on a variety of substrates compared to the base-line expression. Using small interfering RNA (siRNA), integrin  $\beta 1$ -silencing inhibited the positive effects of titanium surface roughness on the activity of ALP and the secretion levels of OC, TGF- $\beta 1$ , prostaglandin E2 and OPG [218]. Due to the complex multi-protein and cellular in vivo environment it should be kept in mind that there is no specific or cell-limited expression of integrins and all cells express various integrins in different combinations depending on their stage of maturation, activity and the intermediate protein between different cells and the implant surface. Some integrins have lineage-specificity. For instance, integrin- $\beta 2$  has been shown to be specific for leukocytes [81] and not expressed by cells of osteoblastic lineage [80]. Integrin-  $\beta 2$  [83] and integrin  $\alpha v$  [23, 219] have also been shown to have important role in osteoclastogenesis. The upregulated expressions of these integrins at the oxidized surface suggest their involvement in the upregulated expression of osteoclastic activity at the oxidized surfaces observed during later periods in paper III.

### **Inflammatory, osteogenic and osteoclastogenic gene expression at the interface**

Over the following periods (i.e. from 1 – 28 d), gene expression in implant-adherent cells was analyzed after 1, 3 and 6 d (paper III) and 6, 14 and 28 d (paper IV). Two distinctive phases of expression characterized each period.

In the early period (i.e. during the first week of implantation) (III) both types of implants demonstrated higher expression levels of proinflammatory cytokines, TNF- $\alpha$  and IL-1 $\beta$ , at the first day and significantly lower levels at d 6 after implantation. Generally, the temporal modulation of both proinflammatory genes did not change significantly from d 1 to d 3.

Comparatively, similar results were observed after drill-hole injury without implants in the proximal tibia [98]: peaks of IL-1 $\beta$  and TNF- $\alpha$  were detected after 16 h and 1 d, respectively, and decreased to minimum levels 7 d after injury. These results reflect the early acute and transient inflammation induced by the tissue injury.

A prominent finding in the present study was that the magnitude of inflammatory cytokine expression was significantly modulated by the implant material properties. This was shown by the 5- and 3-fold lower expression level of IL-1 $\beta$  at the oxidized implants in comparison with machined implants after 1 and 6 d, respectively.

Albeit speculative, the temporal modulation of TNF- $\alpha$  at the oxidized implant surface may be important for the osteogenic and osteoclastogenic differentiation since the peak of TNF-expression (after 3 d) coincided with the highest peak expression of ALP, OC, TRAP and CATK (after 3 d). This assumption was supported by the correlation analysis for expression of genes after 3 d at the oxidized implants where significant correlations were observed between TNF- $\alpha$  and Runx2, ALP, TRAP or CATK. Such correlation was not revealed at machined implants. A similar temporal upregulation of TNF- $\alpha$ , showing an early peak of expression after 5 – 7 d in a rat femur ablation model, was associated with peaks of ALP, collagen I, osteonectin, OC, cbfa1/Runx2 and CATK after 5 – 7 d [43]. Moreover, TNF- $\alpha$  is critical for intramembranous bone formation in vivo [51] and increases MSCs migration and proliferation in vitro [58]. On the other hand, whereas the recruitment and proliferation of MSCs was reduced, the expression of transcription factor Runx2/cbfa1 and OC and trabecular bone formation was increased by local inhibition of TNF- $\alpha$  after drill-hole injury [59].

In the late period (i.e. between 6 and 28 d after implantation) (paper IV), the expression of TNF- $\alpha$  and IL-1 $\beta$  was relatively constant for both machined and oxidized implants. Correlating these levels with levels presented in the paper III (1, 3 and 6 d) was not possible since the two analyses were performed separately. A major observation, similar to what was observed during the early (1 d – 6 d) period, was a significantly higher expression of TNF- $\alpha$  and IL-1 $\beta$  detected for machined implants 6 d – 28 d. The significantly lower levels of expression of both cytokines at the oxidized implants (in range of 2- to 3-fold lower expression levels in comparison with machined implants) suggest major role of the physico-chemical properties of the implant surface for influencing the expression of cytokines even after the earlier phase of woven bone formation has been established. This observation is at least partly in agreement with recent studies in an experimental rabbit model [187]. Gene expression in cells adherent to coin shaped titanium implants blasted with TiO<sub>2</sub> particles with or without hydrofluoric acid demonstrated a significant increase in anti-inflammatory IL-10 expression for hydrofluoric acid treated implants between 4 and 8 weeks. Further, titanium implants with medium hydrofluoric acid treatment were associated with lower expression levels of TNF- $\alpha$  and IL-6 and higher expression of IL-10 in comparison with other surface modifications and control 4 w after implantation [188].

In parallel with temporal downregulation of the proinflammatory gene expression during the first week period (study III), a significant temporal upregulation of genes associated with osteoblastic and osteoclastic phenotypes was demonstrated. Peak expression for ALP, OC, TRAP and CATK was detected 3 d after implantation. Previous studies in

bone fracture model (without implants) in rat have shown that ALP and OC expression attained their peaks after 5 d and 11 d, respectively [39]. Further, in a rat femur ablation model, the ALP and OC expression peaked after 5 d and 7 d, respectively [43]. Osteoclastic gene expression levels of TRAP and CATK have been shown to attain their earliest peaks between 7 – 14 d and gradually decrease to lower levels during the following weeks in bone fracture model [120, 134]. The present observations that the peak expression of osteogenic and osteoclastic markers was detected as early as 3 d at the implant surface and that oxidized implants were associated with significantly higher levels than machined implants indicate, firstly, that bone remodeling around implants starts much earlier than what has previously been assumed (mainly based on conclusions from fracture models and in vitro experiments with one cell population), and, secondly, that the implant surface has an influence on the level of expression of bone differentiation and remodeling markers. Possible mechanisms for the accelerated implant-associated bone response include multiple cell participation and cross-talk, influenced by material surface physicochemical properties and topography and the size and micromechanics of the bone defect.

In the present thesis, the oxidized implants, which showed enhanced osteogenic gene expression, were characterized by relatively higher roughness values and thicker oxide layer in contrast to the machined implants. These observations are corroborated by morphological studies showing that anodic oxidation of electropolished titanium surfaces, which produced areas of increased roughness on the submicrometer scale and a thicker surface oxide, had an enhancing effect on the rate of bone formation [220]. Furthermore, the surface chemical analysis, performed in paper IV, revealed substantial amount of phosphorus, both in the outermost layer and deeper along the oxide layer, which together with increased roughness and oxide thickness, might synergistically influenced the osteogenic differentiation. The incorporation of elements in the implant surface has been suggested to improve the early osteogenic gene expression [221], bone contact and biomechanical capacity [222-226] in vivo. For example, an increased expression of osteogenic differentiation markers, Runx2, ALP and BSP, was detected at blasted/hydrofluoric acid treated implants in comparison to blasted implants separated from dissected rat tibia 7 d after implantation [221].

In the present thesis (study IV), the triggering effects of the altered surface properties was also revealed at the later periods of osseointegration. The increased expression of coupled bone formation and bone remodeling markers at the oxidized implants suggests that surface-elicited gene expression was not only limited to the early cellular differentiation and woven bone formation but extended during the major remodeling and maturation phase. On the other hand, a significant decrease in TRAP and CATK expression was observed after 28 d, indicating a decrease in bone remodelling. A coupled upregulation of osteoblastic (OC) and osteoclastic (TRAP) genes was also observed for 0.01 % hydrofluoric acid treated coin-shaped titanium implants after 4 w in a rabbit tibia model [188]. Further, the present data are in agreement with observations on a higher OC expression in bone harvested from dual acid etched hollow implants compared to machined controls, 2 and 4 w after implantation in rat femur [191].



Taken together, the results presented in this thesis show that changing the physico-chemical properties of the titanium implants results in significant acceleration and upregulation of genes crucial for bone formation and remodeling during the period of osseointegration. Furthermore, different surface treatments appeared to influence the temporal differences in the upregulated expressions levels. Nevertheless, consideration for the different animal models and different sample types, whether implant-adherent cells or peri-implant bone, should be accounted.

### **Transcriptional and growth factor regulators of interfacial gene expression**

The mechanisms for the revealed implant-induced modulation of different chemokines, integrins and differentiation markers at the immediate interface most likely involves the generation of signaling molecules, which promote the recruitment, adhesion, and activation of mesenchymal stem cells and osteoblast progenitors in addition to cells belonging to the defense system and osteoclasts. A selection of genes were investigated during the early time stage (1 – 3 d) in order to pin-point some of the chemotactic/growth factors which may be particularly important during the early stage and differently expressed depending on the two implant surfaces oxidized and machined. The expression of both PDGF-B and BMP-2, two growth factors known to have chemotactic effects on different cells including mesenchymal cells with osteogenic potential [227], was associated with a significant temporal increase from 1 d to 3 d at oxidized implants. This increased expression was in parallel to an increased expression of ALP and OC during the same time period. These observations are at variance with the finding of significant reduction of BMP-2 during similar period in a rat ulnar fracture model (without implants) [111]. In fact, observations on growth factor expression in fracture model and for machined implants in the present study point to common temporal expression. This is also supported by the present finding of a significantly higher expression level of TGF- $\beta$ 1 at the machined implant after 1 d of implantation, coinciding with high expression of proinflammatory cytokines. TGF- $\beta$ 1 has dual effects and is considered to possess both proinflammatory and anti-inflammatory effects [93, 228].

Differentiation of the recruited mesenchymal cells requires induction of specific transcription factors. Runx2 is a major differentiation factor responsible for committing MSCs toward the osteoblastic lineage. In paper III of the present thesis, the 5-fold upregulated expression of osteogenic differentiation marker ALP and OC were in parallel with about 6-fold higher expression of Runx2 at the oxidized implants compared to the machined ones after 3 d of implantation. Also after 28 d (paper IV) there was a significant correlation between the expressions levels of Runx2 and OC at the oxidized implants with significantly higher levels of the two genes compared to the machined implants.

The parallel increase in expression of Runx2 and osteogenic differentiation markers was also revealed at blasted/hydrofluoric acid etched implants compared to blasted implants after 7 d and 8 w in rat [221] and rabbit [187] tibiae, respectively. Further, machined implants inserted in transgenic mice, lacking osterix, a downstream factor of Runx2, showed lower expression of OC and BSP and reduced bone formation in comparison

with machined implants in mice receiving local administration of virus encoding for osterix [229].

Taken together, these results suggest that implant surface-induced upregulated expression of osteogenic differentiation markers is mediated via a key transcription factor Runx2. The expression of Runx2 was decreasing with time (6 d – 28 d) whereas OC expression was continuously upregulated at this time period for oxidized implants (paper IV). Although Runx2 is crucial for directing pluripotent mesenchymal cells to the osteoblast lineage and triggering the gene expression during early osteoblast differentiation, Runx2 has been suggested not to play a major role in the maintenance of the expression of OC in the mature osteoblast [117]. Further, maximum level of OC mRNA expression in osteoblast cell line was associated with continuous recruitment of Runx2 protein to the promoter region of the OC gene despite low level of Runx2 mRNA [230].

In study III, there was significant upregulation of adipogenic transcription factor, PPAR- $\gamma$ , at the 3 d period. Furthermore, it showed significant switch from 2.5-fold higher expression level at the machined implant after 1 day to about 6-fold higher expression level at the oxidized implants after 3 d of implantation. It is not known if there is any role for the adipogenic differentiation at the implant site, however, PPAR- $\gamma$  has been suggested as important regulator for Runx2 expression via BMP-2 Smad pathway [231].

### **Molecular activities in the peri-implant bone**

In papers III and IV, peri-implant bone revealed different temporal phases of the gene expression than those observed in the implant-adherent cells.

During the first week after implantation (paper III), peri-implant bone revealed two dissimilarities and one similarity with that of implant-adherent cells. Firstly, there was an increase in the expression of osteogenic and osteoclastic markers from 1 d to 6 d. These temporal changes did not match those observed in the implant adherent cells that demonstrated earlier peaks (3 d) for osteogenic and osteoclastic genes. Secondly, no statistically significant differences between oxidized and machined implants were detected for osteogenic and osteoclastic markers in the peri-implant bone. This was also different from what occurred in implant-adherent cells. Finally, a similar pattern of pro-inflammatory expression was detected in peri-implant bone as in implant-adherent cells.

In study IV, gene expression in the peri-implant bone was analyzed after 14 d and 28 d. The analysis of peri-implant bone revealed three dissimilarities and two similarities with that of implant-adherent cells. The dissimilarities were: Firstly, the temporal expression of proinflammatory and osteogenic markers showed significant increase between 14 d and 28 d in peri-implant bone around the oxidized implants. This was different from that observed in cells adherent to oxidized implants where the temporal expression was constant. Secondly, after 28 d, there was significantly higher expression of proinflammatory cytokines in the peri-implant bone of the oxidized implants compared to the machined ones. This was the opposite in the implant adherent cells, where cells adherent to machined implants demonstrated higher expression of proinflammatory cytokines compared to those adherent to the oxidized ones. Thirdly, after 28 d, there was significantly higher expression of ALP in the peri-implant bone of the oxidized implants

compared to the machined ones. This was different from that observed in the implant-adherent cells where no difference was detected in the expression of ALP between cells adherent to machined or oxidized implants. The similarities between peri-implant bone and the implant cells were: Firstly, similar temporal patterns of osteoclastic markers were observed in peri-implant bone as in implant-adherent cells for both implant types. Secondly, similar temporal patterns of proinflammatory and osteogenic markers were observed in peri-implant bone of machined implants as in implant-adherent cells. The differences between the early and late and implant-adherent or distant peri-implant responses may indicate different modes of surface/matrix attachment and/or cell-cell contact/cross talk of inflammatory, osteogenic and/or osteoclastic cells during the early tissue organization phase and at later time when bone matrix is formed and remodeled.

The temporal changes in the peri-implant bone of oxidized implants appeared to be similar to those observed in the tibial drill-hole injury in rat [98] and transverse fracture in mice [232]. In these studies, the proinflammatory cytokine TNF- $\alpha$  showed an early peak after 1 d, followed by downregulation after 7 d, subsequently reaching a second peak after 4 w. Furthermore, OC demonstrated continuous upregulation to reach highest peaks after the 4 w periods. In the latter study, the expression of the osteoclast differentiation gene, RANKL, showed temporal reduction from the 2 w to level comparable to the base-line value 4 w after fracture.

Data from early and relatively late time points during the process of osseointegration of titanium implants, show that the implant surface-induced effect on pro-inflammatory, osteogenic and osteoclastic markers is expressed with a significant delay in the peri-implant bone in comparison with implant-adherent cells. This is supported by the absence of statistically significant differences in gene expression between the implants in peri-implant bone at the early time period 1 d – 6 d. Data from the relatively late time points also indicate that the implant surface-induced effect on implant-adherent cells is continuous throughout the entire process of osseointegration.

### ***Biomechanics and the correlation with the molecular activities at the interface***

In paper IV, the in vivo interfacial gene expression model was combined with removal torsion analysis to determine possible relationship between cellular and molecular events and the biomechanics of the interface. The measurement of the torsional capacity of the interface before failure and the subsequent gene expression analysis on the same implant allowed the analysis of the relationship between the cellular activity and the biomechanical capacity at the interface. Major and significant observations were demonstrated when evaluating the mechanical capacities of machined and oxidized bone/implant interfaces during the process of osseointegration:

1. Breakpoint torque and gene expression in relation to time
2. Deformation curve

A significant and constant increase in the breakpoint torque was registered for the oxidized implants from 6 d to 14 d and from 14 to 28 days. The major explanation for the

observed findings is an increased amount and/or quality of the newly formed bone in direct contact with the oxidized implant surface. This is supported by morphological data showing an increased number of mesenchymal cells, rapid bone formation and extension of bone into the microporous surface and organization of the tissue within threads. In agreement, gene expression analysis demonstrated up-regulation of bone formation genes (ALP, OC). Interestingly, equally early in the process, markers of gene expression of bone resorption (TRAP, CATK) were detected. Correlation analysis of genes analyzed in the present study did not reveal strong correlation for any particular gene with the increased torque at any specific time period, as the correlation coefficients were always below the strong significance. This probably indicate that the improved implant stability is due to the overall generalized modulation of genes in favor of osteogenic differentiation and coupled bone formation/bone remodeling, hence enhanced bone contact and increased implant stability.

The subsequent high expression of bone formation and bone resorption indicated an intense remodeling throughout the time period. Although no measurement of the maturation and bone density was made, a development of a stronger interface than the surrounding bone was suggested by morphological observations of torques specimens. Hitherto, little attention has been focused on the development of interfacial strength and its associated cellular and molecular background. In agreement with the present observations after 28 d, in two recent studies [188, 233], Lamolle et al. compared the expression of different genes and the pull-out force of coin-shaped titanium modified with different hydrofluoric acid concentrations in rabbit tibia after 4 w. The results indicated that the group of hydrofluoric modification was associated with increased pull-out values, increased expression of osteocalcin, collagen I and TRAP and decreased expression of TNF- $\alpha$  and IL-6 in the implant-adherent cells. The interesting observation seen in the present thesis and the previous studies [188, 233] of the increased co-expression of both bone formation and bone resorption genes in the implant-adherent cells reflect the ongoing bone remodeling activity at the implant surface without decreasing the stability of the implant.

In contrast to oxidized implants, the temporal course of the breakpoint torque of the machined implants did not reveal any significant changes during the evaluation periods 6, 14 and 28 d after implantation. This finding is in agreement with a previous study, using similar animal model and biomechanical equipment, which demonstrated that the breakpoint torque values for machined implants did not increase between 14 d and 28 d but increased significantly between 28 d and 16 w after implantation [174]. In the latter study, the breakpoint torque values for the tested machined implants were almost identical as in study IV in this thesis. Similarly, in a recent study in a similar rat tibia model but using different torque setup, machined, dual acid etched and nano/alumina coated titanium implants had comparable results: for all implant types, the torque did not increase significantly after 7, 14 and 21 d of implantation, but thereafter increased significantly at 56 days [234].

On the basis of previous morphological and biomechanical studies of the initial process of osseointegration [153, 174], it has been suggested that one possible mechanism for the initial reduction and/or plateau in biomechanical shear strength of machined implants could be due to a post-surgical inflammation and/or bone resorption. This is partly supported by the present results. In the present study, increased expression of pro-

inflammatory markers (TNF- $\alpha$  and IL-1 $\beta$ ) in cells adherent to machined implants was detected at all studied time periods during the osseointegration process. Prolonged interfacial expression of pro-inflammatory markers and relatively less expression of bone remodeling markers in cells adherent to machined implants did not lead to increased biomechanical strength whereas for oxidized implants prolonged interfacial expression of bone formation coupled to bone resorption with less expression of pro-inflammatory markers promoted a completely different development of biomechanical strength.

The torsion test is assumed to be primarily probing the interface mechanics, since the threaded implant design will first transfer the stresses to the interface region which is weaker than the intact bone [167]. Two differently distinctive deformation curves were observed for the machined and the oxidized implants. The deformation curve for machined implants was qualitatively similar to that observed in previous study at the same time periods in rat tibia [174] and after 56 days in rabbit tibia [235]. This curve was characterized by a moderate increase in the torsion resistance before the breakpoint and was followed by uniform and slightly increased plateau before complete failure was reached. In contrast, oxidized implants showed a completely different form of deformation. The main difference from the machined implant curve was the significantly higher breakpoint which needed higher rotation angle before it was reached. A second difference was the relatively shorter or absent plateau phase before the complete failure. Similar curve has previously been demonstrated for laser-modified titanium alloy implant when evaluated after 6 weeks with similar instrument [235].

Using different torque setup, both sandblasted/acid etched (sulfuric and hydrochloric acids) and machined/acid etched implants showed similar sharp curves after 4, 8 and 12 w in pig maxilla [236]. When the sandblasted/acid etched implant was tested with or without NaCl treatment and storage, the modified surface showed flattening of the curve after 8 weeks in the pig maxilla [169].

Taken together, the present gene expression, morphological and biomechanical results suggest that an optimal local interface environment for osseointegration is characterized by the recruitment of several cell types, promotion of osteogenic differentiation, modulation of inflammation and control of bone remodeling, hence providing an elaborated bone matrix in intimate contact with the implant surface and enhanced mechanical interlocking and/or bone bonding.



## Summary and Conclusions

An experimental in vivo model was developed which enabled analysis of quantitative gene expression both at the implant surface and in the peri-implant bone, immunohistochemistry and biomechanical test, thereby providing a new combination of tools for the analysis of mechanisms of osseointegration.

Material surface-induced gene expression was detected in implant-adherent cells, whereas no major differences were detected between materials in the peri-implant bone during the first week. After 14 and 28 d, differences in gene expression between the two material surfaces were detected in the peri-implant bone, however, the gene expression fingerprint was not similar to that in the implant-adherent cells.

During the steady-state condition, rat trabecular bone demonstrated higher expression levels of bone formation markers (ALP and OC) and bone resorption markers (TRAP and CATK), whereas cortical bone revealed higher expression of proinflammatory cytokines (TNF- $\alpha$  and IL-1 $\beta$ ). In response to oxidized titanium implants, 3 d after implantation, implant-adherent cells in cortical site expressed higher level of OC while a higher IL-1 $\beta$  expression in implant-adherent cells were detected in trabecular site. It is concluded that rat femoral and tibial bone sites exhibit different constitutive gene expression of inflammatory and remodeling markers. Further, given the limits of the present experimental conditions, it is suggested that gene expression at implant surfaces is dependent on the bone type.

During the initial 24 h after implantation in rat cortical bone, oxidized implants were associated with a greater influx of cells and higher expression of chemokine homing receptor CXCR4 and integrins  $\beta$ 1,  $\beta$ 2 and  $\alpha$ v in comparison with machined implants. In contrast, machined implants exhibited higher expression of proinflammatory cytokines TNF- $\alpha$  and IL-1 $\beta$ . It is concluded that shortly after the surgical trauma, implant surface properties modulate the inflammatory response, cell recruitment, and adhesion during the first stage of osseointegration/bone regeneration.

During the period from 1 d to 28 d, material surface properties resulted in significant modulation of gene expression denoting inflammation, bone formation and bone resorption. The oxidized implant was associated with higher expression levels of osteogenic differentiation and bone formation (Runx2, ALP and OC) and bone remodeling (TRAP and CATK). This implant demonstrated higher magnitude and significant increase in biomechanical resistance during the first 28 d. In contrast, the machined implant was associated with higher expression levels of the proinflammatory cytokines (TNF- $\alpha$  and IL-1 $\beta$ ). This implant showed lower magnitude and non-significant increase in biomechanical resistance during the first 28 d.

According to the load-deformation plots, different failure patterns were demonstrated for oxidized and machined implants subjected to torque. The oxidized implant showed a fracture-like breakpoint while the machined implant showed the typical curve with mainly separation in the immediate bone-implant interface.

In conclusion, the present experimental studies show, firstly, that the gene expression of implant-adherent cells is a more sensitive indicator of the biological response around implants than that obtained by analyzing the peri-implant bone collar. Secondly, the material surface properties (physicochemical and topography) extremely rapidly govern the rate of osseointegration by modulating inflammation, cell recruitment, adhesion, bone regeneration and remodeling. Finally, these early interfacial cellular responses are strongly influencing the development of implant torsion stability.



## Topics for future research

Future studies may focus on the effect of each specific material surface property on the regulation of gene expression in close vicinity to the implant surface. Furthermore, it is of great importance to analyze the biological components that might be implicated in the interfacial processes of inflammation and bone formation, like for example, MAPK system and the Smad and WNT signaling pathways. The determination of specific role of particular molecules or group of molecules in the osseointegration process may require the modulation of specific target genes by, for instance, the local application of specific growth factors, the use of small interfering RNA (siRNA) or the employment of the knock-out or gene-deficient animals. Such information will be important and vital for our future research on exploring the potential for using the ex vivo genetic modification of cells to produce osteoinductive factors to enhance bone regeneration at the implant surface.

Currently, studies are being designed to combine the present model with other techniques. Some of these studies focus on the distinct proof and quantification of specific cellular subsets adherent to the retrieved implants or at different locations within the interface area.

Furthermore, the clinical application of the sampling procedure and the subsequent qPCR may be evaluated as screening and monitoring procedure for the biological conditions associated with implant treatment.



## Acknowledgements

- At the foremost, I would like to express my heartfelt gratitude to my supervisor, Professor Peter Thomsen, for his guidance through my PhD. project. Along the years of my PhD study, Professor Thomsen guided me from scratch and showed tremendous patience in developing my knowledge and capabilities to conduct quality research. I am really thankful for your several hours discussing new ideas for my research, helping me with the writing and the corrections of this thesis. Thanks for your suggestions about the possible new tools for investigating the biological events at the interface. You are always full of new ideas and willing to learn and explore in new areas.
- I would like to thank my other co-supervisors, Felicia Suska and Ulf Nannmark, for your support, great knowledge and constructive comments and criticism during my PhD work.
- I would like to thank my co-authors, Jan Hall, Neven Zoric and Stina Wigren for your valuable contributions in different studies of this thesis.
- Great thanks to Lena, Anna and Birgitta, for your indispensable and skillful helps during the surgical procedures, the histological preparations and analysis, and for all interesting discussions about life.
- Very special thanks to: Anders Palmquist, for all helps since I started my PhD work at the Department of Biomaterials. Special thanks to Maria Lennerås, for your fundamental and prompt work on the gene expression analysis. Honestly, I was lucky that both of you were there during my PhD study.
- I am also thankful to all ex and present colleagues at the Department of Biomaterials, especially, the administrative team, Anna Öhlund, Micaela Wilberg and Ann-Charlotte Nyrén; Professors Tomas Albrektsson, Pentti Tengvall, Jukka Lausmaa, Lars Sennerby, Christer Dahlin, Young-Taeg Sul, and all others, and the lab staff, for the nice and inspiring conversations around the cafe table and offices. Great thanks to Ahmed, Sofia, Sara, Necati, Giuseppe, Cecilia, Camilla, Byung-Soo, Viktoria, Rick, Karin and all other doctoral and postdoctoral friends at the department. Thanks for your friendship and great companion.
- Great thanks to:

Dr. Abdalla Albergli and Professor Mikael Kubista, the founders of MENA education group, for introducing me to this project.

All participants in Project Alpha and other IBCT projects and all people at GöteborgBIO.

All the staff at the Libyan embassy, for processing and administrating my scholarship.

All of my teachers, friends and colleagues at the Faculty of Dentistry in Benghazi, Libya; and all of the Libyan students at the Swedish universities.

Above all

- All thanks to:

My God, who gave me the patience, courage and ability to do what I needed to do.

And then, to:

My wife, Rima, and my child, Ahmed, the most meaningful of my life.

My mother, sisters and brothers, being far away, it did not stop your unconditional support and love.

My father, I am always remembering you, thanks for all of your self-sacrifice.

During the time of my PhD graduate, my study was supported by a scholarship from the Libyan General Committee for Higher Education. Further, different parts of my studies have been funded by the following grants:

VINNOVA VinnVäxt Program Biomedical Development in Western Sweden (Institute of Biomaterials and Cell Therapy, IBCT, together with Nobel Biocare and TATAA Biocenter).

The present thesis was made in collaboration with the Department of Biomaterials at Sahlgrenska Academy at University of Gothenburg and the Institute of Biomaterials and Cell Therapy (IBCT) (part of GöteborgBIO), Göteborg, Sweden.

VINNOVA Vinn Excellence Center of Biomaterials and Cell Therapy (BIOMATCELL)

Swedish Research Council (grants K2006-73X-09495-16-3 And K2009-52X-09495-22-3)

Region Västra Götaland.

Other research grants from :

Hjalmar Svensson Research Foundation

Kungl och Hvitfeldtska Stiftelsen

Personal funding for students from abroad from Adlerbertska Hospitiestiftelsen.

## References

1. Branemark PI, Adell R, Breine U, Hansson BO, Lindstrom J, Ohlsson A. Intraosseous anchorage of dental prostheses. I. Experimental studies. *Scand J Plast Reconstr Surg* 1969;3(2):81-100.
2. Branemark PI, Hansson BO, Adell R, Breine U, Lindstrom J, Hallen O, et al. Osseointegrated implants in the treatment of the edentulous jaw. Experience from a 10-year period. *Scand J Plast Reconstr Surg Suppl* 1977;16:1-132.
3. Sennerby L, Thomsen P, Ericson LE. Early tissue response to titanium implants inserted in rabbit cortical bone. Part I *Light microscopic observations*. *Journal of Materials Science: Materials in Medicine* 1993;4(3):240-250.
4. Sennerby L, Thomsen P, Ericson LE. Early tissue response to titanium implants inserted in rabbit cortical bone. Part II *Ultrastructural observations*. *Journal of Materials Science: Materials in Medicine* 1993;4(5):494-502.
5. Larsson C, Esposito M, Liao H, Thomsen P. The Titanium-Bone Interface In Vivo. In: Brunette DM, Tengvall P, Textor M, Thomsen P, editors. *Titanium in Medicine*. New York: Springer, 2001. p. 587-648.
6. Esposito M, Hirsch JM, Lekholm U, Thomsen P. Biological factors contributing to failures of osseointegrated oral implants. (II). Etiopathogenesis. *Eur J Oral Sci* 1998 Jun;106(3):721-764.
7. Yin T, Li L. The stem cell niches in bone. *J Clin Invest* 2006 May;116(5):1195-1201.
8. Aubin JE. Bone stem cells. *J Cell Biochem Suppl* 1998;30-31:73-82.
9. Long MW. Osteogenesis and bone-marrow-derived cells. *Blood Cells Mol Dis* 2001 May-Jun;27(3):677-690.
10. Rottmar M, Hakanson M, Smith M, Maniura-Weber K. Stem cell plasticity, osteogenic differentiation and the third dimension. *J Mater Sci Mater Med* 2010 Mar;21(3):999-1004.
11. Lian JB, Stein GS, Stein JL, van Wijnen AJ. Osteocalcin gene promoter: unlocking the secrets for regulation of osteoblast growth and differentiation. *J Cell Biochem Suppl* 1998;30-31:62-72.
12. Gordeladze JO, Reseland JE, Duroux-Richard I, Apparailly F, Jorgensen C. From stem cells to bone: phenotype acquisition, stabilization, and tissue engineering in animal models. *ILAR J* 2009;51(1):42-61.
13. Blumer MJ, Schwarzer C, Perez MT, Konakci KZ, Fritsch H. Identification and location of bone-forming cells within cartilage canals on their course into the secondary ossification centre. *J Anat* 2006 Jun;208(6):695-707.
14. Marks SC, Jr, Odgren PR. Structure and Development of the Skeleton. In: Bilezikian JP, Raisz LG, Rodan GA, editors. *Principles of Bone Biology*. San Diego, California: ACADEMIC PRESS, 2002. p. 3-15.
15. Franz-Odenaal TA, Hall BK, Witten PE. Buried alive: how osteoblasts become osteocytes. *Dev Dyn* 2006 Jan;235(1):176-190.
16. Aarden EM, Burger EH, Nijweide PJ. Function of osteocytes in bone. *J Cell Biochem* 1994 Jul;55(3):287-299.

17. Cowin SC, Moss-Salentijn L, Moss ML. Candidates for the mechanosensory system in bone. *J Biomech Eng* 1991 May;113(2):191-197.
18. Arai F, Hirao A, Suda T. Regulation of hematopoiesis and its interaction with stem cell niches. *Int J Hematol* 2005 Dec;82(5):371-376.
19. Calvi LM, Adams GB, Weibrecht KW, Weber JM, Olson DP, Knight MC, et al. Osteoblastic cells regulate the haematopoietic stem cell niche. *Nature* 2003 Oct 23;425(6960):841-846.
20. Zhang J, Niu C, Ye L, Huang H, He X, Tong WG, et al. Identification of the haematopoietic stem cell niche and control of the niche size. *Nature* 2003 Oct 23;425(6960):836-841.
21. Everts V, Delaisse JM, Korper W, Jansen DC, Tigchelaar-Gutter W, Saftig P, et al. The bone lining cell: its role in cleaning Howship's lacunae and initiating bone formation. *J Bone Miner Res* 2002 Jan;17(1):77-90.
22. Udagawa N, Takahashi N, Akatsu T, Tanaka H, Sasaki T, Nishihara T, et al. Origin of osteoclasts: mature monocytes and macrophages are capable of differentiating into osteoclasts under a suitable microenvironment prepared by bone marrow-derived stromal cells. *Proc Natl Acad Sci U S A* 1990 Sep;87(18):7260-7264.
23. Komano Y, Nanki T, Hayashida K, Taniguchi K, Miyasaka N. Identification of a human peripheral blood monocyte subset that differentiates into osteoclasts. *Arthritis Res Ther* 2006;8(5):R152.
24. Katagiri T, Takahashi N. Regulatory mechanisms of osteoblast and osteoclast differentiation. *Oral Dis* 2002 May;8(3):147-159.
25. Yasuda H, Shima N, Nakagawa N, Yamaguchi K, Kinosaki M, Mochizuki S, et al. Osteoclast differentiation factor is a ligand for osteoprotegerin/osteoclastogenesis-inhibitory factor and is identical to TRANCE/RANKL. *Proc Natl Acad Sci U S A* 1998 Mar 31;95(7):3597-3602.
26. Takahashi N, Udagawa N, Suda T. A new member of tumor necrosis factor ligand family, ODF/OPGL/TRANCE/RANKL, regulates osteoclast differentiation and function. *Biochem Biophys Res Commun* 1999 Mar 24;256(3):449-455.
27. Azuma Y, Kaji K, Katogi R, Takeshita S, Kudo A. Tumor necrosis factor-alpha induces differentiation of and bone resorption by osteoclasts. *J Biol Chem* 2000 Feb 18;275(7):4858-4864.
28. Kim N, Kadono Y, Takami M, Lee J, Lee SH, Okada F, et al. Osteoclast differentiation independent of the TRANCE-RANK-TRAF6 axis. *J Exp Med* 2005 Sep 5;202(5):589-595.
29. Chambers TJ, Hall TJ. Cellular and molecular mechanisms in the regulation and function of osteoclasts. *Vitam Horm* 1991;46:41-86.
30. Duong LT, Lakkakorpi P, Nakamura I, Rodan GA. Integrins and signaling in osteoclast function. *Matrix Biol* 2000 May;19(2):97-105.
31. Oursler MJ. Osteoclast synthesis and secretion and activation of latent transforming growth factor beta. *J Bone Miner Res* 1994 Apr;9(4):443-452.
32. Hayden JM, Mohan S, Baylink DJ. The insulin-like growth factor system and the coupling of formation to resorption. *Bone* 1995 Aug;17(2 Suppl):93S-98S.
33. Irie N, Takada Y, Watanabe Y, Matsuzaki Y, Naruse C, Asano M, et al. Bidirectional signaling through ephrinA2-EphA2 enhances osteoclastogenesis and suppresses osteoblastogenesis. *J Biol Chem* 2009 May 22;284(21):14637-14644.

34. Pederson L, Ruan M, Westendorf JJ, Khosla S, Oursler MJ. Regulation of bone formation by osteoclasts involves Wnt/BMP signaling and the chemokine sphingosine-1-phosphate. *Proc Natl Acad Sci U S A* 2008 Dec 30;105(52):20764-20769.
35. Ninomiya JT, Tracy RP, Calore JD, Gendreau MA, Kelm RJ, Mann KG. Heterogeneity of human bone. *J Bone Miner Res* 1990 Sep;5(9):933-938.
36. Kochanowska I, Chaberek S, Wojtowicz A, Marczyński B, Włodarski K, Dytko M, et al. Expression of genes for bone morphogenetic proteins BMP-2, BMP-4 and BMP-6 in various parts of the human skeleton. *BMC Musculoskelet Disord* 2007;8:128.
37. Komori T. Runx2, a multifunctional transcription factor in skeletal development. *J Cell Biochem* 2002;87(1):1-8.
38. Smits P, Dy P, Mitra S, Lefebvre V. Sox5 and Sox6 are needed to develop and maintain source, columnar, and hypertrophic chondrocytes in the cartilage growth plate. *J Cell Biol* 2004 Mar 1;164(5):747-758.
39. Jingushi S, Bolander ME. Biological Cascades of Fracture Healing as Models for Bone-Biomaterial Interface. In: Davies JE, editor. *The Bone-Biomaterial Interface*. Toronto: University of Toronto Press, 1990. p. 250-262.
40. Ai-Aql ZS, Alagl AS, Graves DT, Gerstenfeld LC, Einhorn TA. Molecular mechanisms controlling bone formation during fracture healing and distraction osteogenesis. *J Dent Res* 2008 Feb;87(2):107-118.
41. Wang FS, Yang KD, Kuo YR, Wang CJ, Sheen-Chen SM, Huang HC, et al. Temporal and spatial expression of bone morphogenetic proteins in extracorporeal shock wave-promoted healing of segmental defect. *Bone* 2003 Apr;32(4):387-396.
42. Chung R, Cool JC, Scherer MA, Foster BK, Xian CJ. Roles of neutrophil-mediated inflammatory response in the bony repair of injured growth plate cartilage in young rats. *J Leukoc Biol* 2006 Dec;80(6):1272-1280.
43. Kuroda S, Viridi AS, Dai Y, Shott S, Sumner DR. Patterns and localization of gene expression during intramembranous bone regeneration in the rat femoral marrow ablation model. *Calcif Tissue Int* 2005 Oct;77(4):212-225.
44. Uchida S, Sakai A, Kudo H, Otomo H, Watanuki M, Tanaka M, et al. Vascular endothelial growth factor is expressed along with its receptors during the healing process of bone and bone marrow after drill-hole injury in rats. *Bone* 2003 May;32(5):491-501.
45. Bu R, Borysenko CW, Li Y, Cao L, Sabokbar A, Blair HC. Expression and function of TNF-family proteins and receptors in human osteoblasts. *Bone* 2003 Nov;33(5):760-770.
46. Locksley RM, Killeen N, Lenardo MJ. The TNF and TNF receptor superfamilies: integrating mammalian biology. *Cell* 2001 Feb 23;104(4):487-501.
47. Samad TA, Moore KA, Sapirstein A, Billet S, Allchorne A, Poole S, et al. Interleukin-1beta-mediated induction of Cox-2 in the CNS contributes to inflammatory pain hypersensitivity. *Nature* 2001 Mar 22;410(6827):471-475.
48. Landry P, Sadasivan K, Marino A, Albright J. Apoptosis is coordinately regulated with osteoblast formation during bone healing. *Tissue Cell* 1997 Aug;29(4):413-419.
49. Olmedo ML, Landry PS, Sadasivan KK, Albright JA, Meek WD, Routh R, et al. Regulation of osteoblast levels during bone healing. *J Orthop Trauma* 1999 Jun-Jul;13(5):356-362.
50. Dimitriou R, Tsiridis E, Giannoudis PV. Current concepts of molecular aspects of bone healing. *Injury* 2005 Dec;36(12):1392-1404.

51. Gerstenfeld LC, Cho TJ, Kon T, Aizawa T, Cruceta J, Graves BD, et al. Impaired intramembranous bone formation during bone repair in the absence of tumor necrosis factor-alpha signaling. *Cells Tissues Organs* 2001;169(3):285-294.
52. Doherty TM, Asotra K, Fitzpatrick LA, Qiao JH, Wilkin DJ, Detrano RC, et al. Calcification in atherosclerosis: bone biology and chronic inflammation at the arterial crossroads. *Proc Natl Acad Sci U S A* 2003 Sep 30;100(20):11201-11206.
53. Helske S, Oksjoki R, Lindstedt KA, Lommi J, Turto H, Werkkala K, et al. Complement system is activated in stenotic aortic valves. *Atherosclerosis* 2008 Jan;196(1):190-200.
54. Bocker W, Docheva D, Prall WC, Egea V, Pappou E, Rossmann O, et al. IKK-2 is required for TNF-alpha-induced invasion and proliferation of human mesenchymal stem cells. *J Mol Med* 2008 Oct;86(10):1183-1192.
55. Hess K, Ushmorov A, Fiedler J, Brenner RE, Wirth T. TNFalpha promotes osteogenic differentiation of human mesenchymal stem cells by triggering the NF-kappaB signaling pathway. *Bone* 2009 Aug;45(2):367-376.
56. Guttridge DC, Mayo MW, Madrid LV, Wang CY, Baldwin AS, Jr. NF-kappaB-induced loss of MyoD messenger RNA: possible role in muscle decay and cachexia. *Science* 2000 Sep 29;289(5488):2363-2366.
57. Sitcheran R, Cogswell PC, Baldwin AS, Jr. NF-kappaB mediates inhibition of mesenchymal cell differentiation through a posttranscriptional gene silencing mechanism. *Genes Dev* 2003 Oct 1;17(19):2368-2373.
58. Fu X, Han B, Cai S, Lei Y, Sun T, Sheng Z. Migration of bone marrow-derived mesenchymal stem cells induced by tumor necrosis factor-alpha and its possible role in wound healing. *Wound Repair Regen* 2009 Mar-Apr;17(2):185-191.
59. Zhou FH, Foster BK, Zhou XF, Cowin AJ, Xian CJ. TNF-alpha mediates p38 MAP kinase activation and negatively regulates bone formation at the injured growth plate in rats. *J Bone Miner Res* 2006 Jul;21(7):1075-1088.
60. Ding J, Ghali O, Lencel P, Broux O, Chauveau C, Devedjian JC, et al. TNF-alpha and IL-1beta inhibit RUNX2 and collagen expression but increase alkaline phosphatase activity and mineralization in human mesenchymal stem cells. *Life Sci* 2009 Apr 10;84(15-16):499-504.
61. Gilbert L, He X, Farmer P, Boden S, Kozlowski M, Rubin J, et al. Inhibition of osteoblast differentiation by tumor necrosis factor-alpha. *Endocrinology* 2000 Nov;141(11):3956-3964.
62. Gilbert L, He X, Farmer P, Rubin J, Drissi H, van Wijnen AJ, et al. Expression of the osteoblast differentiation factor RUNX2 (Cbfa1/AML3/Pebp2alpha A) is inhibited by tumor necrosis factor-alpha. *J Biol Chem* 2002 Jan 25;277(4):2695-2701.
63. Kaneki H, Guo R, Chen D, Yao Z, Schwarz EM, Zhang YE, et al. Tumor necrosis factor promotes Runx2 degradation through up-regulation of Smurf1 and Smurf2 in osteoblasts. *J Biol Chem* 2006 Feb 17;281(7):4326-4333.
64. Graves DT, Jiang Y. Chemokines, a family of chemotactic cytokines. *Crit Rev Oral Biol Med* 1995;6(2):109-118.
65. Kuziel WA, Morgan SJ, Dawson TC, Griffin S, Smithies O, Ley K, et al. Severe reduction in leukocyte adhesion and monocyte extravasation in mice deficient in CC chemokine receptor 2. *Proc Natl Acad Sci U S A* 1997 Oct 28;94(22):12053-12058.



66. Schober A, Zerneck A, Liehn EA, von Hundelshausen P, Knarren S, Kuziel WA, et al. Crucial role of the CCL2/CCR2 axis in neointimal hyperplasia after arterial injury in hyperlipidemic mice involves early monocyte recruitment and CCL2 presentation on platelets. *Circ Res* 2004 Nov 26;95(11):1125-1133.
67. Binder NB, Niederreiter B, Hoffmann O, Stange R, Pap T, Stulnig TM, et al. Estrogen-dependent and C-C chemokine receptor-2-dependent pathways determine osteoclast behavior in osteoporosis. *Nat Med* 2009 Apr;15(4):417-424.
68. Xing Z, Lu C, Hu D, Yu YY, Wang X, Colnot C, et al. Multiple roles for CCR2 during fracture healing. *Dis Model Mech* Mar 30.
69. Williams SR, Jiang Y, Cochran D, Dorsam G, Graves DT. Regulated expression of monocyte chemoattractant protein-1 in normal human osteoblastic cells. *Am J Physiol* 1992 Jul;263(1 Pt 1):C194-199.
70. Rahimi P, Wang CY, Stashenko P, Lee SK, Lorenzo JA, Graves DT. Monocyte chemoattractant protein-1 expression and monocyte recruitment in osseous inflammation in the mouse. *Endocrinology* 1995 Jun;136(6):2752-2759.
71. Wuyts A, Proost P, Lenaerts JP, Ben-Baruch A, Van Damme J, Wang JM. Differential usage of the CXC chemokine receptors 1 and 2 by interleukin-8, granulocyte chemotactic protein-2 and epithelial-cell-derived neutrophil attractant-78. *Eur J Biochem* 1998 Jul 1;255(1):67-73.
72. Dar A, Kollet O, Lapidot T. Mutual, reciprocal SDF-1/CXCR4 interactions between hematopoietic and bone marrow stromal cells regulate human stem cell migration and development in NOD/SCID chimeric mice. *Exp Hematol* 2006 Aug;34(8):967-975.
73. Nagase H, Miyamasu M, Yamaguchi M, Imanishi M, Tsuno NH, Matsushima K, et al. Cytokine-mediated regulation of CXCR4 expression in human neutrophils. *J Leukoc Biol* 2002 Apr;71(4):711-717.
74. Furze RC, Rankin SM. Neutrophil mobilization and clearance in the bone marrow. *Immunology* 2008 Nov;125(3):281-288.
75. Ceradini DJ, Kulkarni AR, Callaghan MJ, Tepper OM, Bastidas N, Kleinman ME, et al. Progenitor cell trafficking is regulated by hypoxic gradients through HIF-1 induction of SDF-1. *Nat Med* 2004 Aug;10(8):858-864.
76. Dar A, Goichberg P, Shinder V, Kalinkovich A, Kollet O, Netzer N, et al. Chemokine receptor CXCR4-dependent internalization and resecretion of functional chemokine SDF-1 by bone marrow endothelial and stromal cells. *Nat Immunol* 2005 Oct;6(10):1038-1046.
77. Ji JF, He BP, Dheen ST, Tay SS. Interactions of chemokines and chemokine receptors mediate the migration of mesenchymal stem cells to the impaired site in the brain after hypoglossal nerve injury. *Stem Cells* 2004;22(3):415-427.
78. Kitaori T, Ito H, Schwarz EM, Tsutsumi R, Yoshitomi H, Oishi S, et al. Stromal cell-derived factor 1/CXCR4 signaling is critical for the recruitment of mesenchymal stem cells to the fracture site during skeletal repair in a mouse model. *Arthritis Rheum* 2009 Mar;60(3):813-823.
79. Wynn RF, Hart CA, Corradi-Perini C, O'Neill L, Evans CA, Wraith JE, et al. A small proportion of mesenchymal stem cells strongly expresses functionally active CXCR4 receptor capable of promoting migration to bone marrow. *Blood* 2004 Nov 1;104(9):2643-2645.

80. Hughes DE, Salter DM, Dedhar S, Simpson R. Integrin expression in human bone. *J Bone Miner Res* 1993 May;8(5):527-533.
81. Stewart M, Thiel M, Hogg N. Leukocyte integrins. *Curr Opin Cell Biol* 1995 Oct;7(5):690-696.
82. Arnaout MA. Leukocyte adhesion molecules deficiency: its structural basis, pathophysiology and implications for modulating the inflammatory response. *Immunol Rev* 1990 Apr;114:145-180.
83. Hayashi H, Nakahama K, Sato T, Tuchiya T, Asakawa Y, Maemura T, et al. The role of Mac-1 (CD11b/CD18) in osteoclast differentiation induced by receptor activator of nuclear factor-kappaB ligand. *FEBS Lett* 2008 Sep 22;582(21-22):3243-3248.
84. Ruster B, Gottig S, Ludwig RJ, Bistrrian R, Muller S, Seifried E, et al. Mesenchymal stem cells display coordinated rolling and adhesion behavior on endothelial cells. *Blood* 2006 Dec 1;108(12):3938-3944.
85. Zimmerman D, Jin F, Leboy P, Hardy S, Damsky C. Impaired bone formation in transgenic mice resulting from altered integrin function in osteoblasts. *Dev Biol* 2000 Apr 1;220(1):2-15.
86. Hu D, Lu C, Sapozhnikova A, Barnett M, Sparrey C, Miclau T, et al. Absence of beta3 integrin accelerates early skeletal repair. *J Orthop Res* Jan;28(1):32-37.
87. Okazaki K, Jingushi S, Ikenoue T, Urabe K, Sakai H, Iwamoto Y. Expression of parathyroid hormone-related peptide and insulin-like growth factor I during rat fracture healing. *J Orthop Res* 2003 May;21(3):511-520.
88. Wildemann B, Schmidmaier G, Brenner N, Huning M, Stange R, Haas NP, et al. Quantification, localization, and expression of IGF-I and TGF-beta1 during growth factor-stimulated fracture healing. *Calcif Tissue Int* 2004 Apr;74(4):388-397.
89. Centrella M, Horowitz MC, Wozney JM, McCarthy TL. Transforming growth factor-beta gene family members and bone. *Endocr Rev* 1994 Feb;15(1):27-39.
90. Robey PG, Young MF, Flanders KC, Roche NS, Kondaiah P, Reddi AH, et al. Osteoblasts synthesize and respond to transforming growth factor-type beta (TGF-beta) in vitro. *J Cell Biol* 1987 Jul;105(1):457-463.
91. Wang R, Ghahary A, Shen Q, Scott PG, Roy K, Tredget EE. Hypertrophic scar tissues and fibroblasts produce more transforming growth factor-beta1 mRNA and protein than normal skin and cells. *Wound Repair Regen* 2000 Mar-Apr;8(2):128-137.
92. Letterio JJ, Roberts AB. Regulation of immune responses by TGF-beta. *Annu Rev Immunol* 1998;16:137-161.
93. Li MO, Wan YY, Sanjabi S, Robertson AK, Flavell RA. Transforming growth factor-beta regulation of immune responses. *Annu Rev Immunol* 2006;24:99-146.
94. Yao D, Ehrlich M, Henis YI, Leof EB. Transforming growth factor-beta receptors interact with AP2 by direct binding to beta2 subunit. *Mol Biol Cell* 2002 Nov;13(11):4001-4012.
95. Ishitani T, Ninomiya-Tsuji J, Nagai S, Nishita M, Meneghini M, Barker N, et al. The TAK1-NLK-MAPK-related pathway antagonizes signalling between beta-catenin and transcription factor TCF. *Nature* 1999 Jun 24;399(6738):798-802.
96. Shibuya H, Yamaguchi K, Shirakabe K, Tonegawa A, Gotoh Y, Ueno N, et al. TAB1: an activator of the TAK1 MAPKKK in TGF-beta signal transduction. *Science* 1996 May 24;272(5265):1179-1182.

97. Fox SW, Lovibond AC. Current insights into the role of transforming growth factor-beta in bone resorption. *Mol Cell Endocrinol* 2005 Nov 24;243(1-2):19-26.
98. Zhou FH, Foster BK, Sander G, Xian CJ. Expression of proinflammatory cytokines and growth factors at the injured growth plate cartilage in young rats. *Bone* 2004 Dec;35(6):1307-1315.
99. Cho TJ, Gerstenfeld LC, Einhorn TA. Differential temporal expression of members of the transforming growth factor beta superfamily during murine fracture healing. *J Bone Miner Res* 2002 Mar;17(3):513-520.
100. Distler JH, Hirth A, Kurowska-Stolarska M, Gay RE, Gay S, Distler O. Angiogenic and angiostatic factors in the molecular control of angiogenesis. *Q J Nucl Med* 2003 Sep;47(3):149-161.
101. Tallquist M, Kazlauskas A. PDGF signaling in cells and mice. *Cytokine Growth Factor Rev* 2004 Aug;15(4):205-213.
102. Fierro F, Illmer T, Jing D, Schleyer E, Ehninger G, Boxberger S, et al. Inhibition of platelet-derived growth factor receptorbeta by imatinib mesylate suppresses proliferation and alters differentiation of human mesenchymal stem cells in vitro. *Cell Prolif* 2007 Jun;40(3):355-366.
103. Tokunaga A, Oya T, Ishii Y, Motomura H, Nakamura C, Ishizawa S, et al. PDGF receptor beta is a potent regulator of mesenchymal stromal cell function. *J Bone Miner Res* 2008 Sep;23(9):1519-1528.
104. Rasubala L, Yoshikawa H, Nagata K, Iijima T, Ohishi M. Platelet-derived growth factor and bone morphogenetic protein in the healing of mandibular fractures in rats. *Br J Oral Maxillofac Surg* 2003 Jun;41(3):173-178.
105. Wozney JM, Rosen V. Bone morphogenetic protein and bone morphogenetic protein gene family in bone formation and repair. *Clin Orthop Relat Res* 1998 Jan(346):26-37.
106. Cheng H, Jiang W, Phillips FM, Haydon RC, Peng Y, Zhou L, et al. Osteogenic activity of the fourteen types of human bone morphogenetic proteins (BMPs). *J Bone Joint Surg Am* 2003 Aug;85-A(8):1544-1552.
107. Lee MH, Kim YJ, Kim HJ, Park HD, Kang AR, Kyung HM, et al. BMP-2-induced Runx2 expression is mediated by Dlx5, and TGF-beta 1 opposes the BMP-2-induced osteoblast differentiation by suppression of Dlx5 expression. *J Biol Chem* 2003 Sep 5;278(36):34387-34394.
108. Lee MH, Kwon TG, Park HS, Wozney JM, Ryoo HM. BMP-2-induced Osterix expression is mediated by Dlx5 but is independent of Runx2. *Biochem Biophys Res Commun* 2003 Sep 26;309(3):689-694.
109. Jung Y, Song J, Shiozawa Y, Wang J, Wang Z, Williams B, et al. Hematopoietic stem cells regulate mesenchymal stromal cell induction into osteoblasts thereby participating in the formation of the stem cell niche. *Stem Cells* 2008 Aug;26(8):2042-2051.
110. Bostrom MP, Lane JM, Berberian WS, Missri AA, Tomin E, Weiland A, et al. Immunolocalization and expression of bone morphogenetic proteins 2 and 4 in fracture healing. *J Orthop Res* 1995 May;13(3):357-367.
111. Kidd LJ, Stephens AS, Kuliwaba JS, Fazzalari NL, Wu AC, Forwood MR. Temporal pattern of gene expression and histology of stress fracture healing. *Bone* 2010 Feb;46(2):369-378.

112. Wang K, Vishwanath P, Eichler GS, Al-Sebaei MO, Edgar CM, Einhorn TA, et al. Analysis of fracture healing by large-scale transcriptional profile identified temporal relationships between metalloproteinase and ADAMTS mRNA expression. *Matrix Biol* 2006 Jul;25(5):271-281.
113. Stein GS, Lian JB, van Wijnen AJ, Stein JL, Montecino M, Javed A, et al. Runx2 control of organization, assembly and activity of the regulatory machinery for skeletal gene expression. *Oncogene* 2004 May 24;23(24):4315-4329.
114. Komori T, Yagi H, Nomura S, Yamaguchi A, Sasaki K, Deguchi K, et al. Targeted disruption of Cbfa1 results in a complete lack of bone formation owing to maturational arrest of osteoblasts. *Cell* 1997 May 30;89(5):755-764.
115. Franceschi RT, Xiao G, Jiang D, Gopalakrishnan R, Yang S, Reith E. Multiple signaling pathways converge on the Cbfa1/Runx2 transcription factor to regulate osteoblast differentiation. *Connect Tissue Res* 2003;44 Suppl 1:109-116.
116. Komori T. Regulation of osteoblast differentiation by transcription factors. *J Cell Biochem* 2006 Dec 1;99(5):1233-1239.
117. Komori T. Regulation of osteoblast differentiation by runx2. *Adv Exp Med Biol* 2010;658:43-49.
118. Yoshida CA, Yamamoto H, Fujita T, Furuichi T, Ito K, Inoue K, et al. Runx2 and Runx3 are essential for chondrocyte maturation, and Runx2 regulates limb growth through induction of Indian hedgehog. *Genes Dev* 2004 Apr 15;18(8):952-963.
119. Mori K, Kitazawa R, Kondo T, Maeda S, Yamaguchi A, Kitazawa S. Modulation of mouse RANKL gene expression by Runx2 and PKA pathway. *J Cell Biochem* 2006 Aug 15;98(6):1629-1644.
120. Nagashima M, Sakai A, Uchida S, Tanaka S, Tanaka M, Nakamura T. Bisphosphonate (YM529) delays the repair of cortical bone defect after drill-hole injury by reducing terminal differentiation of osteoblasts in the mouse femur. *Bone* 2005 Mar;36(3):502-511.
121. Heikkinen S, Auwerx J, Argmann CA. PPARgamma in human and mouse physiology. *Biochim Biophys Acta* 2007 Aug;1771(8):999-1013.
122. Chinetti G, Griglio S, Antonucci M, Torra IP, Delerive P, Majd Z, et al. Activation of proliferator-activated receptors alpha and gamma induces apoptosis of human monocyte-derived macrophages. *J Biol Chem* 1998 Oct 2;273(40):25573-25580.
123. Jeon MJ, Kim JA, Kwon SH, Kim SW, Park KS, Park SW, et al. Activation of peroxisome proliferator-activated receptor-gamma inhibits the Runx2-mediated transcription of osteocalcin in osteoblasts. *J Biol Chem* 2003 Jun 27;278(26):23270-23277.
124. Ponce ML, Koelling S, Kluever A, Heinemann DE, Miosge N, Wulf G, et al. Coexpression of osteogenic and adipogenic differentiation markers in selected subpopulations of primary human mesenchymal progenitor cells. *J Cell Biochem* 2008 Jul 1;104(4):1342-1355.
125. Mbalaviele G, Abu-Amer Y, Meng A, Jaiswal R, Beck S, Pittenger MF, et al. Activation of peroxisome proliferator-activated receptor-gamma pathway inhibits osteoclast differentiation. *J Biol Chem* 2000 May 12;275(19):14388-14393.
126. Wan Y, Chong LW, Evans RM. PPAR-gamma regulates osteoclastogenesis in mice. *Nat Med* 2007 Dec;13(12):1496-1503.

127. Bouhleb MA, Derudas B, Rigamonti E, Dievart R, Brozek J, Haulon S, et al. PPARgamma activation primes human monocytes into alternative M2 macrophages with anti-inflammatory properties. *Cell Metab* 2007 Aug;6(2):137-143.
128. Ek-Rylander B, Bill P, Norgard M, Nilsson S, Andersson G. Cloning, sequence, and developmental expression of a type 5, tartrate-resistant, acid phosphatase of rat bone. *J Biol Chem* 1991 Dec 25;266(36):24684-24689.
129. Andersson GN, Ek-Rylander B, Hammarstrom LE, Lindskog S, Toverud SU. Immunocytochemical localization of a tartrate-resistant and vanadate-sensitive acid nucleotide tri- and diphosphatase. *J Histochem Cytochem* 1986 Mar;34(3):293-298.
130. Perez-Amodio S, Beertsen W, Everts V. (Pre-)osteoclasts induce retraction of osteoblasts before their fusion to osteoclasts. *J Bone Miner Res* 2004 Oct;19(10):1722-1731.
131. Littlewood-Evans A, Kokubo T, Ishibashi O, Inaoka T, Wlodarski B, Gallagher JA, et al. Localization of cathepsin K in human osteoclasts by in situ hybridization and immunohistochemistry. *Bone* 1997 Feb;20(2):81-86.
132. Garnero P, Borel O, Byrjalsen I, Ferreras M, Drake FH, McQueney MS, et al. The collagenolytic activity of cathepsin K is unique among mammalian proteinases. *J Biol Chem* 1998 Nov 27;273(48):32347-32352.
133. Saftig P, Hunziker E, Wehmeyer O, Jones S, Boyde A, Rommerskirch W, et al. Impaired osteoclastic bone resorption leads to osteopetrosis in cathepsin-K-deficient mice. *Proc Natl Acad Sci U S A* 1998 Nov 10;95(23):13453-13458.
134. Uusitalo H, Hiltunen A, Soderstrom M, Aro HT, Vuorio E. Expression of cathepsins B, H, K, L, and S and matrix metalloproteinases 9 and 13 during chondrocyte hypertrophy and endochondral ossification in mouse fracture callus. *Calcif Tissue Int* 2000 Nov;67(5):382-390.
135. Wang LC, Takahashi I, Sasano Y, Sugawara J, Mitani H. Osteoclastogenic activity during mandibular distraction osteogenesis. *J Dent Res* 2005 Nov;84(11):1010-1015.
136. Cooper LF. Biologic determinants of bone formation for osseointegration: clues for future clinical improvements. *J Prosthet Dent* 1998 Oct;80(4):439-449.
137. Albrektsson T, Wennerberg A. Oral implant surfaces: Part 1--review focusing on topographic and chemical properties of different surfaces and in vivo responses to them. *Int J Prosthodont* 2004 Sep-Oct;17(5):536-543.
138. Ellingsen JE, Thomsen P, Lyngstadaas SP. Advances in dental implant materials and tissue regeneration. *Periodontol* 2000 2006;41:136-156.
139. Thomsen P, Ericson LE. Inflammatory Cell Response to Bone Implant Surfaces. In: Davies JE, editor. *The Bone-Biomaterial Interface*. Toronto: University of Toronto Press, 1991. p. 153-169.
140. Muller-Mai CM, Voigt C, Gross U. Incorporation and degradation of hydroxyapatite implants of different surface roughness and surface structure in bone. *Scanning Microsc* 1990 Sep;4(3):613-622; discussion 622-614.
141. van Blitterswijk CA, Grote JJ, Kuypers W, Blok-van Hoek CJ, Daems WT. Bioreactions at the tissue/hydroxyapatite interface. *Biomaterials* 1985 Jul;6(4):243-251.
142. Chehroudi B, Ghrebi S, Murakami H, Waterfield JD, Owen G, Brunette DM. Bone formation on rough, but not polished, subcutaneously implanted Ti surfaces is preceded by macrophage accumulation. *J Biomed Mater Res A* 2010 May;93(2):724-737.

143. Takebe J, Champagne CM, Offenbacher S, Ishibashi K, Cooper LF. Titanium surface topography alters cell shape and modulates bone morphogenetic protein 2 expression in the J774A.1 macrophage cell line. *J Biomed Mater Res A* 2003 Feb 1;64(2):207-216.
144. Jansson E, Kalltorp M, Thomsen P, Tengvall P. Ex vivo PMA-induced respiratory burst and TNF-alpha secretion elicited from inflammatory cells on machined and porous blood plasma clot-coated titanium. *Biomaterials* 2002 Jul;23(13):2803-2815.
145. Suska F, Esposito M, Gretzer C, Kalltorp M, Tengvall P, Thomsen P. IL-1alpha, IL-1beta and TNF-alpha secretion during in vivo/ex vivo cellular interactions with titanium and copper. *Biomaterials* 2003 Feb;24(3):461-468.
146. Refai AK, Textor M, Brunette DM, Waterfield JD. Effect of titanium surface topography on macrophage activation and secretion of proinflammatory cytokines and chemokines. *J Biomed Mater Res A* 2004 Aug 1;70(2):194-205.
147. Boyan BD, Dean DD, Lohmann CH, Cochran DL, Sylvia VL, Schwartz Z. The Titanium-Bone Cell Interface In Vitro: The Role of the Surface in Promoting Osteointegration. In: Brunette DM, Tengvall P, Textor M, Thomsen P, editors. *Titanium in Medicine*. New York: Springer, 2001. p. 561-585.
148. Sinha RK, Tuan RS. Regulation of human osteoblast integrin expression by orthopedic implant materials. *Bone* 1996 May;18(5):451-457.
149. ter Brugge PJ, Jansen JA. Initial interaction of rat bone marrow cells with non-coated and calcium phosphate coated titanium substrates. *Biomaterials* 2002 Aug;23(15):3269-3277.
150. ter Brugge PJ, Torensma R, De Ruijter JE, Figdor CG, Jansen JA. Modulation of integrin expression on rat bone marrow cells by substrates with different surface characteristics. *Tissue Eng* 2002 Aug;8(4):615-626.
151. Siebers MC, Walboomers XF, van den Dolder J, Leeuwenburgh SC, Wolke JG, Jansen JA. The behavior of osteoblast-like cells on various substrates with functional blocking of integrin-beta1 and integrin-beta3. *J Mater Sci Mater Med* 2008 Feb;19(2):861-868.
152. Minkin C, Marinho VC. Role of the osteoclast at the bone-implant interface. *Adv Dent Res* 1999 Jun;13:49-56.
153. Dhert WJ, Thomsen P, Blomgren AK, Esposito M, Ericson LE, Verbout AJ. Integration of press-fit implants in cortical bone: a study on interface kinetics. *J Biomed Mater Res* 1998 Sep 15;41(4):574-583.
154. Gilles JA, Carnes DL, Windeler AS. Development of an in vitro culture system for the study of osteoclast activity and function. *J Endod* 1994 Jul;20(7):327-331.
155. Gomi K, Lowenberg B, Shapiro G, Davies JE. Resorption of sintered synthetic hydroxyapatite by osteoclasts in vitro. *Biomaterials* 1993;14(2):91-96.
156. de Bruijn JD, Bovell YP, Davies JE, van Blitterswijk CA. Osteoclastic resorption of calcium phosphates is potentiated in postosteogenic culture conditions. *J Biomed Mater Res* 1994 Jan;28(1):105-112.
157. Yamada S, Heymann D, Boulter JM, Daculsi G. Osteoclastic resorption of biphasic calcium phosphate ceramic in vitro. *J Biomed Mater Res* 1997 Dec 5;37(3):346-352.

- 
158. Tan KS, Qian L, Rosado R, Flood PM, Cooper LF. The role of titanium surface topography on J774A.1 macrophage inflammatory cytokines and nitric oxide production. *Biomaterials* 2006 Oct;27(30):5170-5177.
159. Schneider GB, Zaharias R, Seabold D, Keller J, Stanford C. Differentiation of preosteoblasts is affected by implant surface microtopographies. *J Biomed Mater Res A* 2004 Jun 1;69(3):462-468.
160. Park JW, Kim YJ, Jang JH. Enhanced osteoblast response to hydrophilic strontium and/or phosphate ions-incorporated titanium oxide surfaces. *Clin Oral Implants Res* 2010 Feb 1;21(4):398-408.
161. Mendonca G, Mendonca DB, Aragao FJ, Cooper LF. The combination of micron and nanotopography by H(2)SO(4)/H(2)O(2) treatment and its effects on osteoblast-specific gene expression of hMSCs. *J Biomed Mater Res A* 2010 Feb 2.
162. Schwartz Z, Lohmann CH, Vocke AK, Sylvia VL, Cochran DL, Dean DD, et al. Osteoblast response to titanium surface roughness and 1alpha,25-(OH)(2)D(3) is mediated through the mitogen-activated protein kinase (MAPK) pathway. *J Biomed Mater Res* 2001 Sep 5;56(3):417-426.
163. Olivares-Navarrete R, Hyzy SL, Hutton DL, Erdman CP, Wieland M, Boyan BD, et al. Direct and indirect effects of microstructured titanium substrates on the induction of mesenchymal stem cell differentiation towards the osteoblast lineage. *Biomaterials* 2010 Apr;31(10):2728-2735.
164. Setzer B, Bachle M, Metzger MC, Kohal RJ. The gene-expression and phenotypic response of hFOB 1.19 osteoblasts to surface-modified titanium and zirconia. *Biomaterials* 2009 Feb;30(6):979-990.
165. Makihira S, Mine Y, Kosaka E, Nikawa H. Titanium surface roughness accelerates RANKL-dependent differentiation in the osteoclast precursor cell line, RAW264.7. *Dent Mater J* 2007 Sep;26(5):739-745.
166. Branemark PI. Osseointegration and its experimental background. *J Prosthet Dent* 1983 Sep;50(3):399-410.
167. Branemark R. A Biomechanical Study of Osseointegration [Doctoral thesis]. Gothenburg: University of Gothenburg; 1996.
168. Choi JW, Heo SJ, Koak JY, Kim SK, Lim YJ, Kim SH, et al. Biological responses of anodized titanium implants under different current voltages. *J Oral Rehabil* 2006 Dec;33(12):889-897.
169. Ferguson SJ, Brogini N, Wieland M, de Wild M, Rupp F, Geis-Gerstorfer J, et al. Biomechanical evaluation of the interfacial strength of a chemically modified sandblasted and acid-etched titanium surface. *J Biomed Mater Res A* 2006 Aug;78(2):291-297.
170. Klokkevold PR, Johnson P, Dadgostari S, Caputo A, Davies JE, Nishimura RD. Early endosseous integration enhanced by dual acid etching of titanium: a torque removal study in the rabbit. *Clin Oral Implants Res* 2001 Aug;12(4):350-357.
171. Son WW, Zhu X, Shin HI, Ong JL, Kim KH. In vivo histological response to anodized and anodized/hydrothermally treated titanium implants. *J Biomed Mater Res B Appl Biomater* 2003 Aug 15;66(2):520-525.
172. Sul YT, Johansson C, Albrektsson T. Which surface properties enhance bone response to implants? Comparison of oxidized magnesium, TiUnite, and Osseotite implant surfaces. *Int J Prosthodont* 2006 Jul-Aug;19(4):319-328.

- 
173. Yeo IS, Han JS, Yang JH. Biomechanical and histomorphometric study of dental implants with different surface characteristics. *J Biomed Mater Res B Appl Biomater* 2008 Nov;87(2):303-311.
174. Branemark R, Ohnells LO, Nilsson P, Thomsen P. Biomechanical characterization of osseointegration during healing: an experimental in vivo study in the rat. *Biomaterials* 1997 Jul;18(14):969-978.
175. Sennerby L, Thomsen P, Ericson LE. A morphometric and biomechanic comparison of titanium implants inserted in rabbit cortical and cancellous bone. *Int J Oral Maxillofac Implants* 1992 Spring;7(1):62-71.
176. Haga M, Fujii N, Nozawa-Inoue K, Nomura S, Oda K, Uoshima K, et al. Detailed process of bone remodeling after achievement of osseointegration in a rat implantation model. *Anat Rec (Hoboken)* 2009 Jan;292(1):38-47.
177. Ayukawa Y, Takeshita F, Inoue T, Yoshinari M, Shimono M, Suetsugu T, et al. An immunoelectron microscopic localization of noncollagenous bone proteins (osteocalcin and osteopontin) at the bone-titanium interface of rat tibiae. *J Biomed Mater Res* 1998 Jul;41(1):111-119.
178. Neo M, Voigt CF, Herbst H, Gross UM. Analysis of osteoblast activity at biomaterial-bone interfaces by in situ hybridization. *J Biomed Mater Res* 1996 Apr;30(4):485-492.
179. Neo M, Voigt CF, Herbst H, Gross UM. Osteoblast reaction at the interface between surface-active materials and bone in vivo: a study using in situ hybridization. *J Biomed Mater Res* 1998 Jan;39(1):1-8.
180. Zhou H, Choong P, McCarthy R, Chou ST, Martin TJ, Ng KW. In situ hybridization to show sequential expression of osteoblast gene markers during bone formation in vivo. *J Bone Miner Res* 1994 Sep;9(9):1489-1499.
181. Jarmar T, Palmquist A, Branemark R, Hermansson L, Engqvist H, Thomsen P. Technique for preparation and characterization in cross-section of oral titanium implant surfaces using focused ion beam and transmission electron microscopy. *J Biomed Mater Res A* 2008 Dec 15;87(4):1003-1009.
182. Jarmar T, Palmquist A, Branemark R, Hermansson L, Engqvist H, Thomsen P. Characterization of the surface properties of commercially available dental implants using scanning electron microscopy, focused ion beam, and high-resolution transmission electron microscopy. *Clin Implant Dent Relat Res* 2008 Mar;10(1):11-22.
183. Rozen S, Skaletsky H. Primer3 on the WWW for general users and for biologist programmers. *Methods Mol Biol* 2000;132:365-386.
184. Pfaffl MW. A new mathematical model for relative quantification in real-time RT-PCR. *Nucleic Acids Res* 2001 May 1;29(9):e45.
185. Donath K, Breuner G. A method for the study of undecalcified bones and teeth with attached soft tissues. The Sage-Schliff (sawing and grinding) technique. *J Oral Pathol* 1982 Aug;11(4):318-326.
186. Branemark R, Skalak R. An in-vivo method for biomechanical characterization of bone-anchored implants. *Med Eng Phys* 1998 Apr;20(3):216-219.
187. Monjo M, Lamolle SF, Lyngstadaas SP, Ronold HJ, Ellingsen JE. In vivo expression of osteogenic markers and bone mineral density at the surface of fluoride-modified titanium implants. *Biomaterials* 2008 Oct;29(28):3771-3780.



188. Taxt-Lamolle SF, Rubert M, Haugen HJ, Lyngstadaas SP, Ellingsen JE, Monjo M. Controlled electro-implementation of fluoride in titanium implant surfaces enhances cortical bone formation and mineralization. *Acta Biomater* 2010 Mar;6(3):1025-1032.
189. Kojima N, Ozawa S, Miyata Y, Hasegawa H, Tanaka Y, Ogawa T. High-throughput gene expression analysis in bone healing around titanium implants by DNA microarray. *Clin Oral Implants Res* 2008 Feb;19(2):173-181.
190. Ogawa T, Nishimura I. Different bone integration profiles of turned and acid-etched implants associated with modulated expression of extracellular matrix genes. *Int J Oral Maxillofac Implants* 2003 Mar-Apr;18(2):200-210.
191. Ogawa T, Sukotjo C, Nishimura I. Modulated bone matrix-related gene expression is associated with differences in interfacial strength of different implant surface roughness. *J Prosthodont* 2002 Dec;11(4):241-247.
192. Ozawa S, Ogawa T, Iida K, Sukotjo C, Hasegawa H, Nishimura RD, et al. Ovariectomy hinders the early stage of bone-implant integration: histomorphometric, biomechanical, and molecular analyses. *Bone* 2002 Jan;30(1):137-143.
193. Delany AM, Hankenson KD. Thrombospondin-2 and SPARC/osteonectin are critical regulators of bone remodeling. *J Cell Commun Signal* 2009 Oct 28.
194. Abboud SL, Ghosh-Choudhury N, Liu LC, Shen V, Woodruff K. Osteoblast-specific targeting of soluble colony-stimulating factor-1 increases cortical bone thickness in mice. *J Bone Miner Res* 2003 Aug;18(8):1386-1394.
195. Lacey DC, Simmons PJ, Graves SE, Hamilton JA. Proinflammatory cytokines inhibit osteogenic differentiation from stem cells: implications for bone repair during inflammation. *Osteoarthritis Cartilage* 2009 Jun;17(6):735-742.
196. Haider R, Watzek G, Plenk H. Effects of drill cooling and bone structure on IMZ implant fixation. *Int J Oral Maxillofac Implants* 1993;8(1):83-91.
197. Malmstrom J, Adolfsson E, Arvidsson A, Thomsen P. Bone response inside free-form fabricated macroporous hydroxyapatite scaffolds with and without an open microporosity. *Clin Implant Dent Relat Res* 2007 Jun;9(2):79-88.
198. Mohammadi S, Esposito M, Hall J, Emanuelsson L, Krozer A, Thomsen P. Short-term bone response to titanium implants coated with thin radiofrequent magnetron-sputtered hydroxyapatite in rabbits. *Clin Implant Dent Relat Res* 2003;5(4):241-253.
199. Lu JX, Gallur A, Flautre B, Anselme K, Descamps M, Thierry B, et al. Comparative study of tissue reactions to calcium phosphate ceramics among cancellous, cortical, and medullar bone sites in rabbits. *J Biomed Mater Res* 1998 Dec 5;42(3):357-367.
200. Susin C, Qahash M, Hall J, Sennerby L, Wikesjo UM. Histological and biomechanical evaluation of phosphorylcholine-coated titanium implants. *J Clin Periodontol* 2008 Mar;35(3):270-275.
201. Rashmir-Raven AM, Richardson DC, Aberman HM, DeYoung DJ. The response of cancellous and cortical canine bone to hydroxylapatite-coated and uncoated titanium rods. *J Appl Biomater* 1995 Winter;6(4):237-242.
202. Lee JE, Heo SJ, Koak JY, Kim SK, Han CH, Lee SJ. Healing response of cortical and cancellous bone around titanium implants. *Int J Oral Maxillofac Implants* 2009 Jul-Aug;24(4):655-662.

203. Eriksson C, Lausmaa J, Nygren H. Interactions between human whole blood and modified TiO<sub>2</sub>-surfaces: influence of surface topography and oxide thickness on leukocyte adhesion and activation. *Biomaterials* 2001 Jul;22(14):1987-1996.
204. Tang L, Eaton JW. Fibrin(ogen) mediates acute inflammatory responses to biomaterials. *J Exp Med* 1993 Dec 1;178(6):2147-2156.
205. Shichinohe H, Kuroda S, Yano S, Hida K, Iwasaki Y. Role of SDF-1/CXCR4 system in survival and migration of bone marrow stromal cells after transplantation into mice cerebral infarct. *Brain Res* 2007 Dec 5;1183:138-147.
206. Yu J, Li M, Qu Z, Yan D, Li D, Ruan Q. SDF-1/CXCR4-mediated migration of transplanted bone marrow stromal cells towards areas of heart myocardial infarction via activation of PI3K/Akt. *J Cardiovasc Pharmacol* 2010 Feb 20. [Epub ahead of print]
207. Wang Y, Deng Y, Zhou GQ. SDF-1alpha/CXCR4-mediated migration of systemically transplanted bone marrow stromal cells towards ischemic brain lesion in a rat model. *Brain Res* 2008 Feb 21;1195:104-112.
208. Otsuru S, Tamai K, Yamazaki T, Yoshikawa H, Kaneda Y. Circulating bone marrow-derived osteoblast progenitor cells are recruited to the bone-forming site by the CXCR4/stromal cell-derived factor-1 pathway. *Stem Cells* 2008 Jan;26(1):223-234.
209. Granero-Molto F, Weis JA, Miga MI, Landis B, Myers TJ, O'Rear L, et al. Regenerative effects of transplanted mesenchymal stem cells in fracture healing. *Stem Cells* 2009 Aug;27(8):1887-1898.
210. Laudanna C, Kim JY, Constantin G, Butcher E. Rapid leukocyte integrin activation by chemokines. *Immunol Rev* 2002 Aug;186:37-46.
211. Ley K, Laudanna C, Cybulsky MI, Nourshargh S. Getting to the site of inflammation: the leukocyte adhesion cascade updated. *Nat Rev Immunol* 2007 Sep;7(9):678-689.
212. Karp JM, Leng Teo GS. Mesenchymal stem cell homing: the devil is in the details. *Cell Stem Cell* 2009 Mar 6;4(3):206-216.
213. Woodruff MA, Jones P, Farrar D, Grant DM, Scotchford CA. Human osteoblast cell spreading and vinculin expression upon biomaterial surfaces. *J Mol Histol* 2007 Oct;38(5):491-499.
214. Luthen F, Lange R, Becker P, Rychly J, Beck U, Nebe JG. The influence of surface roughness of titanium on beta1- and beta3-integrin adhesion and the organization of fibronectin in human osteoblastic cells. *Biomaterials* 2005 May;26(15):2423-2440.
215. Keselowsky BG, Wang L, Schwartz Z, Garcia AJ, Boyan BD. Integrin alpha(5) controls osteoblastic proliferation and differentiation responses to titanium substrates presenting different roughness characteristics in a roughness independent manner. *J Biomed Mater Res A* 2007 Mar 1;80(3):700-710.
216. Gronthos S, Simmons PJ, Graves SE, Robey PG. Integrin-mediated interactions between human bone marrow stromal precursor cells and the extracellular matrix. *Bone* 2001 Feb;28(2):174-181.
217. Gronowicz G, McCarthy MB. Response of human osteoblasts to implant materials: integrin-mediated adhesion. *J Orthop Res* 1996 Nov;14(6):878-887.
218. Wang L, Zhao G, Olivares-Navarrete R, Bell BF, Wieland M, Cochran DL, et al. Integrin beta1 silencing in osteoblasts alters substrate-dependent responses to 1,25-dihydroxy vitamin D3. *Biomaterials* 2006 Jul;27(20):3716-3725.

219. Chin SL, Johnson SA, Quinn J, Miroslavljevic D, Price JT, Dudley AC, et al. A role for alphaV integrin subunit in TGF-beta-stimulated osteoclastogenesis. *Biochem Biophys Res Commun* 2003 Aug 8;307(4):1051-1058.
220. Larsson C, Thomsen P, Aronsson BO, Rodahl M, Lausmaa J, Kasemo B, et al. Bone response to surface-modified titanium implants: studies on the early tissue response to machined and electropolished implants with different oxide thicknesses. *Biomaterials* 1996 Mar;17(6):605-616.
221. Guo J, Padilla RJ, Ambrose W, De Kok IJ, Cooper LF. The effect of hydrofluoric acid treatment of TiO<sub>2</sub> grit blasted titanium implants on adherent osteoblast gene expression in vitro and in vivo. *Biomaterials* 2007 Dec;28(36):5418-5425.
222. Sul YT. The significance of the surface properties of oxidized titanium to the bone response: special emphasis on potential biochemical bonding of oxidized titanium implant. *Biomaterials* 2003 Oct;24(22):3893-3907.
223. Sul YT, Byon ES, Jeong Y. Biomechanical measurements of calcium-incorporated oxidized implants in rabbit bone: effect of calcium surface chemistry of a novel implant. *Clin Implant Dent Relat Res* 2004;6(2):101-110.
224. Sul YT, Johansson C, Byon E, Albrektsson T. The bone response of oxidized bioactive and non-bioactive titanium implants. *Biomaterials* 2005 Nov;26(33):6720-6730.
225. Sul YT, Johansson CB, Albrektsson T. Oxidized titanium screws coated with calcium ions and their performance in rabbit bone. *Int J Oral Maxillofac Implants* 2002 Sep-Oct;17(5):625-634.
226. Sul YT, Johansson CB, Kang Y, Jeon DG, Albrektsson T. Bone reactions to oxidized titanium implants with electrochemical anion sulphuric acid and phosphoric acid incorporation. *Clin Implant Dent Relat Res* 2002;4(2):78-87.
227. Ozaki Y, Nishimura M, Sekiya K, Suehiro F, Kanawa M, Nikawa H, et al. Comprehensive analysis of chemotactic factors for bone marrow mesenchymal stem cells. *Stem Cells Dev* 2007 Feb;16(1):119-129.
228. Li MO, Flavell RA. Contextual regulation of inflammation: a duet by transforming growth factor-beta and interleukin-10. *Immunity* 2008 Apr;28(4):468-476.
229. Xu B, Zhang J, Brewer E, Tu Q, Yu L, Tang J, et al. Osterix enhances BMSC-associated osseointegration of implants. *J Dent Res* 2009 Nov;88(11):1003-1007.
230. Pregizer S, Baniwal SK, Yan X, Borok Z, Frenkel B. Progressive recruitment of Runx2 to genomic targets despite decreasing expression during osteoblast differentiation. *J Cell Biochem* 2008 Nov 1;105(4):965-970.
231. Muruganandan S, Roman AA, Sinal CJ. Adipocyte differentiation of bone marrow-derived mesenchymal stem cells: cross talk with the osteoblastogenic program. *Cell Mol Life Sci* 2009 Jan;66(2):236-253.
232. Kon T, Cho TJ, Aizawa T, Yamazaki M, Nooh N, Graves D, et al. Expression of osteoprotegerin, receptor activator of NF-kappaB ligand (osteoprotegerin ligand) and related proinflammatory cytokines during fracture healing. *J Bone Miner Res* 2001 Jun;16(6):1004-1014.
233. Lamolle SF, Monjo M, Lyngstadaas SP, Ellingsen JE, Haugen HJ. Titanium implant surface modification by cathodic reduction in hydrofluoric acid: surface characterization and in vivo performance. *J Biomed Mater Res A* 2009 Mar 1;88(3):581-588.

234. Mendonca G, Mendonca DB, Simoes LG, Araujo AL, Leite ER, Duarte WR, et al. Nanostructured alumina-coated implant surface: effect on osteoblast-related gene expression and bone-to-implant contact in vivo. *Int J Oral Maxillofac Implants* 2009 Mar-Apr;24(2):205-215.
235. Palmquist A. On a novel technique for preparation and analysis of the implant surface and its interface to bone [Doctoral thesis]. Göteborg: University of Gothenburg; 2008.
236. Li D, Ferguson SJ, Beutler T, Cochran DL, Sittig C, Hirt HP, et al. Biomechanical comparison of the sandblasted and acid-etched and the machined and acid-etched titanium surface for dental implants. *J Biomed Mater Res* 2002 May;60(2):325-332.



